Cyg
61
3846
750
Spine Stubbing
packet
watch Trim

STRATIGRAPHY AND GEOCHEMISTRY OF THE TROODOS OPHIOLITE EXTRUSIVE SEQUENCE IN THE MARGI AREA, CYPRUS

by

David G. Bailey

Submitted in partial fulfillment of the
requirements for the degree of
Master of Science

at

Dalhousie University
Halifax, Nova Scotia

June 1984

DALHOUSIE UNIVERSITY

DEPARTMENT OF GEOLOGY

The undersigned hereby certify that they have read and recommended to the Faculty of Graduate Studies for acceptance a thesis entitled " STRATIGRAPHY AND GEOCHEMISTRY OF THE TROODOS OPHIOLITE EXTRUSIVE SEQUENCE IN THE MARGI AREA, CYPRUS. ."

by David G. Bailey

in partial fulfillment of the requirements for the degree of Master of Science.

ted June 19, 1984

External Examiner

Research Supervisor

Examining Committee

Date June 19, 1984

Author David G. Bailey

Title STRATIGRAPHY AND GEOCHEMISTRY OF THE TROODOS OPHIOLITE EXTRUSIVE SEQUENCE IN THE MARGI AREA, CYPRUS.

Department or School Geology

Degree M.Sc. Convocation Fall Year 1984

Permission is herewith granted to Dalhousie University to circulate and to have copied for non-commercial purposes, at its discretion, the above title upon the request of individuals or institutions.

Signature of Author

THE AUTHOR RESERVES OTHER PUBLICATION RIGHTS, AND NEITHER THE THESIS NOR EXTENSIVE EXTRACTS FROM IT MAY BE PRINTED OR OTHERWISE REPRODUCED WITHOUT THE AUTHOR'S WRITTEN PERMISSION.

TABLE OF CONTENTS

page

Table of Contents..... iv

List of Tables..... vii

List of Figures.....viii

List of Plates..... x

List of Maps..... x

Abstract..... xi

Aknowledgements.....xiii

CHAPTER ONE - INTRODUCTION..... 1

1.1 General Statement..... 1

1.2 Geologic Setting..... 3

1.3 Previous Work..... 9

1.4 Location and Purpose of Study..... 13

CHAPTER TWO - VOLCANIC STRUCTURE AND STRATIGRAPHY..... 16

2.1 General Statement..... 16

2.2 Volcanic Rocks..... 18

2.2.1 Unit I..... 18

2.2.2 Unit II..... 24

2.2.3 Unit III..... 40

2.3 Overlying Sedimentary Rocks..... 46

2.4 Alteration and Distribution of Secondary Minerals..... 48

2.5 Fault Stages..... 54

2.6 Summary..... 56

TABLE OF CONTENTS

page

CHAPTER THREE - MINERAL FORM AND CHEMISTRY..... 59

3.1 General Statement..... 59

3.2 Olivine..... 59

3.3 Pyroxene..... 67

3.4 Plagioclase..... 76

3.5 Spinel..... 78

3.6 Summary..... 80

CHAPTER FOUR - WHOLE-ROCK AND GLASS GEOCHEMISTRY..... 85

4.1 General Statement..... 85

4.2 Major Element Geochemistry..... 85

4.3 Major Element Mobility..... 89

4.4 Trace Element Geochemistry..... 91

4.5 Glass and Unaltered Pillow Geochemistry..... 98

4.6 Summary..... 106

CHAPTER FIVE - ULTRAMAFIC LAVAS..... 109

5.1 General Statement..... 109

5.2 Mineralogical and Chemical Features..... 110

5.2.1 Picrite-based Flows..... 110

5.2.2 Picritic Pillows..... 115

5.3 Olivine-Liquid Equilibria..... 116

5.4 Discussion..... 124

5.5 Summary..... 126

TABLE OF CONTENTS

page

CHAPTER SIX - PETROGENESIS..... 128

6.1 General Statement..... 128

6.2 Sequence and Temperatures of Crystallization..... 129

6.3 Closed-System Fractional Crystallization..... 135

6.4 Partial Melting and Parental Magmas..... 148

6.5 Tectonic Environment..... 158

6.6 Summary..... 163

CHAPTER SEVEN - SUMMARY..... 166

7.1 Data Presented..... 166

7.2 Conclusions..... 166

References..... 169

Appendix I - Table of Petrographic Features..... 178

Appendix II - Analytical Methods..... 187

Appendix III - Whole-Rock and Glass Geochemistry..... 192

Appendix IV - Mineral Analyses..... 206

LIST OF TABLES

		page
III-1	Representative olivine analyses.....	63
III-2	Representative pyroxene analyses.....	71
III-3	Representative plagioclase analyses.....	77
III-4	Representative chromite analyses.....	79
V-1	Least-squares mixing calculation relating the ultrabasic lavas to the surrounding extrusives..	117
V-2	Ferrous/ferric iron concentrations of glass and "unaltered" pillow samples.....	120
VI-1	Calculated olivine liquidus temperatures.....	133
VI-2	Least-squares mixing calculations which model the process of fractional crystallization in the Margi area volcanics.....	138
VI-3	Least-squares mixing calculation which models the derivation of Suite B_1 from depleted Suite B_2 compositions.....	142
VI-4	Trace and minor element crystal/liquid partition coefficients used in computer modelling.....	144
VI-5	Least-squares mixing calculations which model the derivation of lithology II-E compositions...	146
VI-6	Chemical and petrographic features of samples from lithology II B.....	156
VI-7	Hypothetical magma chamber and associated extrusive activity for the Margi area.....	164

LIST OF FIGURES

		page
I-1	Simplified geologic map of Cyprus showing location of study area.....	4
I-2	Simplified geologic map of the Margi - Analiondas area.....	14
II-1	Schematic stratigraphic column of lithologies in the Margi area.....	17
II-2	Cross section of a picrite-based massive flow...	32
II-3	Distribution of secondary minerals with respect to stratigraphic depth.....	50
II-4	Distribution of secondary minerals with respect to cooling unit lithology.....	51
III-1	Microprobe traverse across a typical olivine phenocryst.....	65
III-2	Plot of FeO vs. MgO variation in olivines.....	66
III-3a	Plot of FeO vs. SiO2 variation in pyroxenes.....	72
III-3b	Plot of Al2O3 vs. SiO2 variation in pyroxenes...	72
III-4	Pyroxene compositions plotted in the pyroxene quadralateral.....	74
III-5	Plot of Cr/(Cr+Al) vs. Mg/(Mg+Fe) variation in spinels.....	81
IV-1	Variation diagrams of whole-rock major element oxide concentrations	87
IV-2	Variation diagrams of whole-rock trace element concentrations	94
IV-3	Variation diagrams of whole-rock Cr and Ni concentrations.....	97
IV-4	Variation diagrams of glass and unaltered pillow major element oxide concentrations.....	101
IV-5	Variation diagrams of glass and unaltered pillow minor and trace element concentrations...	104

LIST OF FIGURES (cont.)

		page
IV-6	Ti/V ratios of selected whole-rock samples.....	105
IV-7	Correlation of local to regional lithostratigraphic units and chemical suites.....	107
V-1	Major element variation within a picrite-based massive flow.....	113
V-2	Trace element variation within a picrite-based massive flow.....	114
V-3	Plot of FeO vs. MgO of coexisting olivine and liquid.....	123
V-4	Crystallization temperatures and compositions of olivines in equilibrium with a liquid of known FeO and MgO content.....	125
VI-1	Whole-rock compositions projected from silica onto the plane Ol-Plag-Cpx of the normative basalt system.....	136
VI-2	Modelled pathways of partial melting and fractional crystallization for Cr vs. Y.....	151
VI-3	Modelled pathways of partial melting and fractional crystallization for Ti vs. V.....	153
VI-4	Trace element discriminant diagrams.....	159

LIST OF PLATES

		page
II-1	Layer of umberiferous sediment which locally separates stratigraphic Units I and II.....	22
II-2	Clinopyroxene spherulites on weathered surface of a thin flow in Unit II.....	27
II-3	Exposure of picritic pillows in Unit II.....	29
II-4	Ropey "pahoehoe" surface of thin flow in Unit III.....	43
II-5	Black glassy rind on pillow surface in Unit III.	45
III-1	Microphotograph of olivine and pyroxene in a picritic flow base.....	61
III-2	Microphotograph of olivine in a picritic pillow.	61
III-3	Microphotograph of an olivine phenocryst which exhibits broad kink-bands.....	62
III-4	Microphotograph of groundmass clinopyroxenes with quench morphologies.....	68
III-5	Microphotograph of strongly zoned clinopyroxene and plagioclase grains from a medium-grained, massive flow.....	70

LIST OF MAPS

Map 1 Geologic map of the Margi area. Cyprus..(back pocket)

Map 2 Sample location map.....(back pocket)

ABSTRACT

The extrusive rocks of the Troodos Ophiolite in the Margi area of Cyprus are highly variable in form and mineralogy, consisting of ten distinct cooling unit lithologies. The volcanic sequence can be divided into three major lithostratigraphic units, primarily on the basis of phenocryst mineralogy. The lowermost unit, Unit I, consists of aphyric to plagioclase and clinopyroxene microphyric volcanics. Unit II is approximately 175 m thick and consists largely of olivine phyric to picritic pillows and flows. At the top of the volcanic pile lies Unit III, which is an approximately 50 m thick sequence of aphyric to sparsely olivine phyric pillows and thin flows.

The boundary between Units I and II coincides with the previously mapped boundary between the classical "Lower" and "Upper Pillow Lava" sequences, and is often marked by a thin layer of umberiferous sediment. This boundary also separates rocks which belong to the two major chemical suites which are currently recognized within the massif, the "arc-tholeiite" and "boninite" suites, respectively.

The major element compositional variation of the extrusive rocks within Units II and III (the "boninite" suite), can be largely explained by simple closed-system fractionation of olivine, clinopyroxene, and minor chrome

spinel. Incompatible trace element concentrations of the rocks within these units are consistent with derivation from a strongly depleted mantle source and suggest periodic additions of parental melt fractions to a shallow level magma chamber.

The "ultrabasic lavas" of the Margi area all contain 45 to 65 modal percent phenocrystic olivine. The majority of these rocks formed by post-extrusion gravitative settling of olivine phenocrysts from moderately phyric lavas. A small proportion were extruded as "picritic lavas", but these represent samples of magma chamber cumulates that were mixed with small amounts of melt and extruded as a crystal liquid mush during periods of advanced tapping.

ACKNOWLEDGEMENTS

Sincere thanks to my supervisor. Paul T. Robinson, for making this study possible, and to Drs. R. A. Jamieson and J. Malpas for kindly reviewing the manuscript.

I am grateful to Dr. J. N. Ludden for guidance and assistance in whole-rock XRF analysis. S. Parikh and R. MacKay are thanked for assistance in wet chemistry and microprobe analysis, respectively. J. Robinson provided computer plotting programs.

K. Gillis, J. Mehegan, and the Archives Boys are thanked for stimulating discussions and numerous cups of coffee. Special thanks to Jean Williams for providing moral support.

Thanks also to those on the faculty and staff of the Dalhousie Geology Department who have, in one way or another, contributed to this study.

CHAPTER ONE

INTRODUCTION

1.1 General Statement

Interest in the nature of the ocean crust has grown rapidly ever since the concept of plate tectonics became well-established in the early 1960s. Drilling by the Deep Sea Drilling Project (DSDP), along with geophysical studies and dredge sampling of the ocean floor over the past two decades, has greatly enhanced our knowledge of the ocean crust. However. only the uppermost portions of the crust have been sampled directly. and information on the internal structure and chemistry of the oceanic lithosphere is almost non-existent. For this reason, examinations of ophiolites, which are believed to be obducted slabs of oceanic lithosphere. are essential for resolving many of these subsurface features.

Unfortunately. many ophiolites are internally deformed and, in some instances, totally dismembered. These structural complexities, along with the extensive chemical alteration due to seafloor and subaerial weathering, have made it extremely difficult to extract reliable information from ophiolite complexes.

The Troodos ophiolite of Cyprus is unusual in that it is little deformed or altered. It consists of a complete,

relatively intact ophiolite sequence, exposed as a broad dome in the southwestern portion of the island. The degree to which it has been altered, although variable, is markedly less than in most ophiolites, as evidenced by the preservation of fresh volcanic glass throughout the extrusive sequence (Jorgensen et al., 1981; Robinson et al., 1983). Examination of the Troodos ophiolite therefore provides an excellent means of determining the compositional and structural variations within a portion of oceanic lithosphere.

Of particular interest are the magmatic processes which form the ocean crust. for these are intimately related to the tectonic environment and conditions of formation. Clearly, before any integrated tectonic / petrogenetic model of crustal accretion can be formulated for the Troodos ophiolite, it is necessary to delineate these processes throughout the entire massif.

It is, therefore, one of the broad goals of this thesis, which involves detailed mapping of a small portion of the Troodos pillow lava sequence, to establish some of the variations in the form. mineralogy, and chemical evolution of the ophiolite volcanics. In particular. this thesis examines the "ultrabasic lavas" which are locally abundant within the extrusive sequence, for these rocks clearly formed by unusual magmatic processes whose role in the formation of the Troodos

ophiolite must be understood.

1.2 Geologic Setting

The island of Cyprus lies along the 35th parallel in the eastern Mediterranean Sea. Approximately one-third of its 9250 km2 area is formed by the Troodos ophiolite (Figure I-1). Directly to the north and south, the massif is overlain by thick sequences of upper Cretaceous to middle Miocene calcareous sedimentary rocks (Robertson, 1976).

On the northern coast of Cyprus lies the Kyrenia range, which is composed of an allochthonous sequence of highly deformed and thrust faulted shelf sediments of upper Cretaceous to middle Miocene age, and of minor amounts of basalt, serpentinite, and rhyolite (Robertson, 1980). Undeformed late Miocene to Holocene sediments overlie this allochthonous sequence.

In the southwestern corner of Cyprus lies the Mamonia complex, which is essentially a melange, containing a sequence of both autochthonous and allochthonous sedimentary rocks, along with Triassic lavas and tuffs (Moores and Vine, 1971). It is suggested that this complex may have formed in an ancient subduction zone (Moores and Vine, 1971), or along an oceanic spreading center transform (Spray and Roddick, 1981).

Late Tertiary uplift of the massif on the order of 2000

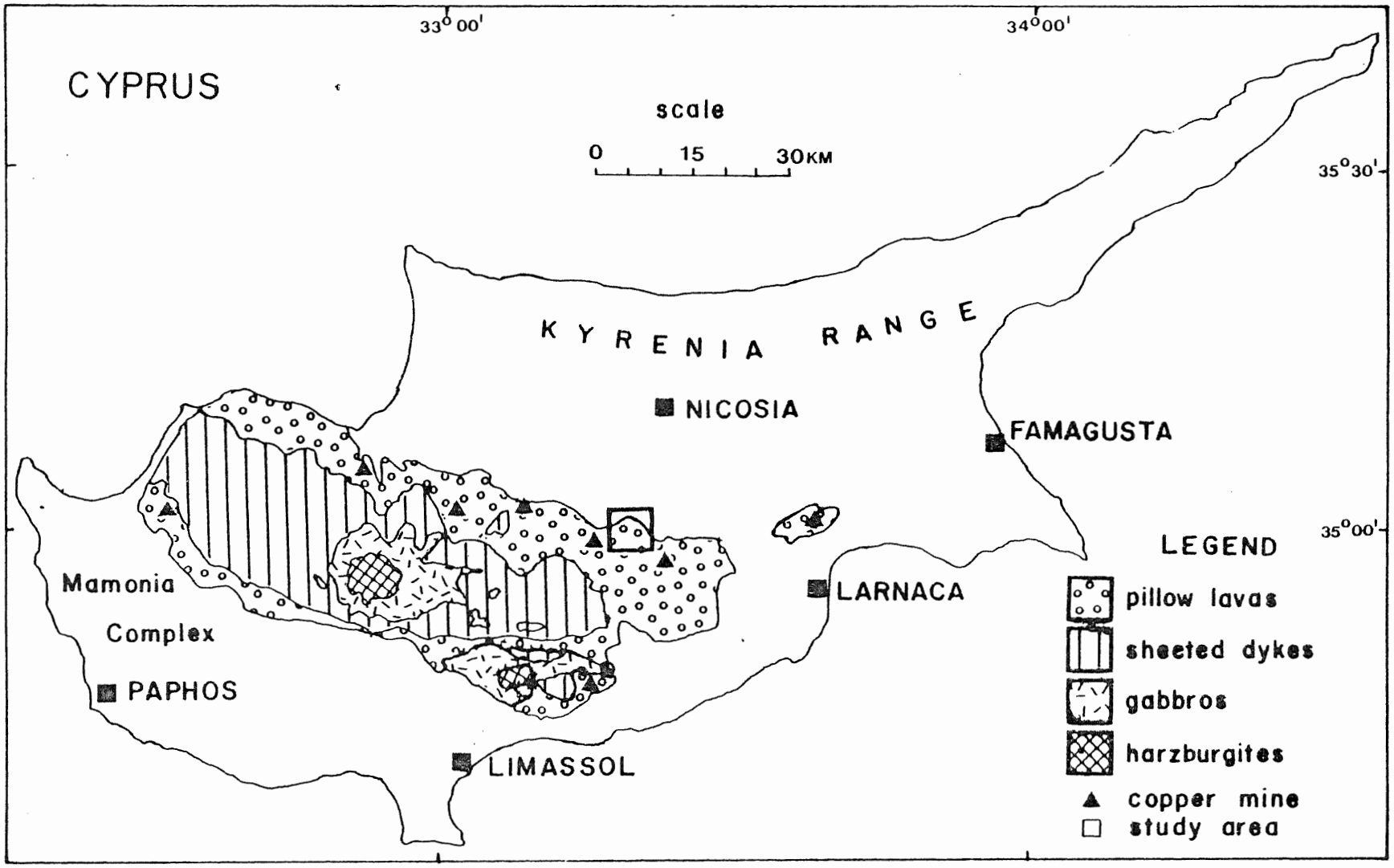

FIGURE I-1. Simplified geologic map of Cyprus showing location of field area.

m has produced a domal structure and, along with subsequent erosion, an annular outcrop pattern (Gass and Masson-Smith, 1963). A complete and undeformed ophiolite sequence, as defined by the 1972 Penrose Ophiolite Conference, is exposed in the massif. A plutonic core is overlain by an extensive sheeted dike complex which, in turn, is overlain by a peripheral ring of pillowed volcanics.

The plutonic rocks consist primarily of tectonized harzburgite, with minor dunite, pyroxenite, olivine gabbro, and quartz diorite (Allen, 1975). Many of the ultramafic rocks are partly to completely serpentinized. The basal harzburgite, which forms the peak of Mt. Olympus, is also the host to economic bodies of asbestos and chromite-rich pods of dunite (Greenbaum, 1972). The harzburgite is overlain by a thick cumulate sequence which ranges in composition from troctolite to plagiogranite. Isotropic olivine gabbro is the predominant cumulate lithology, although layered gabbros which exhibit variations in size and modal abundance of olivine, pyroxene, and plagioclase are common (Moores and Vine, 1971). On the basis of deformational styles and intrusive relations, two distinct magmatic suites have been recognized within the plutonic complex (Dunsworth et al., 1984).

The sheeted dike complex comprises more than 60% of the massif's exposed area. The contact between the dike sequence

and the underlying plutonics is variable. Screens of gabbro and plagiogranite are locally present, with the surrounding dikes chilled against them. In other areas, however, the gabbros clearly intrude the dikes (Wilson, 1959). The complex itself consists of virtually 100% dikes, most of which trend in a north-south direction. Individual dikes range in thickness from 0.2 to 5.0 m, and exhibit poorly developed chilled margins. Most dikes are aphyric, although olivine and clinopyroxene phyric dikes are known. Picritic dikes have also been observed (Desmet, 1976; Mehegan, 1984, pers.comm.), but they appear to be of only minor importance.

Locally. the dikes have been metamorphosed to the greenschist facies and are composed of quartz, epidote, amphibole, and magnetite. The entire dike complex has a thickness on the order of 1 to 1.5 km.

Kidd and Cann (1974) noted that each dike was chilled against those it intruded, and statistical analysis of these chilling directions were interpreted as indicating a spreading center to the west of the present day outcrop. More recent studies, however. have revealed that chilling relationships amongst the dikes are extremely complex, and that there is no apparent chilling direction preference (Baragar et al., 1984).

The contact of the sheeted dike complex with the overlying extrusive rocks is sharp, with a transition from

50% dikes to less than 5% dikes over a zone approximately 100 m thick (Gass,1980). The extrusions form an irregular and incomplete ring around the massif. and range in total thickness from 1 to 2 km. They are predominantly pillowed, but large massive flows, thin sheet flows, and hyaloclastite breccias are common.

The extrusive sequence has been divided into two major units on the basis of field criteria (Wilson, 1959; Gass and Smewing. 1973). The "Lower Pillow Lavas" (or LPL), are predominantly aphyric to slightly clinopyroxene and/or plagioclase phyric basalts and andesites. These rocks typically occur as large, irregular pillows which are gray to greenish-gray in color. This sequence is of variable thickness, but generally comprises around two-thirds of the total extrusive section.

Overlying the LPL are the "Upper Pillow Lavas", (or UPL). The UPL volcanics are largely olivine phyric basalts and picrites, although aphyric and clinopyroxene phyric units do exist. These extrusions typically form small, lobate pillows, and occasionally. large massive flows. The sequence is highly variable in color, (ranging from dark gray to reddish-brown), and in degree of alteration. Commonly, the top 50 m of the section is highly oxidized (Gillis, 1984).

The nature of the boundary between the LPL and the UPL is a matter of great interest and dispute. Locally. the two

sequences are easily distinguished and are confined to distinct stratigraphic intervals separated by thin layers of sediment (e.g. the Pedios canyon area;(Mehegan, 1983; pers.comm.)). In other areas, however, the boundary between the two units is ambiguous and, in fact, it has been suggested that the two sequences may interfinger (e.g. the Yiallias canyon area; (Pearce, 1982; pers. comm.)). Detailed mapping of the Akaki canyon area has also shown that what had been previously mapped as the LPL/UPL boundary does not actually exist (Schminke et al., 1983; Robinson et al., 1983). The actual nature of this boundary throughout the massif, and its relation to major geochemical suites, has yet to be fully determined.

The volcanics are locally overlain by dark brown, manganese-rich umbers, which are in turn overlain by a thick sequence of chalks, marls, and reef limestones. Paleontological and radiometric age determinations on inter-lava sediment and on the overlying pelagic sedimentary rocks have been used to assign an age of approximately 85 m.y. to the Troodos massif (Mantis, 1970; Robertson and Hudson, 1974).

1.3 Previous Work

The Troodos massif of Cyprus is perhaps one of the most studied ophiolites in the world. The numerous massive sulphide bodies that are found throughout the extrusive sequence have been the main focus of geologic interest from ancient times to the present day (e.g. Spooner. 1977). It has only been within the last quarter century that any significant attention has been paid to the geology of the complex as a whole. Recent geologic literature dealing with the Troodos ophiolite, however, is voluminous. reflecting the current interest in the oceanic crust and plate tectonic processes. Therefore, the aim of this section is to present only a broad overview of the history and development of geologic thought with regard to the Troodos ophiolite.

The work of Wilson (1959), Bear (1960), and Carr and Bear (1960), along with other members of the Cyprus Geological Survey made significant contributions to our understanding of the massif. particularly the plutonic sequence and the sheeted dike complex. Work among the extrusive rocks was largely pioneered by Gass (1958, 1960), and Bagnall (1960). Although most of these observations were made prior to the development of the sea-floor spreading hypothesis (Vine and Matthews, 1963), they are still of considerable value.

Gass (1968) was among the first to postulate that the

Troodos massif was an exposed fragment of oceanic lithosphere. This interpretation was supported by early geochemical data on the lavas which were interpreted as showing a tholeiitic composition, and by regional geophysical surveys which produced data compatible with that obtained from similar surveys of the ocean floor (Gass and Masson-Smith, 1963). By the early 1970's, it was generally accepted that the Troodos massif represented a subaerial portion of oceanic crust, and it was identified as an ophiolite (Moores and Vine, 1971; Gass and Smewing, 1973).

In 1973. Miyashiro proposed that the Troodos ophiolite was formed in an island arc environment. Few other papers have received such extensive criticism from the scientific community. The bulk of the criticism (Moores, 1975; Hynes, 1975; and Gass, 1975) centered around Miyashiro's use of major oxide geochemistry to determine the tectonic environment, because virtually all of the extrusive rocks on Cyprus have been, to some degree. mineralogically and chemically altered. The controversy generated by Miyashiro's paper did, however. stimulate additional geologic studies, for interest was now centered around determining more precisely the tectonic setting in which the Troodos ophiolite formed.

Emphasis was placed on minor and trace element geochemical studies for two major reasons. First of all. it

was thought that minor and trace elements could be successfully employed to distinguish between magma types formed in various tectonic environments (e.g. Pearce and Cann, 1971; 1973). Secondly. it was known that certain trace elements remained relatively immobile during weathering and even low-grade metamorphism (Cann, 1970). Since nearly all ophiolites have undergone some form of alteration, it became apparent that minor and trace element studies could potentially be very useful for determining the environment in which they formed.

The results of two trace element studies in the mid-1970's revealed that the Troodos ophiolite extrusive rocks differed significantly from typical ocean-floor basalts (Pearce, 1975; Smewing et al., 1975). On the basis of their results, both authors concluded that the most probable environment of formation for the Troodos Massif was a small, inter-arc, or back-arc basin adjacent to a subduction zone. Such basins have been described from the southwestern Pacific and are believed to be extensional in origin (Karig, 1970).

A major discrepancy between the two studies, however, involved the origin of the Upper Pillow Lava sequence. Smewing et al., (1975) hypothesized that the entire massif formed as a result of spreading in a marginal basin and that the UPL sequence was simply an "off-axis" expression of the same magmatic activity. Pearce (1975), however. concluded

that the UPL sequence represents a distinct phase of volcanism, resulting from the initiation of island-arc magmatism.

Exactly where the Upper Pillow Lavas fit into the tectonic and magmatic evolution of the Troodos massif is still not clear. Chemical analyses of unaltered glass from the extrusive sequence have shown that at least two distinct magmatic suites do exist, though neither is clearly correlative with the classical "Upper" and "Lower" pillow lava sequences (Robinson et al., 1983). Unfortunately, the structural and chronological relationships between the two suites are not yet well-established.

A further problem with regard to the origin of the UPL is presented by the localized occurrence of ultrabasic lavas within the sequence. Gass (1958) originally suggested that these rocks formed directly from "peridotitic" melts, although the more recent work of Malpas and Langdon (1982) suggests that they represent extruded magma chamber cumulates. Both interpretations imply unusual, but vastly different, magmatic processes. It is essential to understand how these ultrabasic lavas formed before a coherent model for the genesis and evolution of the Troodos ophiolite can be formulated.

1.4 Location and Purpose of Study

The area studied for this thesis occupies approximately four square kilometers of the extrusive sequence along the northern flank of the ophiolite complex, near the village of Margi (see Figures I-1 and I-2). The Alykos river flows through the northern and western portions of the field area, occasionally forming a canyon with walls up to 12 meters high. The topography is quite irregular, even though the highest point is only 358 m (asl), and the maximum relief is only 80 meters. Exposure is excellent, especially in the northern portion of the field area where it approaches 80%. Vegetation is sparse, consisting of scattered olive trees and a few shrubs along the major drainages.

Rocks of the classical "Upper Pillow Lava" sequence comprise the majority of the outcrops in the study area (see Figure I-2). A thick cover of sedimentary rocks is present in the northern and eastern portions of the area, and in the south lie the "Lower Pillow Lavas". Of particular geologic interest in the area is the abundance of both umberiferous sediments and ultrabasic lavas. Detailed geologic mapping of this region at a scale of 1:5000, followed up by petrographic and chemical studies, was carried out for two major reasons:

First, mapping of the pillow lavas in a region of such good exposure (instead of just a canyon section), makes it possible to delineate the chemical and structural

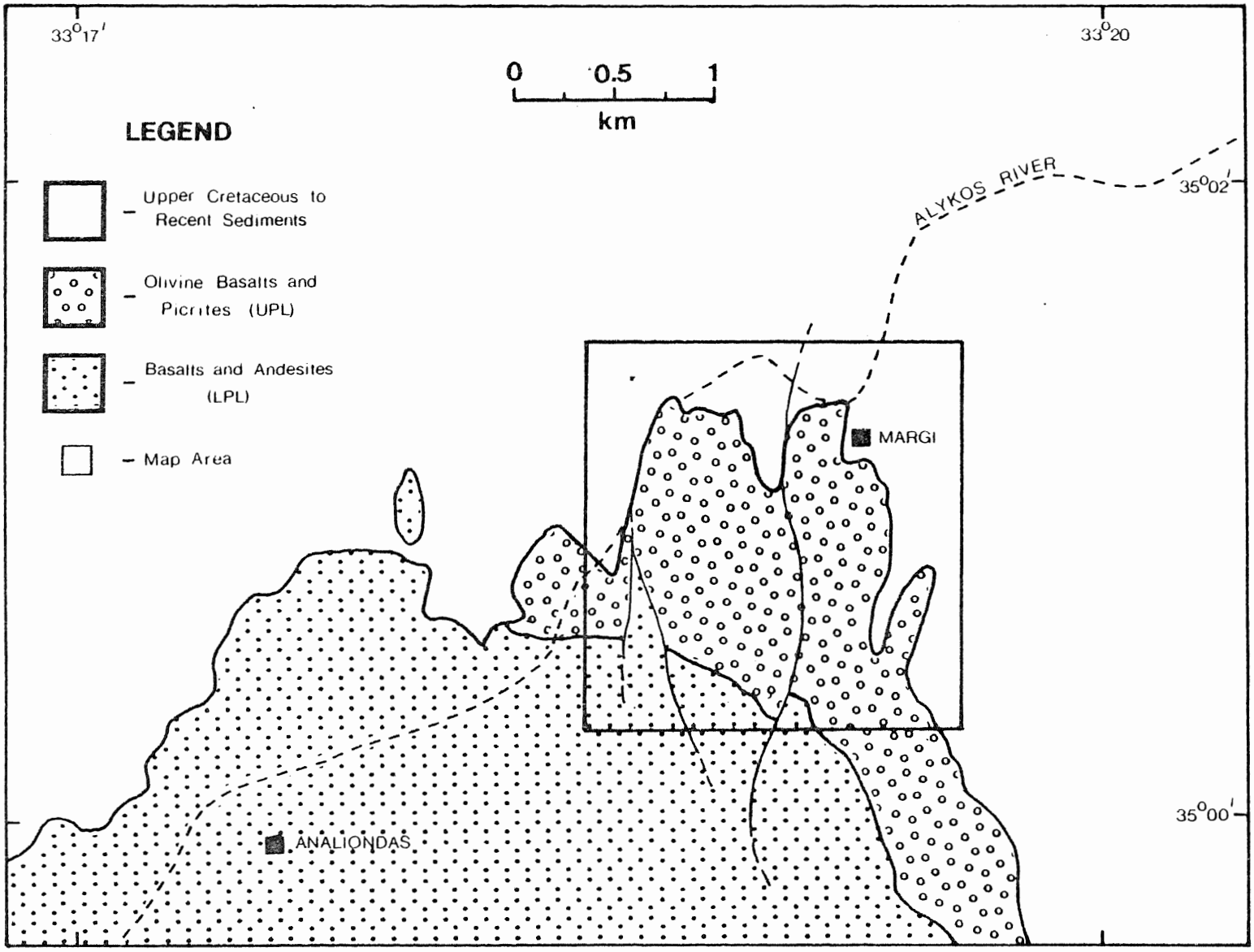

FIGURE I-2. Simplified geologic map of the Margi-Analiondas area (from Geol. Surv. Cyprus Dhali Map).

relationships within the extrusive sequence. Such features must be understood before many of the previously mentioned problems regarding the origin and evolution of the Upper Pillow Lavas, and their relationship with the Lower Pillow Lavas, can be resolved.

Secondly. it is another aim of this thesis to explain the genesis of the locally abundant ultrabasic lavas, for the presence of such rocks implies unusual processes in the magmatic evolution of the Troodos massif.

CHAPTER TWO

VOLCANIC STRUCTURE AND STRATIGRAPHY

2.1 General Statement

The extrusive sequence in the area surrounding the village of Margi is well exposed and easily accessible. In general. the stratigraphy is simple, with a thick sequence of aphyric to clinopyroxene and plagioclase microphyric lavas being overlain by an approximately 200 m thick sequence of olivine phyric volcanics which, in turn, is overlain by calcareous sedimentary rocks. In detail. however, the stratigraphy is much more complex, for the volcanics exhibit an extremely wide variation in both form and lithology.

In order to illustrate and describe some of these features, the sequence has been divided into three major stratigraphic units on the basis of field criteria (See Map 1, back pocket). A simplified stratigraphic column (Figure II-1), schematically shows the vertical distribution of these three units, along with the various lithologies and flow styles that occur within each. Field and petrographic features of all these are described separately below. (For further petrographic descriptions see Chapter Three and Appendix I.) The alteration and faulting of the rocks within these units are also described in this chapter.

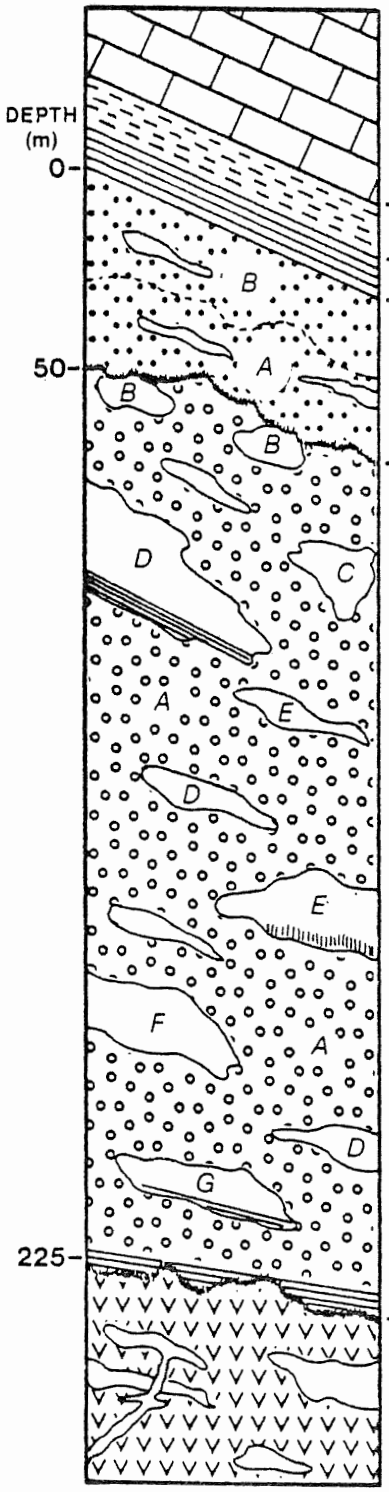

CHALKS

MUDSTONES

UMBERS / CHERTS

UNIT III

A. Aphyric pillows and thin flows

B. Sl. Olivine phyric pillows and flows

UNIT II

A. "Crystalline" olivine phyric pillows and thin flows

B. "Glassy" olivine phyric pillows

C. Picritic pillows

D. Picrite-based flows

E. Aphyric massive flows

F. Olivine microphyric flows

G. Clinopyroxene microphyric flows

UNIT I

A. Aphyric and plagioclase / clinopyroxene microphyric volcanics

FIGURE II-1. Schematic stratigraphic column of the extrusive sequence in the Margi area, Cyprus.

2.2 Volcanic Rocks

The volcanic rocks in the Margi area can be divided into three major lithostratigraphic units, primarily on the basis of phenocryst mineralogy.

Unit I Lack of olivine; presence of clinopyroxene and/or plagioclase microphenocrysts.

Unit II Phenocrystic olivine, 5-50%.

Unit III Phenocrystic olivine, < 5%.

Variations in the form and lithology of the extrusive rocks within each unit are described below.

2.2.1 Unit I

Unit I is stratigraphically the lowest extrusive unit exposed in the field area. It is composed of aphyric to clinopyroxene and plagioclase phyric pillows and thin flows, along with minor intrusives. There is significant variation in many features of the rocks within this unit, however, due to the poor exposures and limited area of the unit that was mapped, it was not practical to distinguish distinct lithologic or flow types.

The upper boundary of this unit is generally obscure, but where visible, there is a sharp contact with Unit II, commonly separated by a thin layer of umberiferous sediment. Significantly, the location of this boundary coincides with that of the previously mapped boundary between the "Lower"

and "Upper Pillow Lava" sequences.

The extent of Unit I down-section is not known, although reconnaissance mapping along with the work of Boyle and Robertson (1983), have shown that olivine phyric lavas are again present approximately 2 km south of the Unit I / Unit II boundary mapped in this study. This suggests the possibility of either structural repetition or interfingering of the two units.

A. Aphyric and Plagioclase/Clinopyroxene Microphyric Volcanics

Pillows in Unit I are variable in size, morphology, and color. They are generally dark brown, with yellow to purple weathering surfaces. All the extrusive rocks are highly vesicular (around 10%), with vesicles ranging in size from 0.5 to 8.0 mm in diameter, and in shape from elongate to spherical. Elongate vesicles are stretched and aligned with local flow directions. Most vesicles are open, although linings of smectite, analcime, or calcite are not uncommon. Chilled margins are indistinct, and glassy rinds totally obliterated.

In thin section, the only primary minerals observed are plagioclase, clinopyroxene and titanomagnetite. Plagioclase typically occurs as elongate microlites in the groundmass, although laths up to 0.80 mm long do occur. Abundance is

highly variable (trace to 35%), and most grains are at least 50% altered.

Clinopyroxene is present in most samples, either as groundmass microlites or as microphenocrysts with diameters up to 0.70 mm. Abundance varies from 0 to 20%, though pyroxene is generally subordinate to plagioclase. Alteration of the pyroxene to smectites is extensive.

Minute (< 0.10 mm), anhedral grains of titanomagnetite are occasionally observed in the groundmass of the least altered samples. In most specimens from the study area, however, its presence is not discernable. The remaining groundmass is completely altered to dark brown, virtually opaque oxides and smectites.

B. Interlava Breccias and Sediments

Hyaloclastites are common in the uppermost portion of Unit I. They tend to occur as thin (less than 1.0 m thick), discontinuous layers within the pillow sequence. They are composed of altered, angular fragments of basaltic glass (up to 3 cm in diameter), set in an off-white matrix of clays and carbonates.

No major breccia zones or sediment horizons were observed within Unit I. However, at the very top of the unit, a thin (10 to 30 cm thick) layer of umberiferous sediment occurs. The best exposure of this sediment occurs

in the southeastern portion of the field area, and is shown in Plate II-1.

In this area, the highly weathered pillows and thin flows of Unit I are locally overlain by hyaloclastite and dark brown volcanic breccia. The breccia consists of subangular to rounded, basalt fragments (1 to 10 mm long), suspended in a basaltic matrix. Clinopyroxene and plagioclase microlites are found in trace amounts in both the fragments and the matrix. The fragments, when elongate, are aligned subparallel to the general flow direction.

Overlying these fragmental rocks is a thin, but continuous, layer of sediment. The basal portion of this sediment layer is dark brown in color, and composed of manganese and iron-rich hydroxides and clays, similar to the umbers which overlie the entire extrusive sequence in the Margi area (See section 2.4). This "umberiferous" sediment grades upward into a dark grey, finely laminated mudstone.

A thin (1 to 2 m), basalt flow is found directly overlying these sediments. Well developed chilled margins (approximately 10 cm thick), are developed along both the top and bottom surfaces of the flow. These margins are fine grained and much more resistant to weathering than the medium grained flow interior. The lower chilled margin is light grey, except for the bottom 4 cm which is dark red to purple, and contains large olivine phenocrysts. These phenocrysts

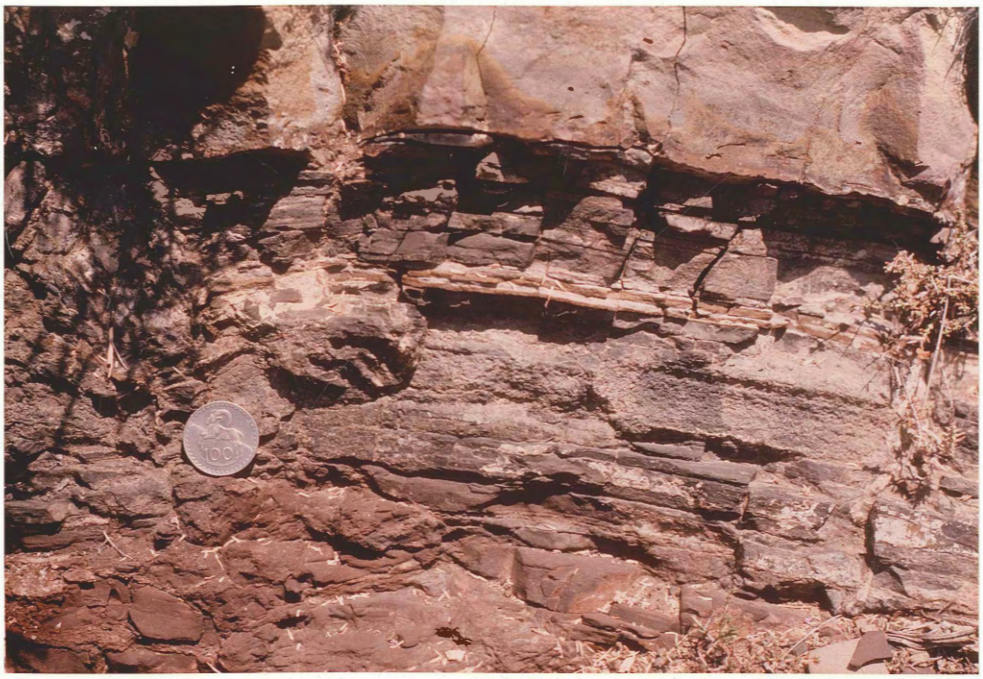

PLATE II-1. Layer of umberiferous sediment which locally separates stratigraphic Units I and II. (Scale: Coin diameter = 30 mm).

are 1 to 10 mm long, and are totally altered, forming pseudomorphs composed largely of limonite. Interestingly, the flow is essentially aphyric except for these large phenocrysts which, at most, comprise only 2% of the entire flow.

It should be noted that the sequence described above is only observed in one locality. In other areas, the sequence of lithologies can be markedly different, and thicknesses are quite variable. The following sequence is the "maximum" observed for the transition from Unit I to Unit II:

7. Unit II — Slightly olivine phyric pillows +/or thin flows
6. Sediment — Mudstone/Umber
5. Basalt — Slightly olivine phyric thin flow
4. Sediment — Mudstone/Umber
3. Basalt — Breccia +/or Hyaloclastite
2. Sediment — Mudstone/Umber
1. Unit I — Aphyric pillows

Any or all of lithologies 2 through 6 may be present in any one section, though there is generally at least one layer of sediment separating the two units. Clearly, there is a significant "lull" in volcanicity between extrusion of Units I and II.

2.2.2 Unit II

The volcanic rocks within Unit II are typically olivine phyric and contain, on average, > 5% phenocrystic olivine. Single cooling units, however, are highly variable in mineralogy and form, and individual samples may contain anywhere from 0 to 60% olivine.

Rocks of Unit II are the most common in the area mapped, comprising over 60% of the exposed volcanic section (see Map 1; back pocket). The actual thickness of this unit is difficult to determine due to faulting, however, it is roughly estimated to be 175 m thick.

A. "Crystalline" Olivine Phyric Pillows and Thin Flows

Olivine phyric pillows (and minor thin flows), comprise between 60 and 70% of the exposed extrusive rocks in all of Unit II. They are highly variable in form, color, and modal mineralogy. The term "crystalline" is used here to refer to pillows which contain discrete grains of clinopyroxene and/or plagioclase in the groundmass. Most pillows are elongate and ellipsoidal, with an average diameter of approximately 60 cm. They are light to dark brown in color, except for the margins which are either light gray or red-brown. Fresh glassy rinds are rarely preserved, most having been altered to green smectites and minor carbonate.

Phenocrysts of olivine (2 to 20%), are sub- to euhedral, and range from 0.5 to 10 mm in diameter. Most grains are completely altered, and form red-brown pseudomorphs composed of smectites, oxides and calcite. Phenocrysts are found throughout a single cooling unit (e.g. from rim to core), though there is a slight tendency for grains to be concentrated in pillow centers. An average modal abundance of 8% is estimated for the entire unit.

Clinopyroxene phenocrysts and microphenocrysts are irregularly distributed, being observed in only 20% of the pillows of Unit II. They are significantly more common in the lower one-third of the unit. Grains are difficult to observe in the field for they are rarely over 1 mm in length. In thin section, however, they are seen to be equant, subhedral crystals with an average diameter of approximately 0.30 mm. Modal abundance ranges from 0-12%, with an average of nearly 8% for the "clinopyroxene phyric" lithologies, but less than 2% for the entire unit. Most grains contain abundant inclusions and show signs of slight alteration.

Microphenocrysts of dark red to black, euhedral spinel are also observed, but are generally present in only trace amounts (0 to 4%). Typically, they occur as inclusions in large olivine grains, although independent grains within the groundmass are not uncommon.

The groundmass of most olivine phyric pillows is tan to

brown in color, and composed largely of clays, disseminated secondary oxides, and calcite. Poorly formed grains and elongate microlites of clinopyroxene are present in all samples, though the actual modal abundance is highly variable (4 to 20%). Minute grains and needles of plagioclase are also common (3 to 15%), but are generally present in subordinate amounts compared to clinopyroxene.

B. "Glassy" Olivine Phyric Pillows

At the top of Unit II, localized exposures of dark black, dense, glassy pillows are common. Individual pillows are small, with diameters ranging from 10 to 60 cm. Fresh glass is occasionally preserved and found as 5 to 10 mm thick rinds on pillow margins. A spherulitic texture is present in some pillows, yet it is most commonly observed on weathered surfaces of thin flows that occur amongst the pillows (Plate II-2). These spherulites range from 5 to 20 mm in diameter and are formed by radiating clinopyroxene microlites.

Olivine is the only phenocryst phase present in these pillows. It is homogeneously distributed, ranging in modal abundance within and between cooling units from only 5 to 10%, averaging around 7%. Crystals are subhedral to skeletal in form, and often contain inclusions of spinel and/or groundmass material. The average diameter is approximately 0.45 mm, although grains up to 2 mm long do occur. Most

PLATE II-2. Clinopyroxene spherulites on weathered surface of a thin flow in Unit II. (Scale: Coin diameter = 30 mm).

crystals are altered to yellow-green clays and oxides along grain boundaries and fractures. Nevertheless, nearly 80% of the olivine in these pillows is fresh.

The groundmass is dark black, hard, and appears glassy. Little fresh glass, however, is actually preserved; most is altered to dark brown smectites. Clinopyroxene microlites are abundant, comprising between 40 and 70% of the groundmass. These microlites exhibit excellent quench morphologies such as radiating trichites and elongate grains with a herringbone structure. Subhedral spinel grains are also common (trace to 4%), both as inclusions in olivine and as grains in the groundmass. Crystals are generally small (<0.20 mm), although phenocrysts up to 0.35 mm in diameter do exist. Plagioclase was not observed in any of the samples studied.

C. Picritic Pillows

Two exposures of picritic pillows occur within Unit II. Both outcrops grade vertically and laterally into typical olivine phyric lavas. Pillows are generally spherical, with diameters ranging from 20 to 60 cm. Individual pillows are often difficult to discern because chilled margins are indistinct. Locally, however, pillow forms are accentuated by the presence of interpillow sediment (see Plate II-3). Unaltered glass is locally preserved along pillow margins,

PLATE II-3. Exposure of picritic pillows in Unit II. Note abundant interpillow sediment. (Scale: Bar = 10 cm).

forming a rind which is never more than 2 mm thick.

Fresh, phenocrystic, olivine is abundant (45 to 65%), and is homogeneously distributed within a single pillow, with only a slight trend of decreasing grain size from core to rim. Grains range from 0.5 to 14.0 mm in diameter, with an average of around 4.0 mm. Crystals are subhedral to euhedral and commonly contain inclusions of spinel and groundmass material. Alteration of the olivine to green-brown clays along fractures and grain boundaries is common.

The groundmass of these pillows is dark brown to black, being largely composed of altered glass. Devitrification of the glassy groundmass is virtually complete, evident from the ubiquitous presence of minute, brown globularites. Clinopyroxene microlites within the groundmass comprise 20 to 30% of most samples. They exhibit rapid growth features similar to those described above, though generally not as well-developed. Anhedral olivine grains are also present, and range in size from incipient crystals to microphenocrysts. Subhedral, dark red to black spinel grains averaging 0.20 mm in diameter are found in minor amounts (trace to 4%).

D. Picrite-based Flows

Throughout Unit II, massive to thin flows with picritic bases are abundant. Thicknesses are extremely variable (from

1 to 30 m), and many of the thicker flows can be traced laterally for over 200 m. In the thinner flows (< 5 m), most olivine is concentrated in the lower one-half of the flow, though it can also be found in the upper portions as well. In the thicker flows, on the other hand, virtually all of the olivine is found in the lower one-third of the flow and there is a sharp boundary between the lower "picritic" zone and the overlying aphyric portion of the flow.

Flow surfaces are highly irregular, and generally indiscernable. It is common for the massive flows to grade both vertically and laterally into "megapillows" (diameters > 4 m), and eventually, into typical pillows. (Similar megapillows have been described by Schminke et al. (1983) in the Akaki canyon and are thought to be feeders for the surrounding pillows).

A cross section of one of the thicker flows is shown in Figure II-2. In general, there are four distinct lithologic zones in these flows: 1) a picritic base, 2) a "transition" zone, 3) an aphyric flow interior, and 4) an olivine phyric, oxidized flow top.

The picritic base is distinct, being dark green to black in color, and relatively resistant to weathering. The basal chilled margin, when exposed, is 5 to 30 cm thick and only moderately olivine phyric. Columnar jointing is invariably present, but poorly developed. Layering on the 5 to 10 cm

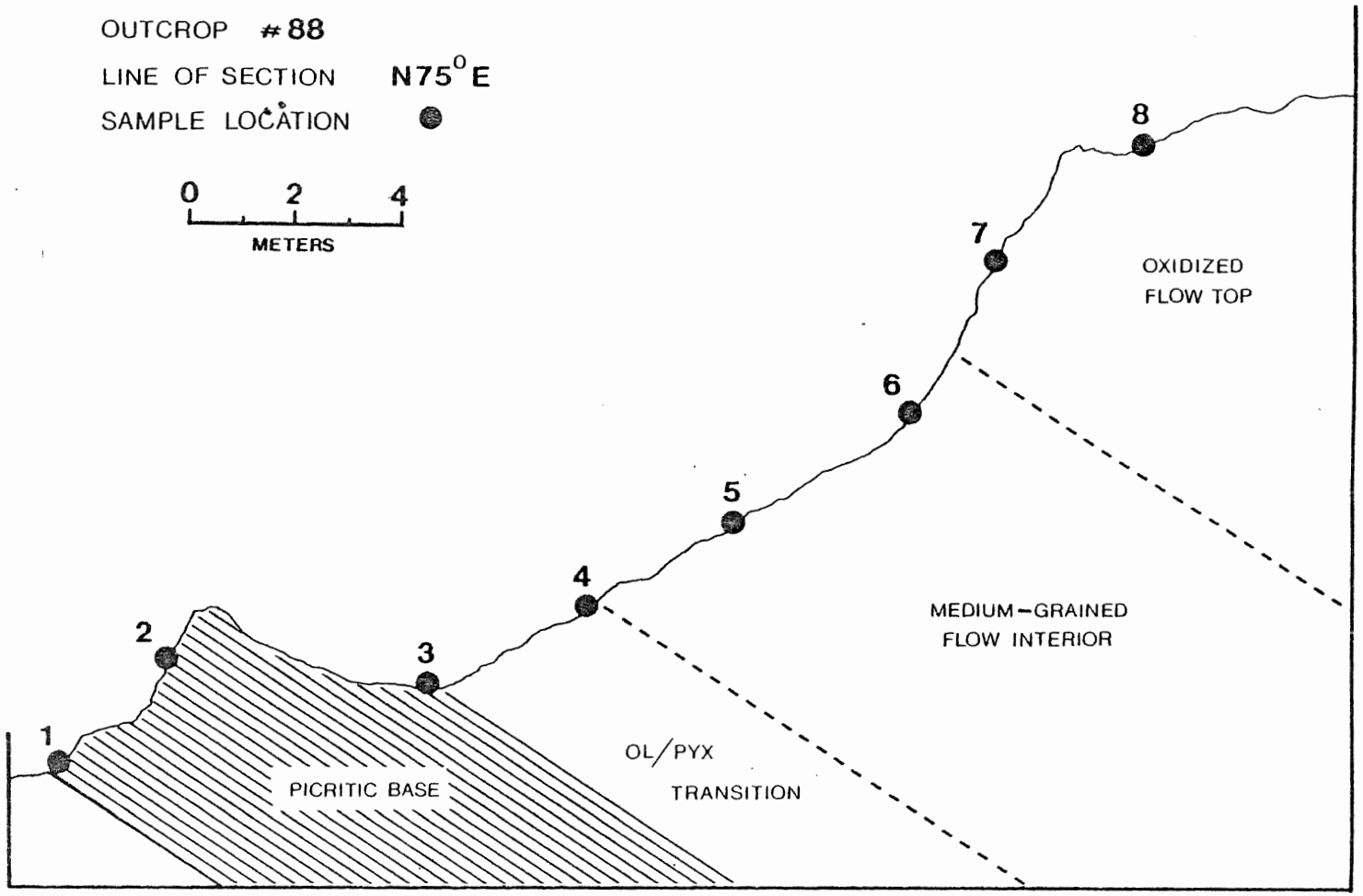

FIGURE II-2. Cross-section traverse across a picrite-based massive flow showing schematic lithologic variations.

scale is also observed, reflecting minor variations in the size and modal abundance of the mineral phases.

Samples from this basal zone are composed of anywhere from 20 to 60% olivine, though most specimens average around 40 modal percent. Olivine grains are subhedral to rounded, with an average diameter of approximately 2.0 mm. Inclusions of spinel and groundmass material are common, and a few of the larger grains are strained and exhibit broad kink-bands. Alteration of the olivine ranges from 10 to 80%, with grain boundaries and fractures being the first areas to be replaced by light green clays and serpentine group minerals.

Clinopyroxene is also present in the flow bases, comprising from 5 to 25% of most samples. Grains are subhedral and elongate, with an average diameter of 0.40 mm. These pyroxenes are predominantly diopsidic augites, although trace amounts of Ca-poor pyroxenes are found overgrowing rounded olivine grains.

Plagioclase grains (4 to 12%), vary in size from minute needles to large laths which reach 2.0 mm in length. The larger grains are often intimately intergrown with pyroxene and strongly zoned. Groundmass and opaque inclusions are ubiquitous, especially within grain cores. Subhedral spinel grains occur with an average abundance of approximately 2%.

The transition from the picritic base to the central portion of the flow is often marked by a relatively thin

"transition" zone, in which clinopyroxene replaces olivine as the dominant ferromagnesium phase.

The central portion of these flows is typically light tan and medium-grained. Subhedral, equant clinopyroxenes comprise up to 45% of samples from this region. Grains average 0.40 mm in diameter, are strongly zoned, and commonly twinned. Minute opaque inclusions are abundant and tend to be zonally distributed. Plagioclase is the only other major phase in this portion of the flow, comprising up to 30% of some samples. Grains are variable in size and shape, typically being anhedral, strongly zoned laths with an average diameter of 0.25 mm.

The transition from the central to the top zone in these flows is gradational. Generally, there is a return to lithologies and textures common to most of the olivine phyric pillows and smaller flow units in the area. Red-brown olivine pseudomorphs are once again present, along with both clinopyroxene and plagioclase microlites. The abundances and average grain sizes of all of these phases, however, are much lower than in the basal portions of the flow.

E. Aphyric Massive Flows

Within Unit II, there are four major exposures of aphyric, massive flows (See Map 1, back pocket). They all occur in the central portion of the unit, though they are

apparently not confined to a single stratigraphic horizon. Thicknesses vary from 3 to 15 m and flows can be traced laterally for up to 150 m. These flows are aphyric throughout, though for purposes of discussion, they will be divided into two portions.

The lower half of a flow is typically brown and medium-grained. Columnar jointing is well-developed, with individual joints ranging in diameter from 50 to 100 cm. Mineralogically, plagioclase is the dominant phase, comprising between 50 and 70% of most samples. Grains are generally subhedral laths (0.20 to 1.20 mm long), are strongly zoned, and exhibit albite twinning. Opaque inclusions are abundant, and alteration along twin planes and grain boundaries is common. Clinopyroxene comprises between 5 and 10% of most samples, although small localized zones along the very base of the flow contain up to 30% as a result of crystal settling. Grains are typically subhedral and equant, with an average diameter of 0.30 mm. Virtually all are optically zoned, and most contain abundant opaque inclusions. The groundmass is totally altered to clays and oxides.

The transition from this medium grained, jointed base to the finer grained flow interior and top is gradational. The uppermost portion of the flow is irregular in form, and light green to gray in color. It is occasionally highly vesicular

(up to 10%), though most flow tops have an average vesicularity of only 3 to 5%. The vesicles are predominantly spherical, and range from 0.2 to 5.0 mm in diameter. The smaller vesicles are completely filled with carbonate and/or clays. Plagioclase is still the predominant primary mineral phase, comprising from 40 to 60% of most samples. Aside from being slightly smaller in size, grains are markedly similar to those in the lower portions of the flow. Likewise, clinopyroxene is slightly less abundant, and grains are smaller than those in the base of the flow. The only other significant petrographic difference between the upper and lower portions of the flow is the higher degree of alteration in the upper portion. Pyroxene and plagioclase grains are difficult to distinguish in samples from this portion, and the groundmass often exhibits a felted texture due to the formation of fibrous secondary minerals. Euhedral grains of secondary quartz are also common, typically found lining large vesicles.

F. Olivine Microphyric Flows

In the lower third of Unit II, three large olivine bearing flows are exposed. These flows are, in many respects, similar to lithologies IIE and IIG, though they are easily distinguished by the presence of olivine. Thicknesses range from 6 to 12 m, and laterally the flows can be traced

up to 100 m. As with most massive flows, the top surface is irregular in form, and highly altered, while the base is less altered and exhibits columnar jointing.

The abundance of olivine in these flows varies from trace amounts to 10% (averaging around 3%), though overall, there is no marked zonation of olivine distribution within a single flow. In the basal portions of the flows, however, grain sizes are larger, and occasional picritic concentrations of olivine and pyroxene do occur. These picrite zones, though, are rarely more than 5 cm thick and 30 cm long.

In general, olivine grains are anhedral to subhedral, 0.25 mm in diameter, and totally altered to smectites and oxides. Pyroxenes are also present, but abundances are difficult to determine due to the effects of alteration. Generally, they comprise from 10 to 20% of most samples, and have an average diameter of roughly 0.20 mm. They are anhedral and elongate, and are commonly intergrown with plagioclase and olivine. Plagioclase (20 to 40%), occurs as subhedral laths which are strongly zoned and have an average diameter of 0.25 mm.

G. Clinopyroxene Microphyric Flows

At the very base of Unit II, flows with thick basal concentrations of clinopyroxene microphenocrysts are exposed.

These flows range from 5 to 15 m in thickness, and can be traced along strike for up to 80 m. Columnar jointing is poorly developed in the bases of these flows, with joints averaging 50 cm in diameter. Layering on the 5 to 10 cm scale, however, is well developed and easily observed in the field. The upper portions of these flows are poorly preserved, but when present, they are fine-grained, aphyric, and moderately vesicular (3 to 6%).

There is a wide variation in modal mineralogy within a single flow, but these variations are gradational. Thus, it is not useful to divide these flows into distinct zones as was done for the picritic flows. In general, flow bases are dark green to brown, and contain from 20 to 40% clinopyroxene. Grains are equant and subhedral, with diameters averaging around 0.20 mm, although occasional grains up to 1.0 mm long do occur. Plagioclase is the only other important phase, comprising around 30 to 40% of most basal samples. Grains are poorly formed, strongly zoned laths, with an average diameter of 0.20 mm. Many of the pyroxene and plagioclase grains are slightly altered, while the surrounding groundmass is totally altered to clays and oxides. Olivine was not identified in any of the samples from these flows. From the bottom to the top of the flow, there is generally a decrease in the total abundance of clinopyroxene, and a corresponding increase in the relative

abundance of plagioclase.

H. Interlava Breccias and Sediments

Pillow breccias are not common within Unit II, with only one major breccia zone being observed. This zone occurs along the major NW - SE trending fault in the central portion of the field area (see Map 1; back pocket). The breccia is composed of angular. slightly olivine phyric basalt fragments (1 to 10 cm in diameter), enclosed in an off-white, carbonate and smectite matrix. The breccia zone averages 3 m in thickness, and grades downward into an extensively veined pillow pile. This pillow breccia zone is distinct, forming a pronounced topographic ridge which is light yellow-brown in color. Smaller breccia zones do occur throughout the unit, but all are of only minor extent.

Thin hyaloclastite layers are most common at the top and base of the unit. Most hyaloclastite layers are less than 1.0 m thick and are of very limited lateral extent. Angular glass fragments (2 to 20 mm in diameter), are suspended in a matrix of clays, smectites, and carbonates. The glass fragments themselves are totally altered to light green smectites. The abundance of hyaloclastite in Unit II is difficult to determine because these layers are easily eroded, and thus, poorly exposed.

Sedimentary material occurs locally among the extrusive

rocks of Unit II. The most widespread is a light yellow, ferruginous material that commonly fills interpillow interstices. It is common in the uppermost portion of the unit, being found amongst the olivine phyric pillows (lithology II-A), and the picritic pillows (lithology II-C)(See Plate II-3). XRD analysis of two samples revealed a compositon of predominantly calcite and iron hydroxides.

2.2.3 Unit III

The transition from Unit II to Unit III is distinct, marked not only by an abrupt decrease in modal olivine concentrations, but also by an increased amount of clinopyroxene microphenocrysts in the volcanic rocks. Fresh glass and hyaloclastite material are also more abundant in Unit III.

The extrusives in Unit III are predominantly pillowed, and show a sharp transition from aphyric to sparsely olivine phyric lithologies approximately half-way through the unit. Unit III is on the order of 50 m thick, and is overlain by a thick sequence of sedimentary rocks.

A. Aphyric Pillows and Thin Flows

The olivine phyric lavas of Unit II are directly overlain by essentially aphyric volcanics. In some areas this change is quite rapid, while in others it is

gradational.

The pillowed extrusions are highly variable in both color and size, typically having light green-gray interiors, and tan to red-brown margins. Pillow diameters range from 30 to 250 cm. with an average of roughly 1 m.

Thin (0.2 to 3.0 m), aphyric flows are commonly found amongst these pillows. They are green-gray, and tend to be hard and coherent compared to the surrounding pillows. Vesicles, 0.3 to 5 mm in diameter, are concentrated in the upper one-third of the flow (up to 10%), and are predominantly spherical. They are commonly filled or lined with calcite and smectites.

In thin section, olivine grains are found in trace amounts. When present, they are small (<0.30 mm), anhedral, and totally altered. The groundmass of most samples is composed largely of brown smectites and clays. Small equant grains of clinopyroxene, along with plagioclase microlites are often present, and they occur in roughly equal proportions; typically around 10 to 15 modal % each. It should be noted, though, that the actual amounts are highly variable and difficult to determine due to the effects of alteration.

B. Sparsely Olivine Phyric Pillows and Thin Flows

The aphyric lavas in the lower portion of Unit III gradually give way to slightly olivine phyric pillows and thin flows. The olivine phyric pillows are generally yellow-tan, although red-brown, highly oxidized pillows are also common. Finer-grained pillow margins (2 to 4 cm thick), are more resistant to weathering, and are a distinct light gray color. Pillow diameters range from 25 to 200 cm, and average roughly 75 cm.

Thin flows, (10 to 200 cm thick), are locally abundant, comprising around 25% of the entire unit. Their average lateral extent is not known, but some flows can be traced along strike for at least 30 m. Many of the thinnest flows have developed a ropey, pahoehoe upper surface (See Plate II-4), whereas the thicker flows tend to have a smooth upper surface, a basal accumulation of olivine, and an increase in vesicle size and abundance towards the top of the flow.

The only phenocryst phase observed in the field is olivine. It varies markedly in modal abundance both between and within flow units, being concentrated in pillow cores and flow bases. It ranges between trace and 5 modal %, with an overall abundance of approximately 2%. Phenocrysts are typically subhedral and small, rarely larger than 1.5 mm in length. The average diameter observed in thin section is around 0.35 mm. Alteration of the olivine is complete,

PLATE II-4. "Ropey" pahoehoe upper surface of a thin flow in Unit III. (Scale: Coin diameter ≈ 30 mm).

resulting in yellow-brown pseudomorphs composed of iron and magnesium-rich oxides and clays, along with minor carbonate.

Microphenocrysts of clinopyroxene are also common, comprising up to 8 modal percent of some flow units, but averaging only around 4%. They are typically small, equant grains with an average diameter of 0.25 mm. although phenocrysts up to 1.2 mm long do occur. Most clinopyroxene grains are "cloudy" due to inclusions and varying degrees of alteration.

Typically. the groundmass is totally altered to smectites and sundry oxides. In the less altered samples, however, clinopyroxene microlites are often recognizable in thin section, and can comprise up to 50% of the groundmass. In some pillows, minute grains of plagioclase are also present, and in the thickest flows, plagioclase can make up nearly 20% of the groundmass.

Despite the extensive alteration of the groundmass, fresh glass is commonly found as 4 to 10 mm thick rinds on pillows and flow surfaces (See Plate II-5). In general, glass is preferentially preserved in areas where thick layers of umbers and/or volcanic flows occur above or within the extrusive sequence. Gillis (1984) has suggested that such units partially "cap" and seal off the underlying lavas from the effects of long term. seawater alteration.

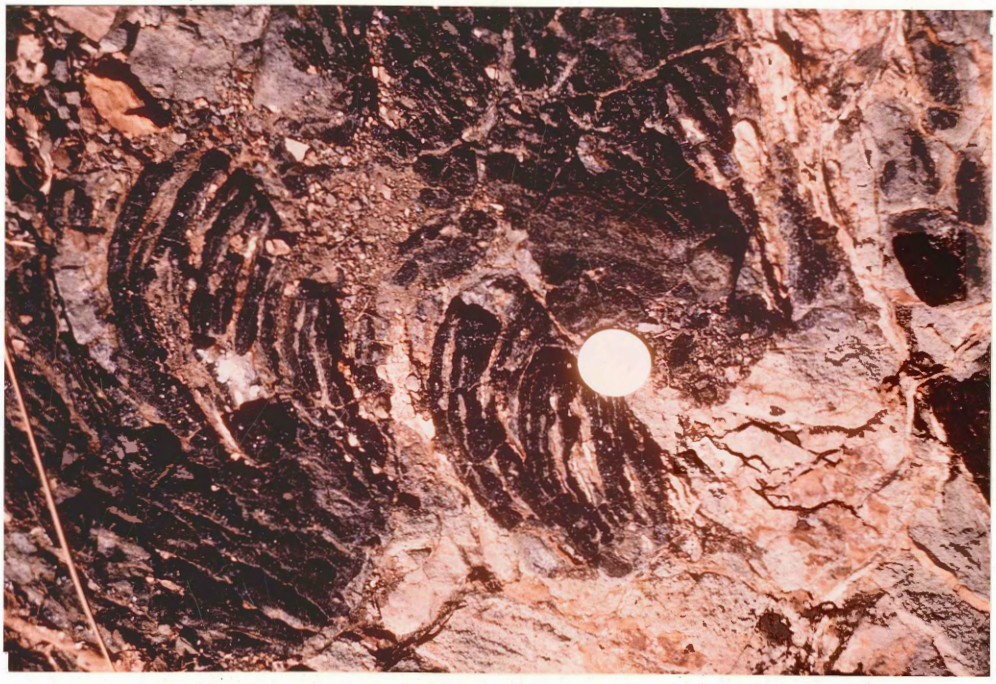

PLATE II-5. Fresh glassy rind on pillow surface in Unit III. (Scale: Coin diameter = 30 mm).

C. Interlava Breccias and Sediments

Pillow breccias and hyaloclastite layers comprise approximately 5% of Unit III, and are concentrated towards the top of the sequence. Pillow breccias range from randomly oriented pillow fragments in a carbonate/clay matrix, to highly fractured and veined pillow piles. Thicknesses are generally on the order of 1 to 5m.

Hyaloclastites are typically thin (< 2 m), poorly sorted layers of altered glass fragments in a matrix of smectite, carbonate, and clay. The total amount of hyaloclastite in this unit is difficult to estimate owing to poor exposures.

Within Unit III, a yellow-orange sedimentary material is found filling open spaces between individual pillows. As noted previously, this material is composed largely of iron oxides and carbonates.

2.3 Overlying Sedimentary Rocks

Where the sedimentary rocks are conformable upon the ophiolite extrusives, it appears that the preferred sequence is pillowed volcanics --> umbers (+/- chert) --> mudstones (+/- chert) --> chalks. (A good example of this sequence is found along the Alykos canyon just north of the village of Margi). It should be noted though, that most of the sediment/ophiolite contacts in the area are either faulted or obscured by overburden. Thus, one should be cautious in

accepting the above sequence as being typical for the massif.

Directly overlying the extrusive rocks of Unit III is a relatively thick layer of umberiferous sediment (0.5 to 5 m thick). The umbers are yellow to dark brown, very fine-grained, poorly laminated and highly hygroscopic. They consist of iron and manganese hydroxides along with various clays, and are commonly fractured and contain thin carbonate and manganese oxide veins.

Lobate bodies of dark brown to black chert are found locally at the base of the umbers. They are generally less than 0.5 m thick and contain thin carbonate veins.

Umbers are abundant all along the northern flank of the Troodos ophiolite, particularly in the Margi-Mathiati area, where mining of the umbers has been extensive. It is interesting to note that in this same area, some of the largest sulfide deposits have been found. This coincidence of major sulfide deposits and abundant chemical sediments has been observed in a number of areas, and some researchers have suggested a genetic relationship between the two (e.g. Boyle and Robertson, 1983).

Overlying the umbers is a layer of finely-laminated, tan to brown mudstone which is 2 to 6 m thick. This mudstone, along with the umbers and cherts, belong to the Perapedhi Formation and have been dated as Campanian in age (Robertson, 1976).

Overlying all of these units, is a thick sequence of calcareous sedimentary rocks. The predominant sedimentary rock in the Margi area is an off-white chalk with pronounced bedding on the 10 cm scale. A weak cleavage is generally developed sub-parallel to bedding. Aside from localized faulting and tilting, these rocks are relatively undeformed, and dip gently to the northeast. These chalks are of Maastrichtian age, and are members of the Lefkara Formation (Robertson and Hudson, 1974).

2.4 Alteration and Distribution of Secondary Minerals

While it is not one of the main objectives of this thesis to explain the styles and types of alteration, it is a feature that cannot be ignored. For, as is evident from the preceding lithologic descriptions, all of the volcanic rocks in the study area have been altered to some degree.

The effects of seawater on rocks of basaltic composition is a subject which has attracted a significant amount of attention in recent years, for it is a process that significantly alters the bulk chemical composition of the ocean crust, and one intimately related to the formation of ore deposits. Many researchers have attempted to classify "stages" or "styles" of alteration on the basis of observed secondary mineral assemblages in DSDP cores (e.g. Cann, 1979; Staudigel et al., 1981). Combined with experimental work on

phase stabilities, these styles or stages are often correlated with discrete temperatures of formation, and categorized as "low temperature assemblages" etc. While temperature is clearly an important parameter of hydrothermal systems, recent literature reveals that there are many other parameters that are perhaps equally as important in controlling the formation of secondary mineral assemblages (e.g. Mottl et al., 1980; Mottl, 1983; Seyfried et al., 1982). Some of these parameters are: initial fluid composition; water/rock ratio; rock compositon and mineralogy; rock permeability; and time. Clearly, the alteration process involves extremely complex physical and chemical systems, and much work remains to be done before the process is fully understood.

Nevertheless, as a first approach to understanding the alteration of rocks exposed in the Margi area, the areal distribution of secondary minerals was examined. The results are summarized in two schematic diagrams. The first (Figure II-3), shows the distribution of secondary minerals with respect to stratigrahic depth, and is based largely on observations made by Gillis during the summer of 1983. Minor changes were made on the basis of field and petrographic observations of the present author. The second diagram (Figure II-4), shows the distribution of secondary minerals with respect to individual cooling unit lithologies. All

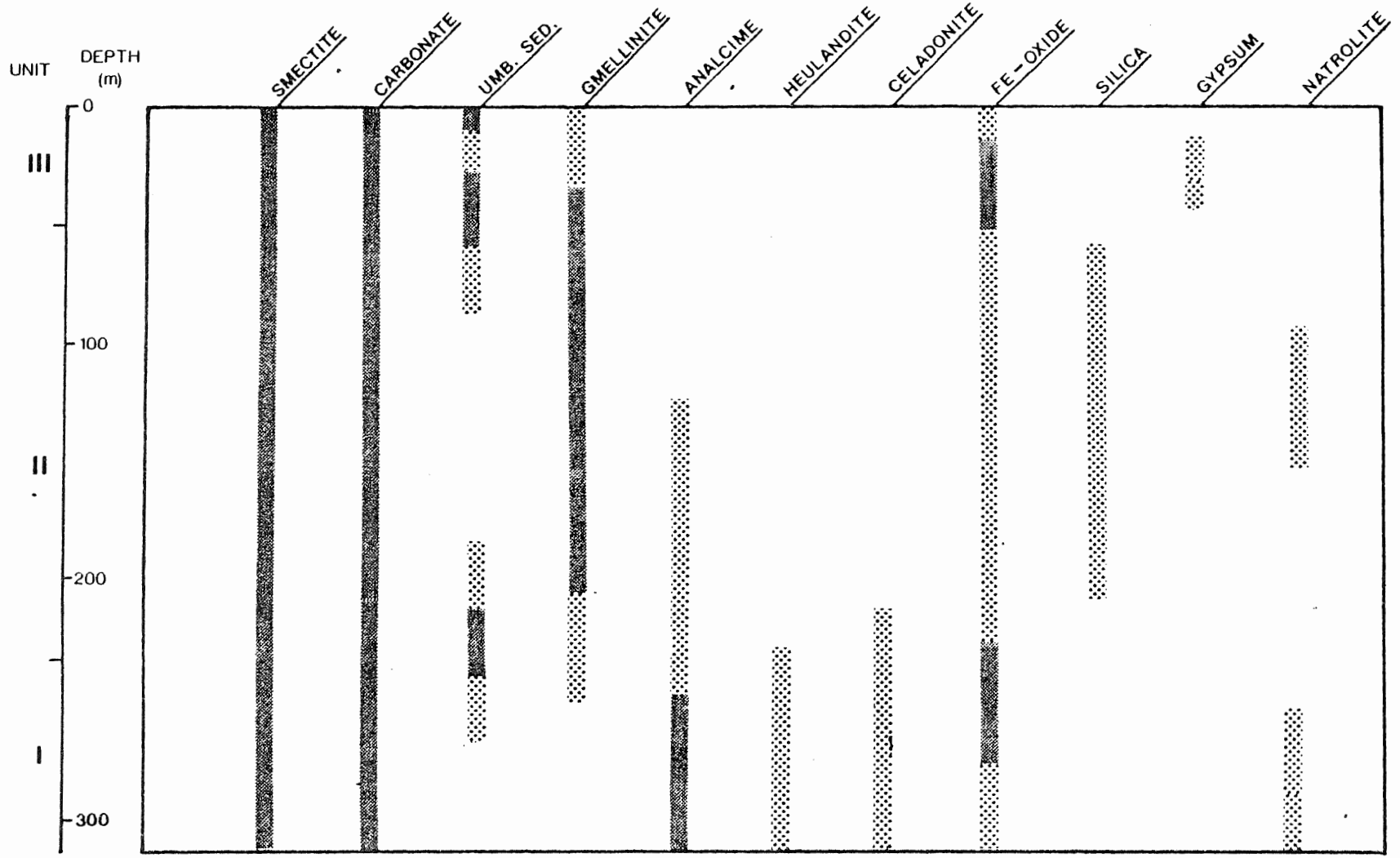

FIGURE II-3. Distribution of secondary minerals with respect to stratigraphic depth. (Grey line = common; dotted line = scarce; no line = not observed)

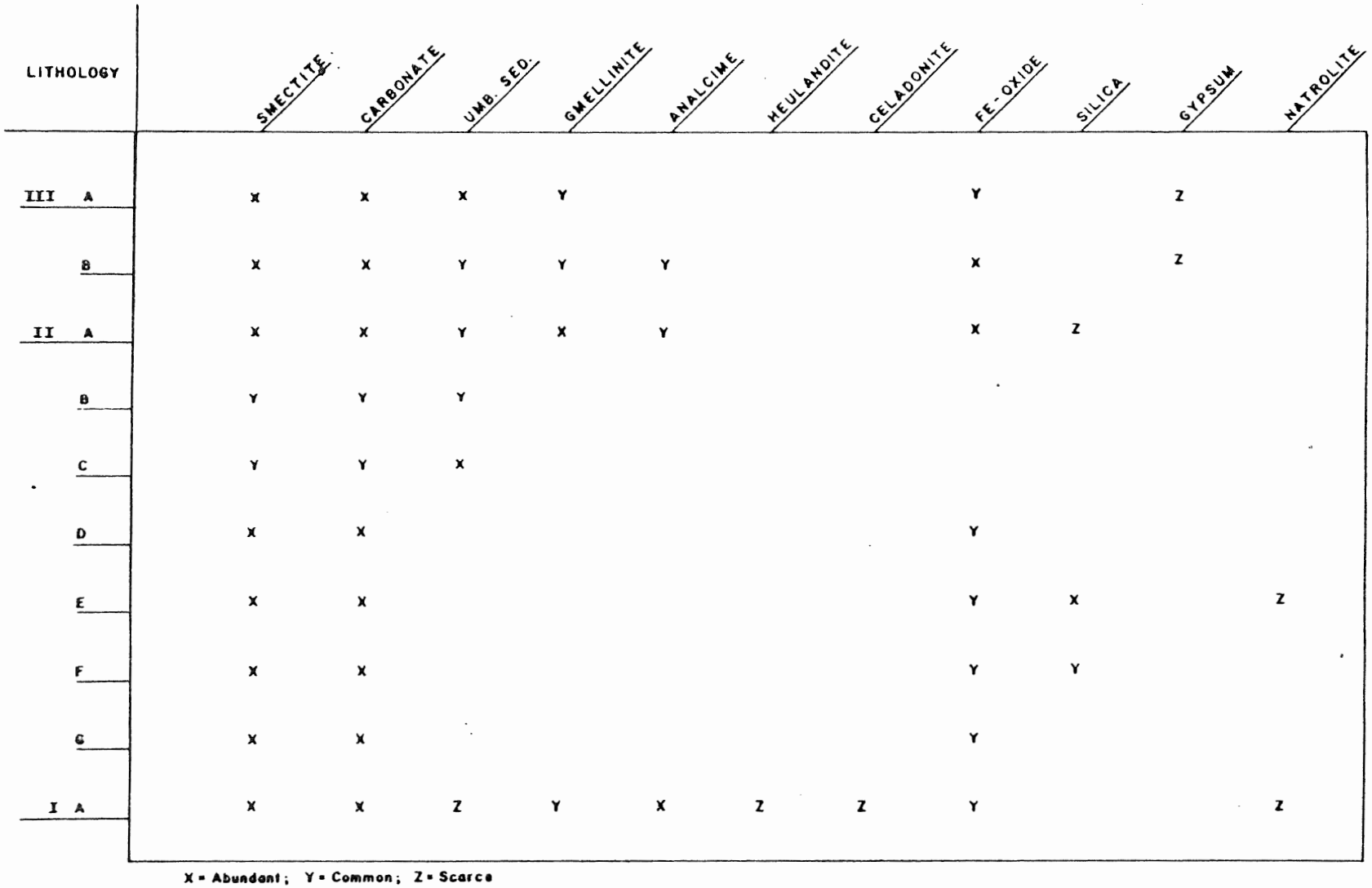

FIGURE II-4. Distribution of secondary minerals with respect to cooling unit lithology.

mineral determinations are based solely on macro- and microscopic observations, although X-ray examinations are currently underway at Dalhousie University (Gillis, in prep.).

A short summary of these diagrams follows.

Smectite and carbonate, while irregularly distributed, are found throughout the sequence and in virtually all lithologies.

Gmelinite and analcime are the two most common zeolites, being found in most pillow units (except lithologies II-B and II-C). Natrolite and heulandite are the only other zeolites observed, though they are both quite scarce. Natrolite is found in the aphyric flows of Unit II (lithology II-E), and in the more coherent pillows of Unit I. Heulandite, on the other hand, is found only in the pillows of Unit I.

Celadonite is uncommon, occuring primarily in the vicinity of intrusives in Unit I.

Secondary silica (quartz), is observed only in thin section, and occurs as subhedral grains within vesicles, or as anhedral grains in the groundmass of massive flows, and rarely, the pillows of Unit II.

Potassium feldspar (adularia), is similarly observed only in thin section, typically replacing plagioclase cores in samples from thick flows and pillows of Unit II.

Gypsum is found in thin veins cutting through the rocks

of Unit III. These veins are rarely over 1.0 cm wide, and they are found only in the easternmost portion of the field area.

Interlava umberiferous sediments are found throughout Unit III, and at the top of Unit II. Related ferruginous material is also common amongst the picrite pillows (lithology II-C).

Secondary iron oxides are irregularly distributed throughout all units. Flow tops and pillow margins are generally the most oxidized portions of individual flow units.

In summary, the following four points are stressed:

1) Smectite, carbonate, and iron-oxides are virtually ubiquitous.
2) Gmelinite and analcime are the most common zeolites, with gmelinite predominant in Units II and III, and analcime predominant in Unit I.
3) Lithologies IIB and IIC are unusual in that they are little altered and contain few secondary minerals.
4) The rocks of Unit I are extensively altered and exhibit the widest range of observed secondary minerals.

Clearly, there are variations in the secondary mineral assemblage which coincide with discrete stratigraphic depths and lithologic types. Whether these are the controlling

parameters, however, can not be easily ascertained.

Nevertheless, the overall secondary mineral assemblage is one typical of oceanic basalts which have undergone low-temperature, seawater alteration (or submarine weathering) (Cann, 1979; Honnorez, 1981). Following the definition of Honnorez (1981), low temperature alteration comprises both diagenesis and the beginning of zeolite facies metamorphism; suggesting maximum temperatures of only 100oC. So while the process of alteration is, in detail, extremely complex, we can at least conclude that in the Margi area, the process was predominantly one of low temperature basalt/seawater interaction.

It should be noted, that the observed secondary minerals and their relative abundances are markedly different in other portions of the ophiolite extrusive sequence. It is suggested that the unusually thick cover of umbers, and/or the high percentage of massive flows in the Margi area are responsible for significantly influencing the conditions of alteration, and in turn, for producing the observed secondary mineral assemblage (Gillis, 1984).

2.5 Fault Stages

In the mapped area, two distinct phases of faulting were observed (See Map 1; back pocket). The oldest stage trends NW-SE, and dips 60 to 80o to the southwest. Correcting for

the regional tilt of the volcanic pile and the overlying sedimentary rocks (approx. 25°E), reveals that these faults were originally close to vertical, and sub-parallel to the trend of dikes in the surrounding area. These faults cut only the extrusive units, and are best exposed in Unit II. Vertical offset along these faults is difficult to determine, but for the major fault in the central portion of the field area, it is roughly estimated at 150 m. This estimate is based on the location of "glassy" olivine phyric pillow outcrops, for this is the only lithology cut by the fault that is distinctive and appears to occur at the same stratigraphic level throughout the sequence. These faults form prominant topographic ridges associated with zones of extensive brecciation. Carbonate and smectite veining is abundant in the surrounding rocks.

The second stage of faulting is a much later event, cutting through both the extrusive rocks and the overlying sedimentary rocks, forming many of the basalt/sediment contacts. Unfortunately, these faults are poorly exposed, tending to form topographic lows. Generally, there are two distinct sets of these faults; one trending N-S, and the other trending roughly E-W. On the basis of jointing patterns in the surrounding chalks, dips are estimated as being nearly vertical (+/- 10°).

Boyle and Robertson (1983), claim to have observed two

distinct phases of normal faulting that predate the formation of the pelagic sediment cover in the Margi area. The earliest phase, or "type 1" faults, trend NW-SE, and displace only the lavas of Unit I (their Units A and B). The later phase, or "type 2" faults, trend predominantly N-S (and occasionally NW-SE), displace type 1 faults, and formed during eruption of Units II and III (their units C and D). Evidence for the earlier phase of faulting is not observed in the mapped area, but this is most likely a result of the limited exposure of Unit I in the area atudied. The NW-SE trending faults described in this study therefore correspond to the "type 2" faults of Boyle and Robertson, 1983). It is perhaps significant that they follow the general trend of both the dikes and the "type 1" faults, and not the N-S trend of most "type 2" faults described by Boyle.

The N-S (and E-W), trending faults observed in the Margi area are much later. post-sediment faults, perhaps related to the uplift and/or emplacement of the entire Troodos Massif. Many of these may simply be reactivated "type-2" faults.

2.6 Summary

A synthesis of the major stratigraphic and structural features of the extrusive sequence in the Margi area follows:

1) A thick sequence of aphyric to clinopyroxene and plagioclase microphyric lavas (Unit I), were extruded as

pillows and thin flows. "Type 1" normal faults were presumably active throughout this period of extrusion (Boyle and Robertson, 1983).

2) A significant hiatus in volcanism followed, during which the uppermost portion of the Unit I extrusives underwent extensive sea-floor weathering. The relatively continuous horizon of mudstones and umbers located between Units I and II formed during this hiatus.

3) Volcanism resumed sporadically, with the extrusion of slightly olivine phyric pillows and thin flows. Massive olivine and clinopyroxene microphyric flows formed locally amongst these pillows (lithologies IIF and IIG, respectively). As volcanism proceeded, the slightly olivine phyric lithologies gave way to more olivine-rich (and clinopyroxene-poor), pillows and flows. (It should be noted that the aphyric massive flows (lithology IIE), are the only major exception to this generalization.) Massive flows, and in particular, flows with picritic bases, became more abundant.

4) As volcanism continued, the abundance of massive flows rapidly decreased, leaving olivine phyric pillows as the dominant lithology. Interpillow sediment became more common, and hyaloclastite layers much more extensive.

5) The glassy olivine phyric pillows (lithology IIB) represent a small "spurt" of volcanic activity prior to the

extrusion of Unit III lavas. The sharp boundary between Units II and III, along with the abundance of hyaloclastite in this portion of the extrusive sequence suggests another short break in volcanicity.

6) Volcanism resumed with the extrusion of aphyric pillows and thin flows (lithology IA), followed by the extrusion of slightly olivine phyric lithologies (lithology IB).

7) Volcanism ceased, and the extrusive sequence was quickly covered by umberiferous sediments and pelagic chalks.

8) Finally, the entire sequence was cut by N-S and E-W trending normal faults which accompanied the uplift (+/or emplacement) of the entire massif, and the topography was shaped by subaerial erosion.

CHAPTER THREE

MINERAL FORM AND CHEMISTRY

3.1 General Statement

Four primary mineral phases occur in the extrusive rocks of the Margi area. These are olivine, pyroxene, plagioclase, and spinel. Variations in the morphology, composition, and alteration of these phases are described below. All chemical analyses were obtained using an energy dispersive microprobe system at Dalhousie University (see Appendix IV for complete listing of analyses).

3.2 Olivine

Olivine is the dominant phenocryst phase in Units II and III, though its distribution is highly irregular. Pillows and massive flows both exhibit ranges in olivine contents from 0 to over 50 modal percent. This wide range in abundance is significant, for it indicates the complexity of volcanic processes that formed these rocks.

Over 80% of the olivine in the pillowed extrusions has been replaced by smectites, iron oxides / hydroxides, and carbonates during subaerial and seafloor weathering. In the picritic units (particularly in the massive flows), olivine grains are partially altered (10 to 60%) along grain boundaries and fractures to smectites and serpentine group

minerals which range in color from straw-yellow to olive-green. Minor fine-grained, disseminated magnetite is commonly associated with these grains.

Fresh olivine is preserved primarily in the picritic lithologies, and in the "glassy" olivine phyric pillows. Grains in the lower parts of the large picrite-based flows range in size from 0.2 to over 12.0 mm in diameter, but average only around 2.5 mm (see Plate III-1). Original grain forms are difficult to discern due to alteration along the margins, however, subhedral to rounded grains appear to be the most common. In the picritic pillows, however, grains are less altered, and are typically euhedral in form (see Plate III-2). Inclusions of spinel and groundmass material are common in the larger grains of both the pillows and massive flows.

Interestingly, some grains exhibit broad "kink-bands" (See Plate III-3). Such banding is commonly observed in olivines of mantle peridotites (Augistithis, 1978), and has been shown to be the result of high-temperature dislocation creep (Poirier and Nicolas, 1976; Kohlstedt et al., 1976).

Approximately 100 analyses of olivines were obtained from these lithologies. Compositions are generally Mg-rich (up to Fo 93), and many grains contain traces of Ni, Mn, Ca, and Cr (see Table III-1 for representative analyses).

Olivine grains from the picritic lithologies show

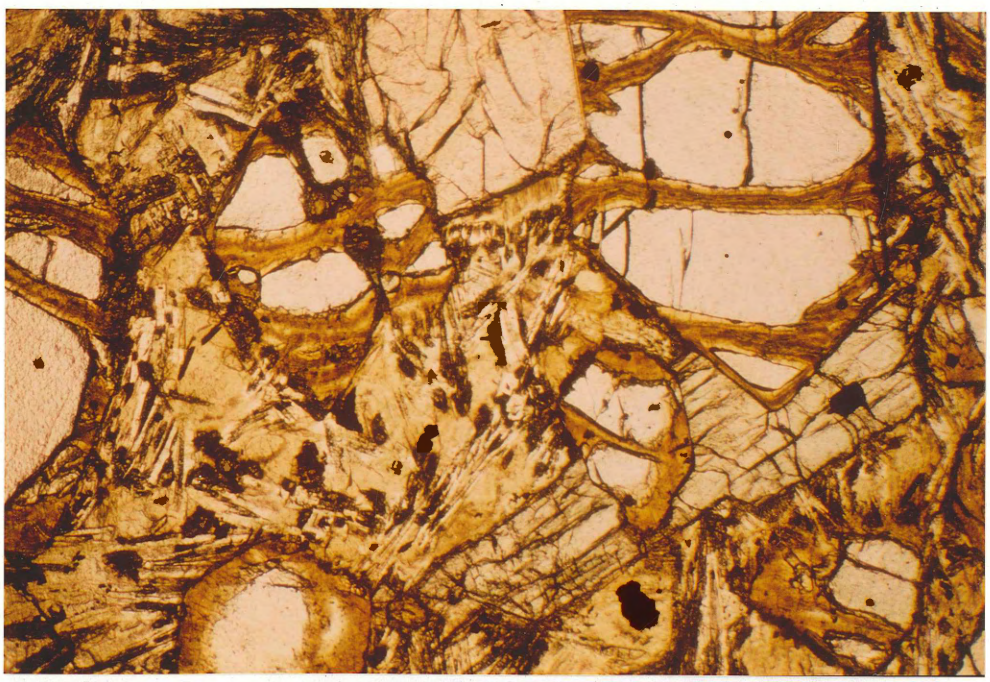

PLATE III-1. Subhedral olivine and clinopyroxene in picritic flow base. Note alteration of olivine along margins and fractures. (Sample #53; plane light; 40X).

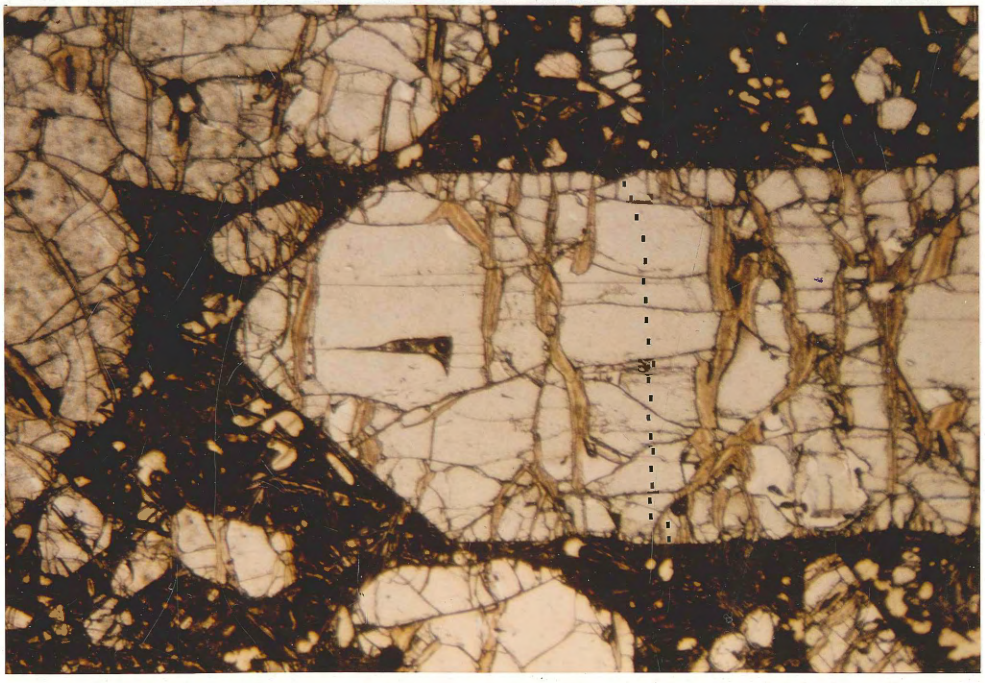

PLATE III-2. Large sub- to euhedral olivine phenocrysts in a glassy matrix which contains quench microlites of clinopyroxene. Location of microprobe traverse (Figure III-1) marked by dashed line. (Sample #127; plane light; 15X).

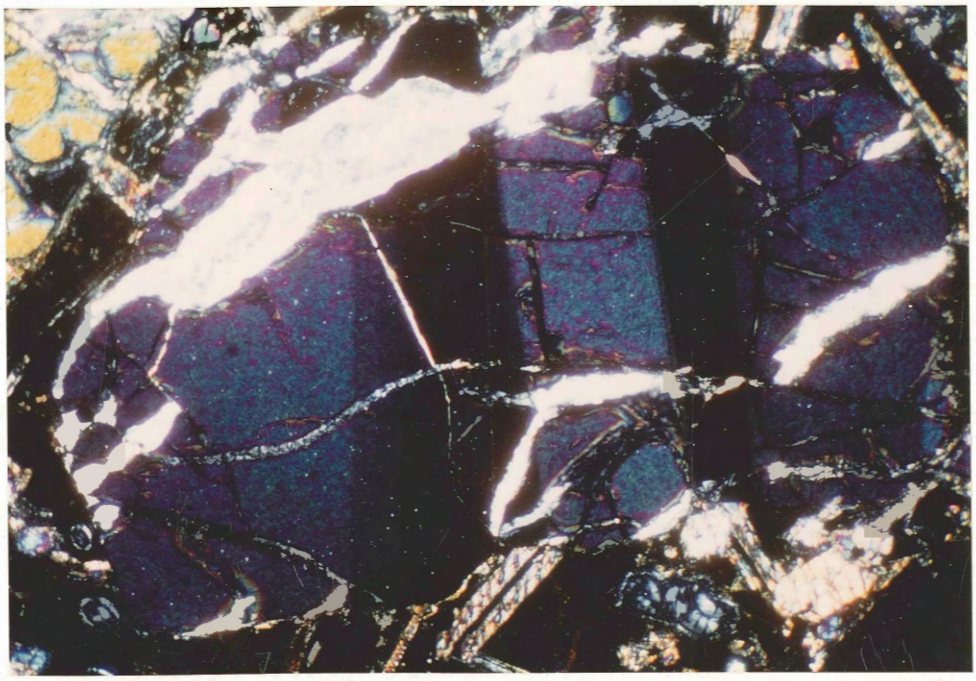

PLATE III-3. Olivine phenocryst in picritic flow base exhibiting broad, subparallel, "kink bands". (Sample #44; X-nicols; 40X).

TABLE III-1 Representative olivine analyses

Sample #	99-5	53-2	10-3	35-1	83-5	86-6
SiO2	40.12	39.73	39.66	39.31	38.99	38.65
FeO*	7.99	9.35	10.75	11.50	12.88	15.23
MnO	0.05	0.04	0.11	0.04	-	0.23
MgO	50.50	49.33	48.80	48.75	47.02	45.19
Cr2O3	0.19	0.11	0.05	-	-	-
NiO	0.29	0.18	0.22	0.11	0.08	0.05
CaO	0.20	0.15	0.18	0.07	0.14	0.18
TOTAL	99.35	98.90	99.77	99.79	99.12	99.54
MINERAL FORMULA (on basis of 4 oxygen)						
Si	0.986	0.986	0.982	0.976	0.981	0.980
Fe2+	0.164	0.194	0.223	0.239	0.271	0.323
Mn	0.001	0.001	0.002	0.001	-	0.005
Mg	1.851	1.825	1.801	1.804	1.763	1.707
Ni	0.006	0.004	0.004	0.002	0.002	0.001
Ca	0.005	0.004	0.005	0.002	0.004	0.005
Σ(Tet.)	0.986	0.986	0.982	0.996	0.981	0.980
Σ(Oct.)	2.027	2.028	2.035	2.048	2.040	2.041
Atomic Ratios						
Mg/(Mg+Fe)	0.92	0.90	0.89	0.88	0.87	0.84
Fe/(Mg+Fe)	0.08	0.10	0.11	0.12	0.13	0.16

99-5) Phenocryst core/ Picritic flow base
53-2) Phenocryst core/ Picritic flow base
10-3) Phenocryst core/ "Glassy" olivine phyric pillow
35-1) Phenocryst core/ "Glassy" olivine phyric pillow
83-5) Groundmass grain/ Picritic flow base
86-6) Groundmass grain/ Olivine phyric pillow
(FeO*=Total iron)

considerable chemical variation, and within a single sample, there is often a bimodal distribution of compositions. Large phenocrysts are generally homogeneous, and exhibit little chemical zonation (See Figure III-1). Smaller, poorly formed groundmass grains and phenocryst rims, however, are commonly poorer in magnesium compared to these phenocrysts (e.g. Fo 88 vs. Fo 92). Overall, olivines from the picritic lithologies span a range of composition from Fo 86 to 93 (See Figure III-2).

Fresh olivine also occurs in the "glassy" olivine phyric pillows (lithology IIB) and in a few pillow margins of lithologies IIIA and IIA. These grains are typically skeletal to subhedral, and range in size from phenocrysts (up to 2.5 mm in diameter), to incipient groundmass grains (see Plate III-2). Margins of these grains are commonly altered to yellow-brown smectites and oxides, and many contain minute spinel inclusions.

Compositionally, these grains are iron-rich compared to those of the picritic units, with Fo values ranging from 83 to 89 (see Figure III-2). This entire range of compositions may be present within a single sample, though phenocryst compositions are generally between Fo 87 and Fo 89.

The wide range of olivine compositions in the samples studied is an indication of marked differences in the conditions of crystallization. Petrographic features of the

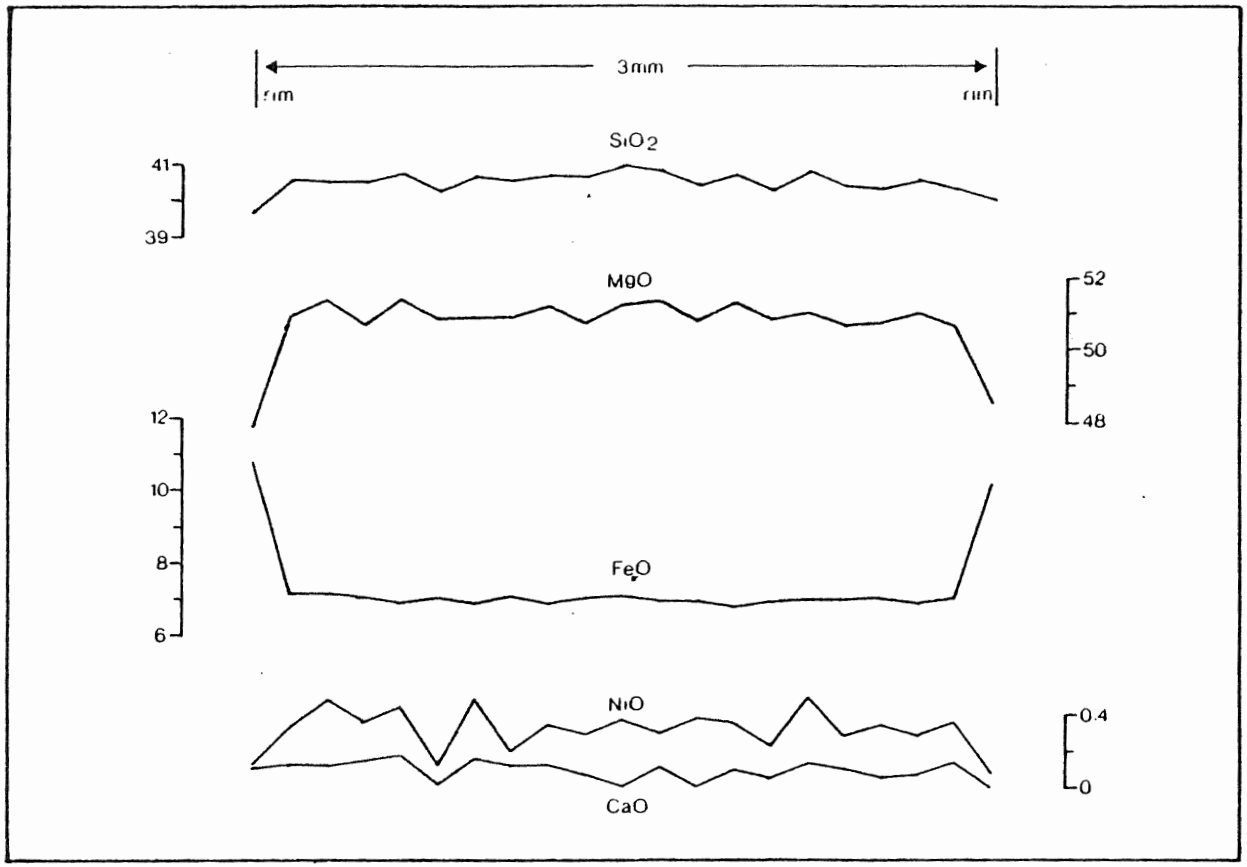

FIGURE III-1. Microprobe traverse across a large olivine phenocryst in a picritic pillow. (See Plate III-2 for location of traverse). Composition of the grain interior is Fo 92; rim composition Fo 88/89.

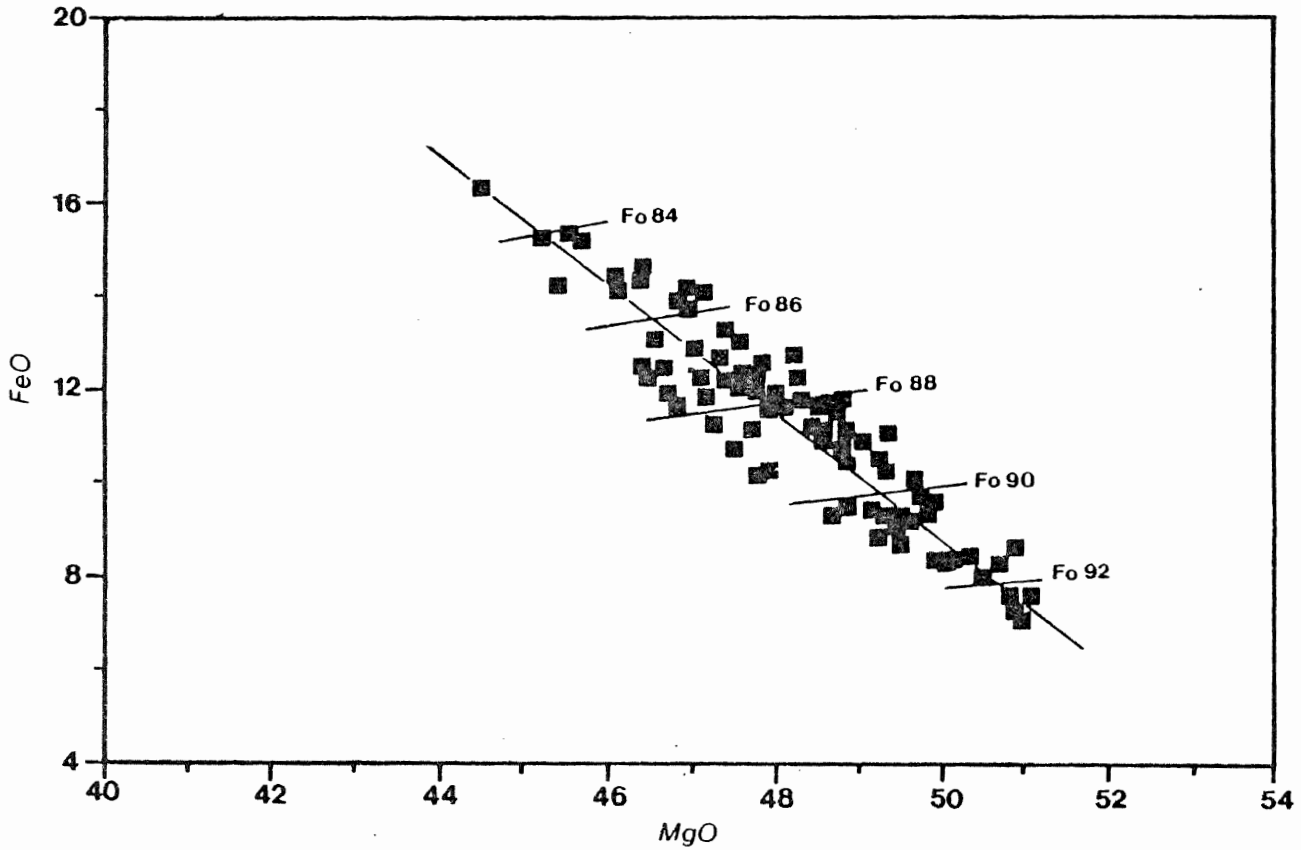

FIGURE III-2. FeO vs. MgO variation in olivines from the Margi area. (FeO = Total Iron).

large olivine grains in the picritic units (e.g. spinel inclusions, kink-bands, and rounded grain boundaries), along with their high Fo content, suggest that they crystallized from magnesium-rich liquids at relatively high temperatures, and that they are not in equilibrium with the melts in which they were extruded. Conversely, the relatively iron-rich grains found in the surrounding pillows appear to be liquidus phases at the time of extrusion. A closer examination of olivine-liquid equilibria will follow in Chapter Five.

3.3 Pyroxene

Calcium-rich clinopyroxene is the second most abundant phase observed in the volcanic rocks of the Margi area. Large phenocrysts are rare, however, microphenocrysts ranging from 0.2 to 0.6 mm in diameter are common. As with olivine, the distribution and abundance of clinopyroxene is highly variable. In general, distinct, subhedral clinopyroxene microphenocrysts are most common in the rocks of Unit I, the lower portion of Unit II, and the upper portion of Unit III. They are conspicuously absent from lithologies IIB and IIC. Groundmass microlites are abundant in almost all samples, typically exhibiting rapid growth and quench morphologies in the glassy groundmass of pillowed units (see Plate III-4).

Clinopyroxene grains within the picrite-based flows (lithology IID) are quite variable in abundance and form.

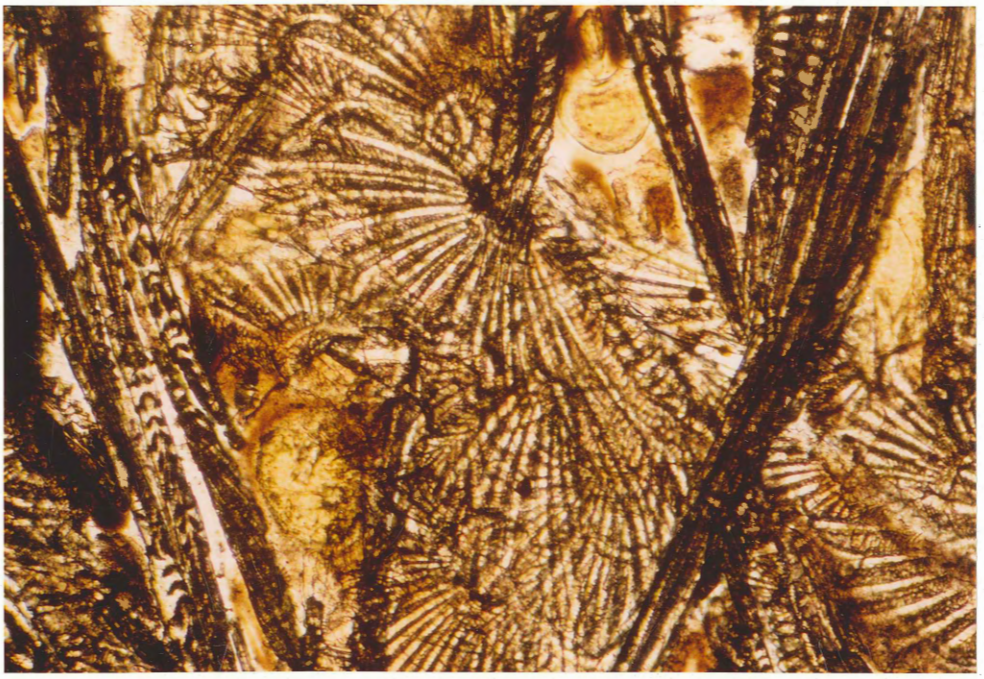

PLATE III-4. Groundmass clinopyroxene in "glassy" olivine phyric pillow. Radiating trichites and herringbone morphology indicative of rapid cooling. (Sample #38; plane light; 150X).

They make up 5 to 20% of the rock in the lower parts of the flows, are typically elongate to bladed in form, and vary from 0.1 to 3.0 mm in diameter (see Plate III-1). Calcium-poor pyroxenes are occasionally found in these zones as minute grains (<0.20 mm) rimming larger Ca-rich pyroxenes, or olivines.

In the aphyric, massive flows, clinopyroxene typically occurs as subhedral to euhedral, strongly zoned, equant grains which range from (0.20 to 1.00 mm) in diameter (see Plate III-5).

Fresh pyroxenes suitable for microprobe analyses were found in all of the lithologies studied, except those of Unit I. Samples from this unit are extensively altered and most pyroxene grains are replaced by smectites and oxides. Pyroxene analyses from similar lithologies in the Pedios area (from Mehegan, unpub. data.), are therefore used for comparison.

Major element compositions of over 200 pyroxenes are listed in Appendix IV. Representative analyses are shown in Table III-2. Variation diagrams (Figure III-2 a+b), clearly show four groups of pyroxene compositions.

Type 1: Ca/Mg-rich clinopyroxenes

This is the most common composition of pyroxene phenocrysts and microphenocrysts in rocks from nearly all lithologies in Units II and III. There is a range in

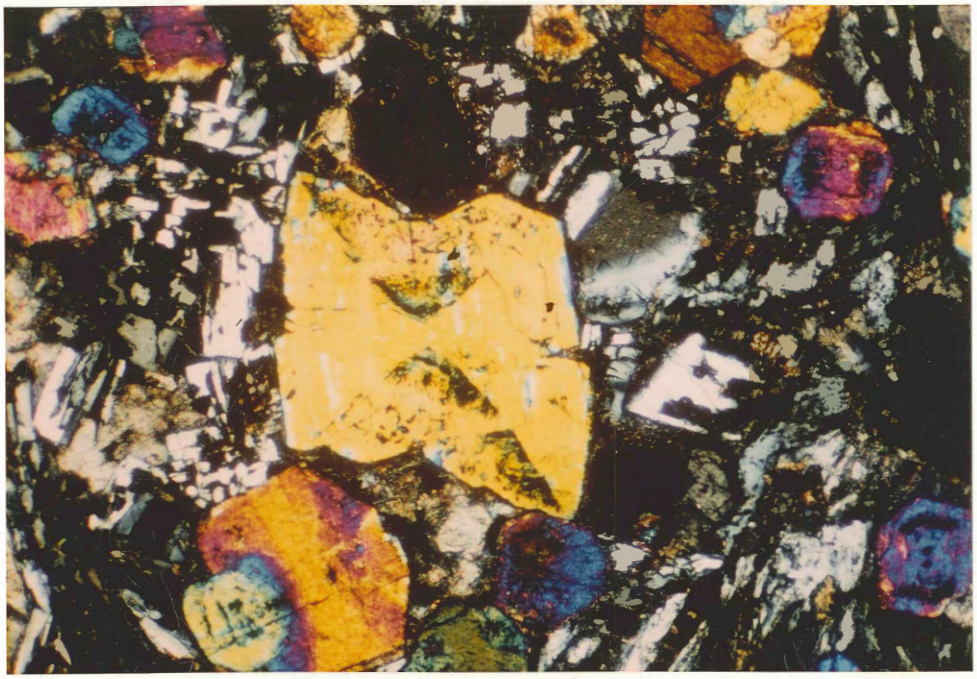

PLATE III-5. Clinopyroxene (and plagioclase) in medium-grained flow interior. Note strong optical zonation and abundant inclusions. Large grain in center exhibits "hourglass" zonation of inclusions. (Sample #120A; X-nicols; 46X).

TABLE III-2 Representative pyroxene analyses

Sample #	35-6	121-5	162-1	14-7	136-10	83-4
SiO2	46.06	48.35	50.50	52.83	53.21	54.62
TiO2	0.89	0.96	0.46	0.18	0.28	0.15
Al2O3	11.05	7.75	5.32	2.61	2.33	1.27
Cr2O3	-	0.14	0.31	0.48	0.52	0.33
FeO*	11.16	6.92	6.13	5.71	5.90	5.16
MgO	10.55	12.51	14.75	16.90	18.16	18.55
CaO	20.20	23.05	22.09	20.76	19.16	19.75
TOTAL	99.90	99.67	99.57	99.47	99.57	99.82
MINERAL FORMULA (basis of 6 oxygen)						
Si	1.731	1.800	1.868	1.941	1.945	1.983
Al	0.269	0.200	0.132	0.059	0.055	0.017
Al	0.220	0.140	0.099	0.054	0.046	0.038
Ti	0.025	0.027	0.013	0.005	0.008	0.004
Fe2+	0.351	0.215	0.190	0.175	0.180	0.157
Mg	0.591	0.694	0.813	0.925	0.990	1.004
Cr	-	0.004	0.009	0.014	0.015	0.009
Ca	0.813	0.920	0.875	0.817	0.751	0.768
Σ(Z)	2.000	2.000	2.000	2.000	2.000	2.000
Σ(Y)	1.186	1.082	1.124	1.174	1.239	1.212
Σ(X)	0.813	0.920	0.875	0.817	0.751	0.768
Atomic Ratios						
Fe/(Fe+Mg)	0.372	0.237	0.189	0.159	0.154	0.135

35-6) Quench groundmass grain/ "Glassy" olivine phyric pillow
121-5) Quench groundmass grain/ Olivine phyric pillow
162-1) Groundmass grain/ Picritic flow base
14-7) Microphenocryst rim/ Sl. Olivine phyric pillow
136-10) Microphenocryst core/ Olivine phyric pillow
83-4) Phenocryst interior/ Picritic flow base
(FeO*=Total iron; (Z)=Si,Al; (Y)=Al,Ti,Fe,Mg,Cr; (X)=Ca,Na)

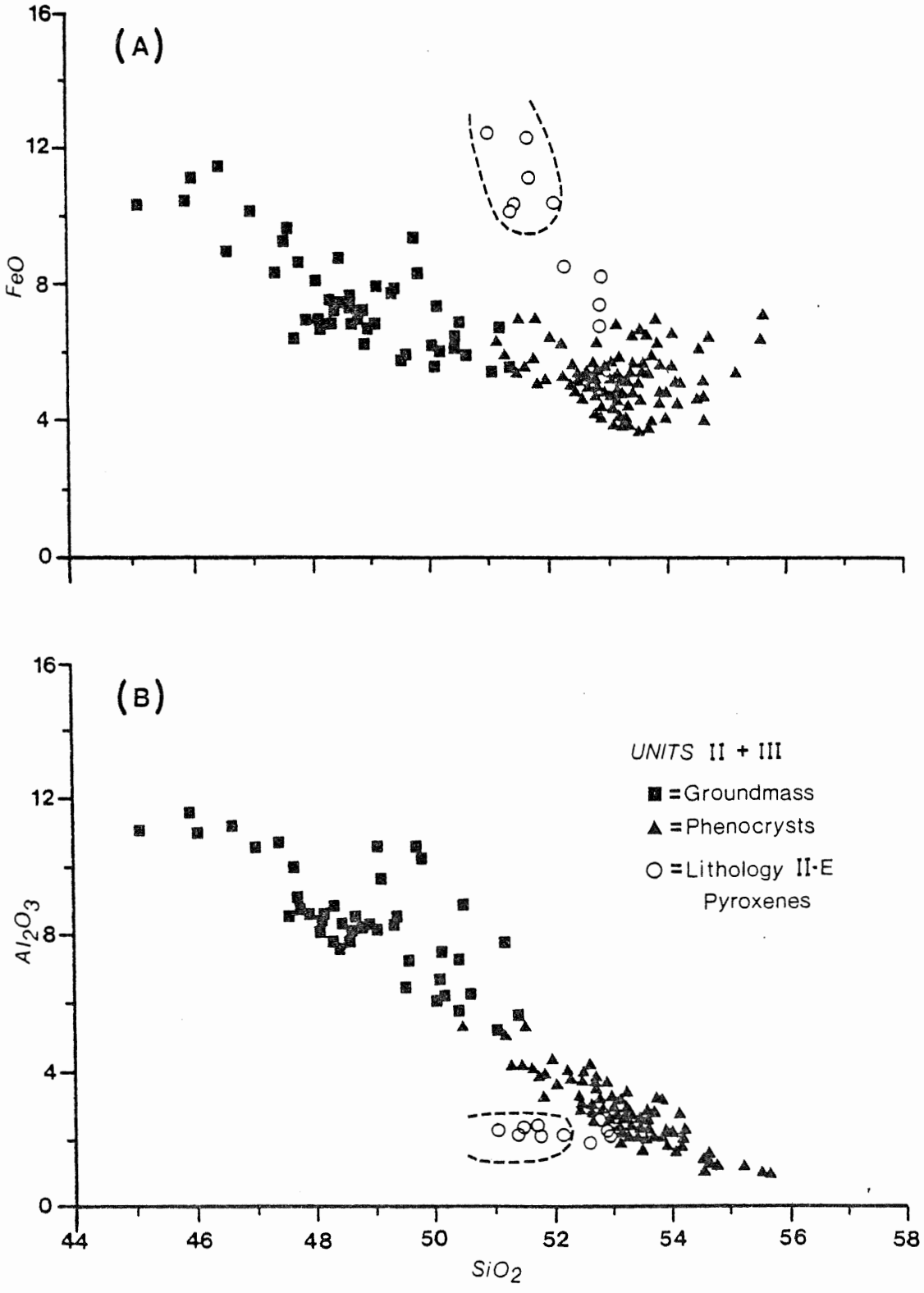

FIGURE III-3. Compositional variation of clinopyroxenes. (Dotted line encloses field of pyroxene phenocryst compositions in "Unit I" type lavas from the Pedios canyon - Mehegan; unpub. data.).

composition, however, the majority can be classified as either endiopsides or diopsides (see Figure III-4). Most contain significant amounts of chromium (0.5 to 1.5wt.%), and only minor amounts of titanium (<0.50 wt.%).

Type 2: Al-rich clinopyroxenes

Highly aluminous (and correspondingly Si-poor) pyroxenes occur as groundmass microlites and quench crystals in rocks from Units II and III (See Plate III-4 and Figure III-3). Plotted in the pyroxene quadralateral, most of the analyses lie in the diopside or salite fields, although many plot above the diopside - hedenbergite tie-line (see Figure III-4). The unusual compositions of these grains (e.g. the high Al and Fe, and low Si, Mg and Cr contents), may be the result of the rapid cooling which the host lithologies have undergone, for studies of DSDP basalts and experimental work on lunar basalts have shown that fast rates of cooling favor the entry of Al, Fe, Ca, and Ti into the pyroxene structure (Lofgren et al., 1974; Coish and Taylor, 1979).

Type 3: Fe-rich clinopyroxenes

Compositions of pyroxene phenocrysts from the aphyric massive flows of Unit II (lithology II-E), are distinct from those in the surrounding lithologies. Although some overlap does occur, they are generally enriched in Fe, and depleted in Al with respect to type 1 pyroxenes (see Figure III-3). Most of the analyses plot in the augite field of the pyroxene

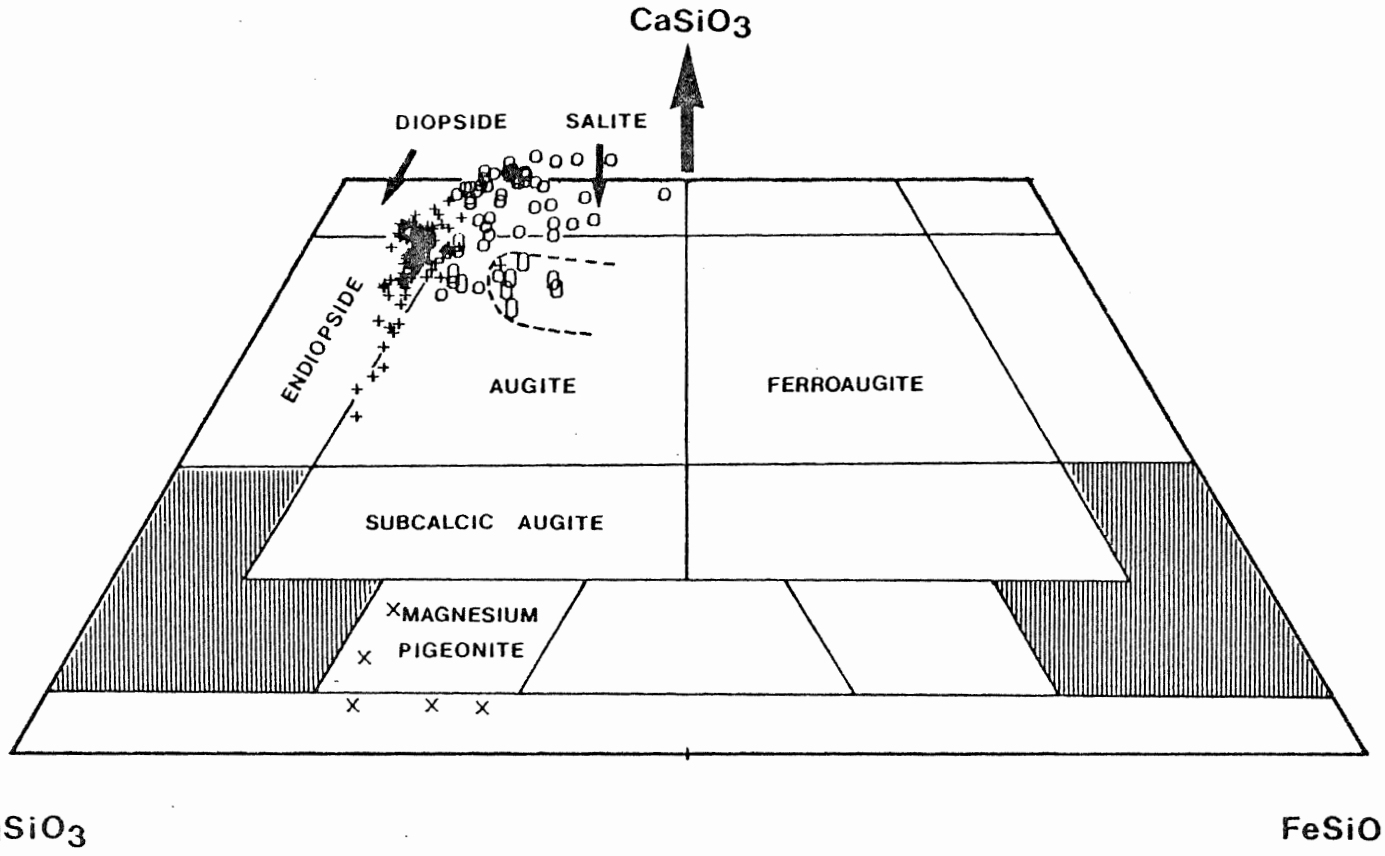

FIGURE III-4. Pyroxene compositions plotted in the pyroxene quadralateral. (+ = Unit II and III phenocrysts; o = Unit II and III groundmass grains; O = lithology II-E phenocrysts; X = Ca-poor groundmass grains in picritic flow bases.

quadralateral (Figure III-4).

Clinopyroxene phenocrysts from rocks correlative with those in Unit I are compositionally similar to those described above (Mehegan, unpub. data, 1984). They are, however, typically even more evolved, being considerably enriched in Fe and depleted in Al (see Figure III-3). Cr_2O_3 contents of these pyroxenes are also lower, typically under 0.50 wt.%, while TiO_2 contents are higher, averaging over 0.50 wt.%. These pyroxenes are predominantly augite, although some grains approach a ferroaugite composition (see Figure III-4).

Type 4: Ca-poor pyroxenes

As mentioned earlier, Ca-poor pyroxenes are found in the picrite-based flows, often rimming large Ca-rich pyroxenes. Unfortunately, obtaining good microprobe analyses of these grains is difficult for they are extremely small, and generally, slightly altered. The few analyses that were obtained show considerable chemical variation both within and between grains, indicating disequilibrium, which is typical of groundmass grains in rapidly cooled basalts. Compositions range from hypersthene to magnesium pigeonite (1.5 to 6.0 wt.% CaO). It should be noted, however, that these pyroxenes are not an important phase in the volcanic rocks of the Margi area, for they occur only within this one lithology, and only as minute, "late-stage" grains.

3.4 Plagioclase

Plagioclase is found in the groundmass of all lithologies, with the notable exception of the "glassy" olivine phyric pillows and the picritic pillows (lithologies II-B and II-C). In general, the greater the thickness of a flow unit, the larger and more abundant are the groundmass plagioclase grains. This suggests that the crystallization of plagioclase occurs predominantly post-extrusion, during the cooling of individual flow units. Most grains are small, lath-shaped microlites, except for those in the thickest flows which are large, anhedral grains commonly intergrown with pyroxene. Phenocrystic plagioclase is not observed in any of the rocks in Units II and III, although, elongate microphenocrysts do occur in samples from Unit I.

Much of the plagioclase is partially altered to fine-grained clay minerals and, as a result, is optically "cloudy". Microprobe analyses also reveal that the cores of some of the larger grains have been replaced by potassium feldspar (adularia).

Compositions of approximately 50 feldspars are listed in Appendix IV. Representative analyses are given in (Table III-3). Most plagioclase grains are highly calcic, with compositions between An70 and An80 (bytownite). More sodic compositions do exist (up to An52), but these are restricted

TABLE III-3 Representative plagioclase analyses

Sample #	101-3c	74-1	74-5	101-4	120-5	101-3b
SiO2	55.94	54.42	53.65	51.62	49.98	49.32
Al2O3	26.46	28.13	28.35	28.85	30.31	31.20
FeO*	0.62	0.56	0.60	0.62	0.57	0.39
MgO	-	-	-	-	0.16	-
CaO	11.01	12.17	13.16	14.52	15.75	16.39
Na2O	5.31	4.74	4.23	3.52	2.64	2.35
K2O	0.10	-	0.27	-	-	-
TOTAL	99.45	100.03	100.32	99.14	99.41	99.65
MINERAL FORMULA (basis of 32 oxygen)						
Si	10.160	9.856	9.738	9.508	9.207	9.072
Al	5.663	6.004	6.064	6.262	6.580	6.763
Fe2+	0.094	0.085	0.091	0.095	0.088	0.060
Mg	-	-	-	-	0.044	-
Ca	2.142	2.362	2.559	2.865	3.109	3.230
Na	1.870	1.664	1.489	1.257	0.943	0.838
K	0.023	-	0.063	-	-	-
Σ(Tet.)	15.917	15.945	15.892	15.865	15.919	15.894
Σ(Oct.)	4.035	4.026	4.110	4.122	4.052	4.068
Compositional Ratios						
OR	0.01	-	0.02	-	-	-
AB	0.46	0.41	0.36	0.30	0.23	0.21
AN	0.53	0.59	0.62	0.70	0.77	0.79

101-3c) Groundmass grain/ Olivine phyric flow
74-1) Rim of moderate (1 mm) lath/ Aphyric massive flow
74-5) Rim of irregular grain/ Aphyric massive flow
101-4) Core of moderate lath/ Olivine phyric flow
120-5) Core of large grain/ Picritic flow base
101-3b) Core of large grain/ Olivine phyric flow
(FeO*=Total iron)

to the rims of only a few grains. No major compositonal differences exist between the various units or lithologies, although grains from Unit I and lithology II-E are commonly more sodic than those from Units II and III.

3.5 Spinel

Within Unit I, small, anhedral spinels are found in the groundmass of many of the thicker cooling units (trace to 2%). In most samples, these grains are completely altered, though in one sample they were positively identified by microprobe analysis as titanomagnetites. Unfortunately, however, no reliable analyses were obtained.

Subhedral spinel grains are common accessories (trace to 4%) in many of the rocks from Units II and III, particularly in the picritic and highly olivine phyric lithologies. Most grains are less than 0.50 mm in diameter, although discrete phenocrysts up to 2.0 mm long do exist. In thin section, the spinels are deep red to opaque, and are commonly found as inclusions within large olivine phenocrysts. Subhedral groundmass grains are also present in trace amounts.

Compositionally, the spinels within Units II and III are members of the chromite series, with Cr_2O_3 contents between 40 and 60wt.%. Representative analyses are given in Table III-4. Elemental ratios of Cr/(Cr+Al) and Mg/(Mg+Fe) are plotted for all the obtained chromite analyses in Figure

TABLE III-4 Representative chromite analyses

Sample #	154a-5	127-2r	127-8	120-7	120-8	154a-7
SiO2	-	-	-	-	-	-
TiO2	0.27	0.18	-	0.29	0.31	0.82
Al2O3	11.79	11.19	12.29	13.72	14.69	15.52
Cr2O3	57.45	55.22	53.16	51.54	48.10	43.77
FeO*	16.84	18.63	20.53	20.77	26.91	26.12
MnO	-	0.16	0.15	0.09	0.18	0.16
MgO	13.92	13.78	12.51	12.78	9.03	12.36
CaO	0.06	-	-	-	-	0.05
TOTAL	100.27	99.16	98.64	99.19	99.22	98.75
MINERAL FORMULA (basis of 32 oxygen)						
Si	-	-	-	-	-	-
Ti	0.052	0.035	-	0.056	0.061	0.158
Al	3.532	3.394	3.759	4.144	4.531	4.672
Cr	11.547	11.238	10.910	10.445	9.954	8.841
Fe3+	0.807	1.296	1.328	1.296	1.391	2.163
Fe2+	2.772	2.712	3.126	3.153	4.498	3.414
Mn	-	0.035	0.033	0.020	0.040	0.035
Mg	5.275	5.287	4.840	4.583	3.523	4.706
Ca	0.016	-	-	-	-	0.014
Σ(Tet.)	15.938	15.963	15.998	15.942	15.937	15.833
Σ(Oct.)	8.064	8.035	8.000	8.056	8.061	8.169
Atomic Ratios						
Mg/(Mg+Fe2)	0.655	0.658	0.605	0.606	0.437	0.577
Cr/(Cr+Al)	0.766	0.768	0.744	0.716	0.687	0.654

154a-5) Microphenocryst core/ Olivine phyric pillow
127-2r) Round inclusion in olivine/ Picritic pillow
127-8) Groundmass grain core/ Picritic pillow
120-7) Groundmass grain core/ Picritic flow base
120-8) Groundmass grain rim/ Picritic flow base
154a-7) Groundmass grain rim/ Olivine phyric pillow
(FeO*=Total iron; Fe2+ and Fe3+ calculated on basis of stoichiometry)

III-5. Most phenocryst / microphenocryst compositions cluster within the dotted line which encloses the compositional field of spinels from the Troodos plutonic sequence (from Cameron et al., 1980).

3.6 Summary

The extrusive rocks in the Margi area are highly variable with respect to the relative abundances and compositions of the four primary phases previously discussed. The most significant differences in phase relations and compositions occur between the rocks of Unit I and those of Units II and III.

1) UNIT I: Plag + Cpx + Ti-Mt

Samples from Unit I invariably lack olivine, and generally, contain plagioclase and/or clinopyroxene phenocrysts. Modal abundances and proportions of the two phases are variable, and many samples are completely aphyric. Phenocrysts are commonly small, subhedral grains, present in only minor amounts (generally < 5 modal percent).

Most samples contain sparse plagioclase and clinopyroxene microphenocrysts along with groundmass microlites of plagioclase and minute titanomagnetite grains. This suggests a relatively short period of bytownitic plagioclase crystallization, coincident with, or followed

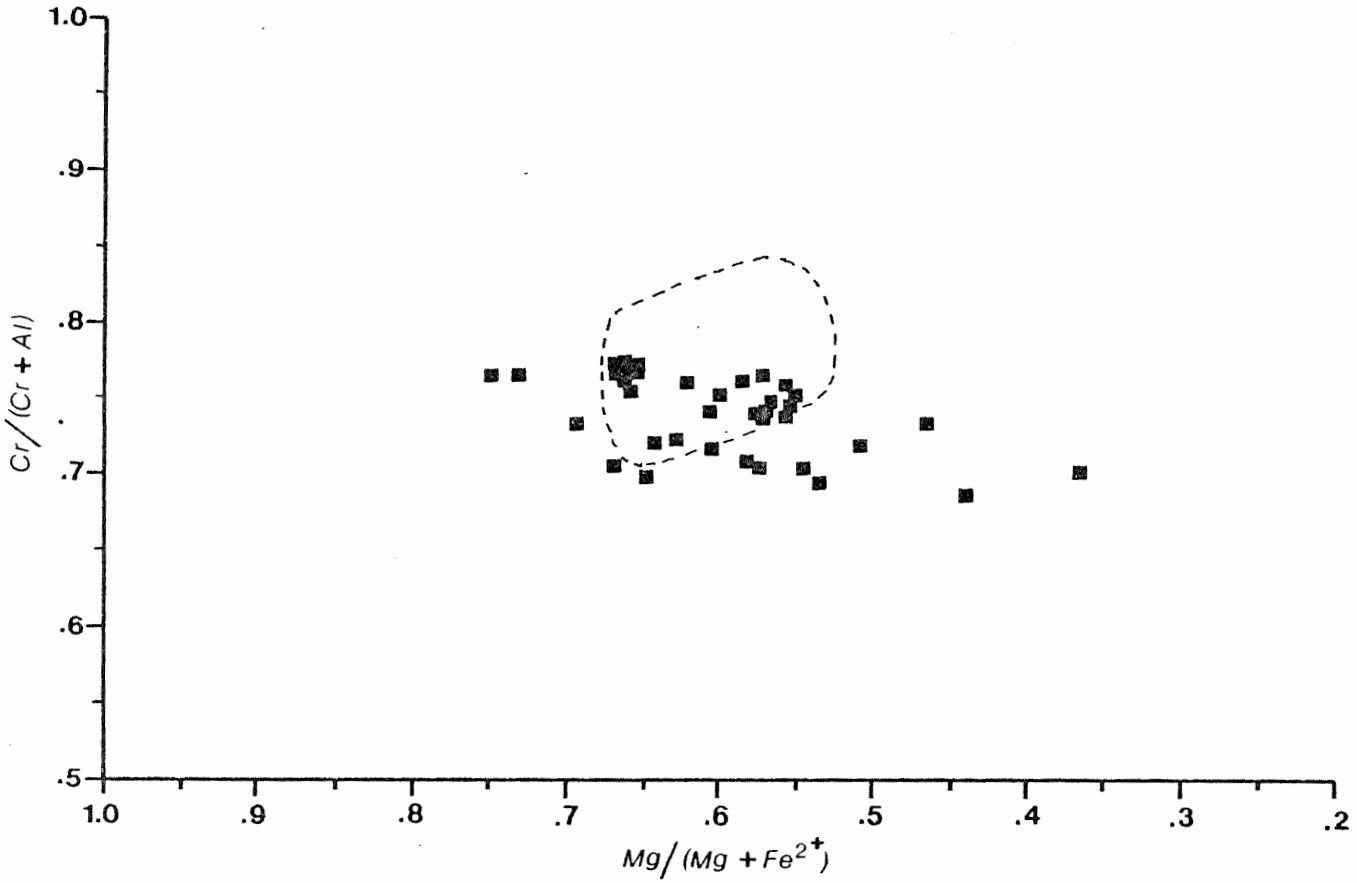

FIGURE III-5. Cr/(Cr+Al) vs. Mg/(Mg+Fe) variation in spinels from Units II and III. Dotted line encloses field of spinel compositions from the Troodos plutonic sequence (from Cameron et al., 1980).

rapidly by crystallization of "type-3" clinopyroxenes prior to extrusion. Titanomagnetite was apparently a liquidus phase at the time of extrusion for some of the lavas. The abundance and size of groundmass grains was strongly influenced by the rates of cooling of individual flow units.

2) UNITS II and III: Ol + Cpx + Cr-Sp

Virtually all the rocks from Units II and III contain olivine (+/- spinel, +/- clinopyroxene) as phenocryst phases. The modal abundance of olivine is highly variable (trace to 55%), but this variation is believed to be largely a result of pre- and post extrusion sorting processes (See Chapter Five for further discussion of this phenomenon).

Rocks in this group appear to have undergone a long period of olivine crystallization, along with, or perhaps preceded by, minor chrome spinel crystallization. This was followed, in some instances, by a period of "type-1" clinopyroxene formation prior to extrusion. During the process of extrusion, quenching conditions were responsible for the formation of clinopyroxenes with rapid growth morphologies (See Plate III-4), and unusual "type-2" compositions. This occurred predominantly in the pillowed lithologies, particularly in lithologies II-B and II-C. The thicker, more massive flow units underwent slower cooling, allowing time for the formation and growth of both "type-1"

clinopyroxenes and bytownitic plagioclase.

The aphyric massive flows within Unit II exhibit markedly different mineralogical features than those described above. Samples from this lithology lack olivine, and contain only large groundmass grains of clinopyroxene and plagioclase.

It appears that these thick flows were extruded essentially as liquids, though the possibility exists that microphenocrysts of clinopyroxene and/or plagioclase might have been present in substantial quantities prior to extrusion. Cooling of these units was relatively slow due to their thickness, and during this period, the formation and/or growth of both "type-3" clinopyroxenes and bytownitic to labradoritic plagioclase took place. Most of the pyroxenes are strongly zoned, with core compositions similar to those of "type-1" pyroxenes, while the rims tend to be significantly enriched in iron. Feldspar compositions show a similar trend, with rims often being enriched in sodium relative to the bytownitic cores.

The unusual phase relations (i.e. the lack of both olivine and spinel), and pyroxene compositions in samples from these flows (see Figure III-3), are believed to be largely the result of post-extrusion differentiaton within individual flow units.

It should be noted that the above groups and "crystallization sequences" are simplified, and based only on petrographic observations of samples from the Margi-Analiondas area, and may not be typical of the entire massif. For although there are broad similarities in many features of the ophiolite volcanics, there are also many local variations, as evidenced by the presence of orthopyroxene as an important phenocryst phase in the extrusive rocks on the southern flank of the massif (Mehegan; pers.comm.,1984).

CHAPTER FOUR

WHOLE-ROCK AND GLASS GEOCHEMISTRY

4.1 General Statement

Seventy-eight rock samples representing all the major lithologies in the study area were analyzed for nine major, and thirteen trace elements by X-ray fluorescence at the Universite de Montreal. Weight percents of the volatiles (CO_2, H_2O^+, and H_2O^-), and ferrous iron were determined by wet chemistry at Dalhousie University. (See Appendix III for analyses and Appendix II for analytical methods.)

Twenty-six samples of fresh volcanic glass were analyzed at the Smithsonian Institute in Washington, D.C. for major elements by a wavelength dispersive microprobe system (See Appendix III for analyses.)

In this chapter, major compositional differences between lithologic and stratigraphic units are delineated. A brief discussion of the effects of alteration on major element mobility is also included. Major petrologic interpretations, however, are reserved for Chapter Six.

4.2 Major Element Geochemistry

Whole-rock samples were collected with the aim of obtaining representative analyses from as wide a range of lithologies and stratigraphic levels as possible. Samples

range from highly picritic flow bases and pillow cores, to aphyric pillow margins and flow interiors. Extensively "altered" samples were avoided when possible.

Plots of the major oxides against MgO are shown in Figure IV-1(a-g). Symbols correspond to the two rock "groups" delineated in Chapter Three, along with separate symbols for the picritic lithologies and the aphyric massive flows of Unit II. The field of extrusive glass compositions for the Margi area (from Units II and III only), is also shown on each plot, enclosed by a dashed line. All of the variation diagrams are of the "raw" (volatile free) XRF data, though plots of data corrected for excess calcium carbonate and for ferrous iron are not significantly different.

The diagrams clearly show the unusual, ultrabasic compositions of the picritic lithologies, with MgO contents ranging from 20 to 40 wt.%, and SiO2 contents generally less than 45 wt.%. Details of the chemistry and genesis of this group of rocks will be discussed in Chapter Five.

Rocks in the three remaining groups are predominantly basalt to basaltic andesite in composition, though it should be noted that those in Units II and III have unusually low TiO2 and high MgO and SiO2 contents compared to typical MORB, and are therefore similar to "boninites" and high-Mg andesites (see Cameron and Nisbet, 1982). The three groups cannot, with any confidence, be distinguished on most of the

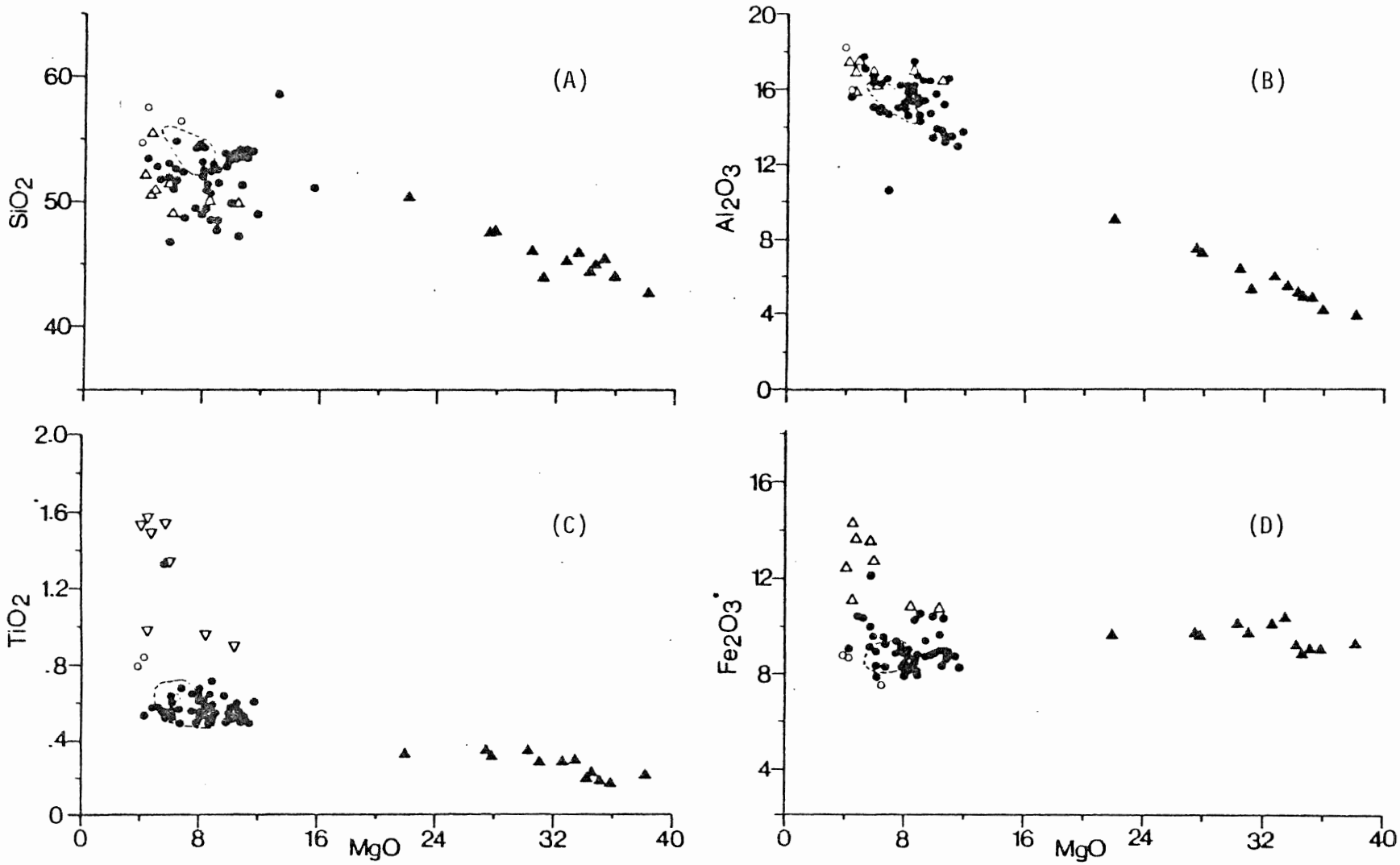

FIGURE IV-1. Variation diagrams of whole-rock major element oxide concentrations. (Key to symbols on following page).

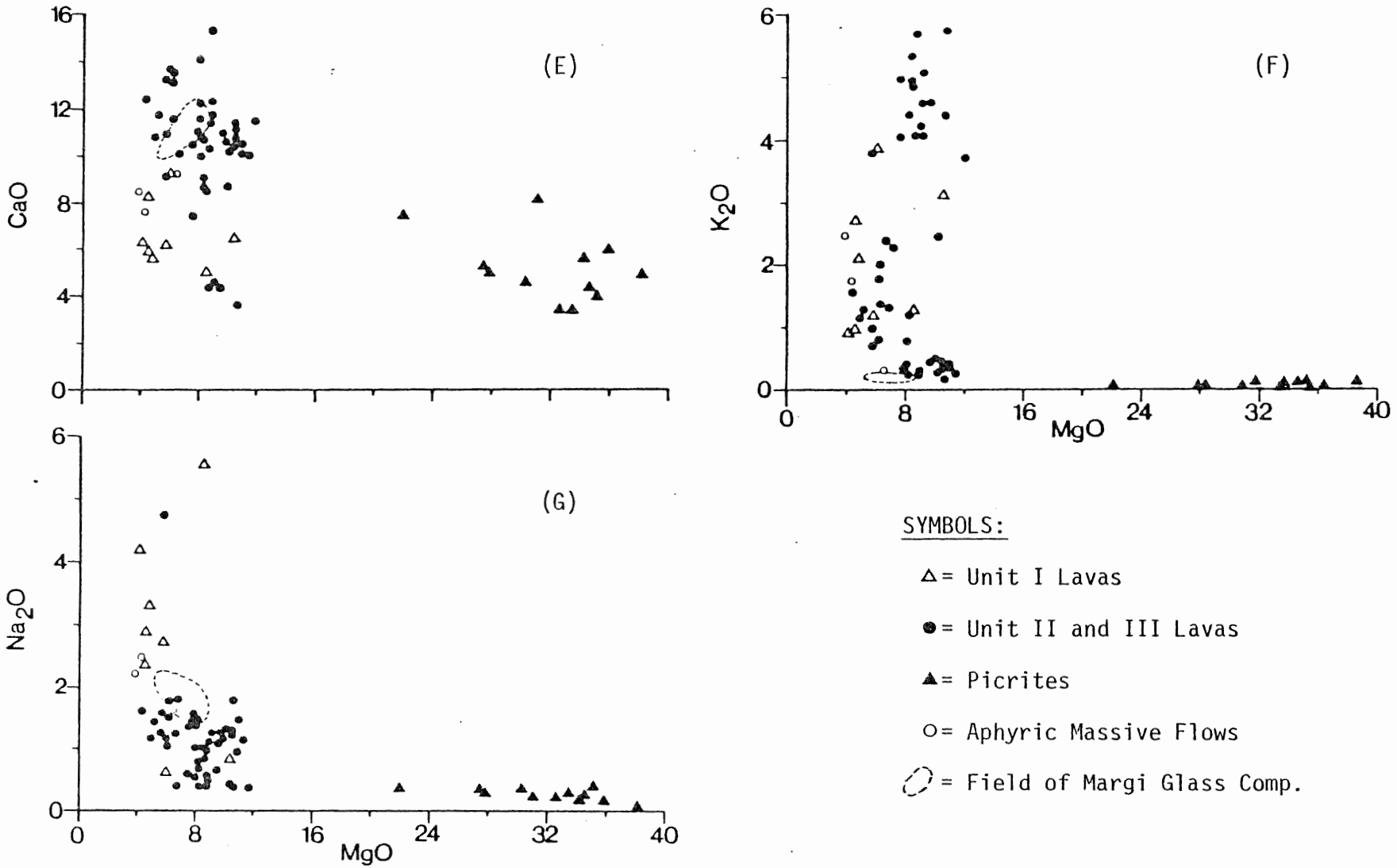

FIGURE IV-1.(cont.) Variation diagrams of whole-rock major element oxide concentrations.

major element variation diagrams. Samples from Unit I, however, are separated from those of Units II and III on both the Fe2O3-MgO, and TiO2-MgO diagrams (See Figure IV-1c+d). These two groups are also separated, albeit poorly, on the CaO-MgO and Na2O-MgO plots, though the wide scatter of points on these diagrams makes this distinction tenuous. In general, samples from Unit I contain significantly higher amounts of titanium and total iron than do any other rocks in the Margi area.

Unfortunately, only five samples from the aphyric massive flows of Unit II (lithology II-E) were analyzed, and few conclusions can be drawn as to their chemical characteristics. Generally, they exhibit compositions that are intermediate to those of most samples from Units I and II.

4.3 Major Element Mobility

As was previously discussed in Chapter Two (section 2.4), all of the whole-rock samples collected have undergone some degree of mineralogic alteration as a result of having been subjected to subaqueous and subaerial weathering. Unfortunately, the formation of secondary minerals, whether at the expense of primary minerals or not, is generally not an isochemical process.

Depending upon the system(s) involved, particular

elements may be enriched or depleted in the bulk rock relative to original values. Comparison of fresh glass compositions with those of whole rock samples from the same lithologic units is , therefore, used as a means of estimating the relative mobility of the major elements during alteration. The field of glass compositions from Units II and III, are shown in the variation diagrams of Figure IV-1, enclosed by a dashed line. Relative to this field, the major elements in the whole-rock samples from the same units exhibit the following behaviour:

Enriched: K
Depleted: Na, Ca, Si
Unchanged: Ti, Al, Fe, Mg

Such behaviour of the major elements is typical for basalts which have been altered under low temperature, hydrous conditions (e.g. sea-floor weathering conditions), though studies of element mobility are far from unanimous (Honnorez, 1981). The marked depletion in sodium may also be significant, for experimental work by Mottl (1983), suggests that sodium is leached from basalt only at high water/rock ratios.

Preliminary results from a study on the alteration of samples from drill hole CY-2A also indicate the same relative changes in element abundances (Cann, ICRDG board meeting; Sep. 1983). It should be noted though, that in Cann's study, magnesium was found initially to increase and then slowly

decrease in abundance as alteration progressed, commonly returning to, or dropping below, original values. This illustrates the fact that "unchanged" values are not necessarily indicative of an "immobile" element, and that simple enrichment or depletion may not be the case for any of the elements mentioned above. All we are examining is the net result of an extremely complex and variable process.

Nevertheless, it should be stressed that the observed changes in major element compositions can be explained by low temperature, sea-floor alteration, most likely under water-dominated conditions. This is in good agreement with the observed secondary mineral assemblages and their stabilities, as discussed in Chapter Two.

4.4 Trace Element Geochemistry

For most of the seventy-eight whole-rock samples, the following trace and minor elements were analyzed by XRF: Rb, Sr, Y, Zr, Nb, Ba, V, Zn, Cu, Ni, Cr, Ti, and P. All analyses are expressed in parts per million (ppm), and listed in Appendix III. Niobium and barium values are typically at or below detection levels (approx. 3 ppm and 20 ppm, respectively), and are not shown in any of the following diagrams.

The remaining elements, except for Ni, Cr and Cu, tend to behave incompatibly in basaltic magmas (Carmichael et al.,

1974). Plots between pairs of incom patible elements are often useful for distinguishing magma suites, since the interelement ratios are not significantly influenced by simple fractional crystallization processes. Unfortunately, the behaviour of the incompatible trace elements in basalts subjected to conditions of low-temperature, hydrous alteration are highly variable. Saunders et al.(1979), have proposed a division of these elements into two groups based on the ionic character of the elements. Elements with large ionic radii and low charges (or high radius/charge ratios), are termed "low field strength" (LFS) cations, and these have been shown to be mobile during low-temperature alteration (Pearce and Cann, 1973; Smith et al., 1976; Ludden et al., 1979). The LFS group is composed of Cs, Rb, K, Sr, Ba, Th, U, Pb, and the light REE. Elements with a low radius/charge ratio are labelled "high field strength" (HFS) elements, and these are generally considered to be immobile during alteration of basalts (Pearce and Norry, 1979; Shervais, 1982). This group includes Zr, Hf, Ti, P, Nb, V, and Ta. The heavy REE (and Y), have intermediate radius/charge ratios, but in many aspects their behaviour resembles that of the HFS cations (Saunders et al., 1979). The HFS and heavy rare-earth elements are, therefore, the most useful for examining the primary geochemical features of altered basaltic rocks.

Titanium was chosen as a common plotting parameter for the following reasons: 1) as noted above, it is generally regarded as "immobile" under conditions of low-temperature, seawater alteration (Cann; 1970), and the tight cluster of data points on the TiO2-MgO diagram (Figure IV-1c), supports this conclusion; 2) since it is a minor element, it is present in relatively high concentrations when expressed as a trace element which results in an increased resolution of the data; and 3) samples contain a wide range of titanium concentrations (over one order of magnitude!), and this also enhances the separation of chemical "suites". The resulting variation diagrams are shown in Figure IV-2(a-h).

The four rock "groups" previously discussed (i.e. the picritic lithologies, the aphyric massive flows, Unit II and III lavas, and Unit I lavas), can be distinguished on most of these diagrams, primarily as a result of distinct differences in their titanium contents.

Not suprisingly, plots of the HFS elements (particularly Zr, V, and Y vs. Ti), exhibit the most marked separation of these four groups. The picritic samples invariably plot in a very restricted field, and contain the lowest observed values of all the incompatible elements. Rocks from Unit I, on the other hand, are relatively enriched in these elements, and span the widest compositional range. Samples from Units II and III generally have compositions intermediate to those of

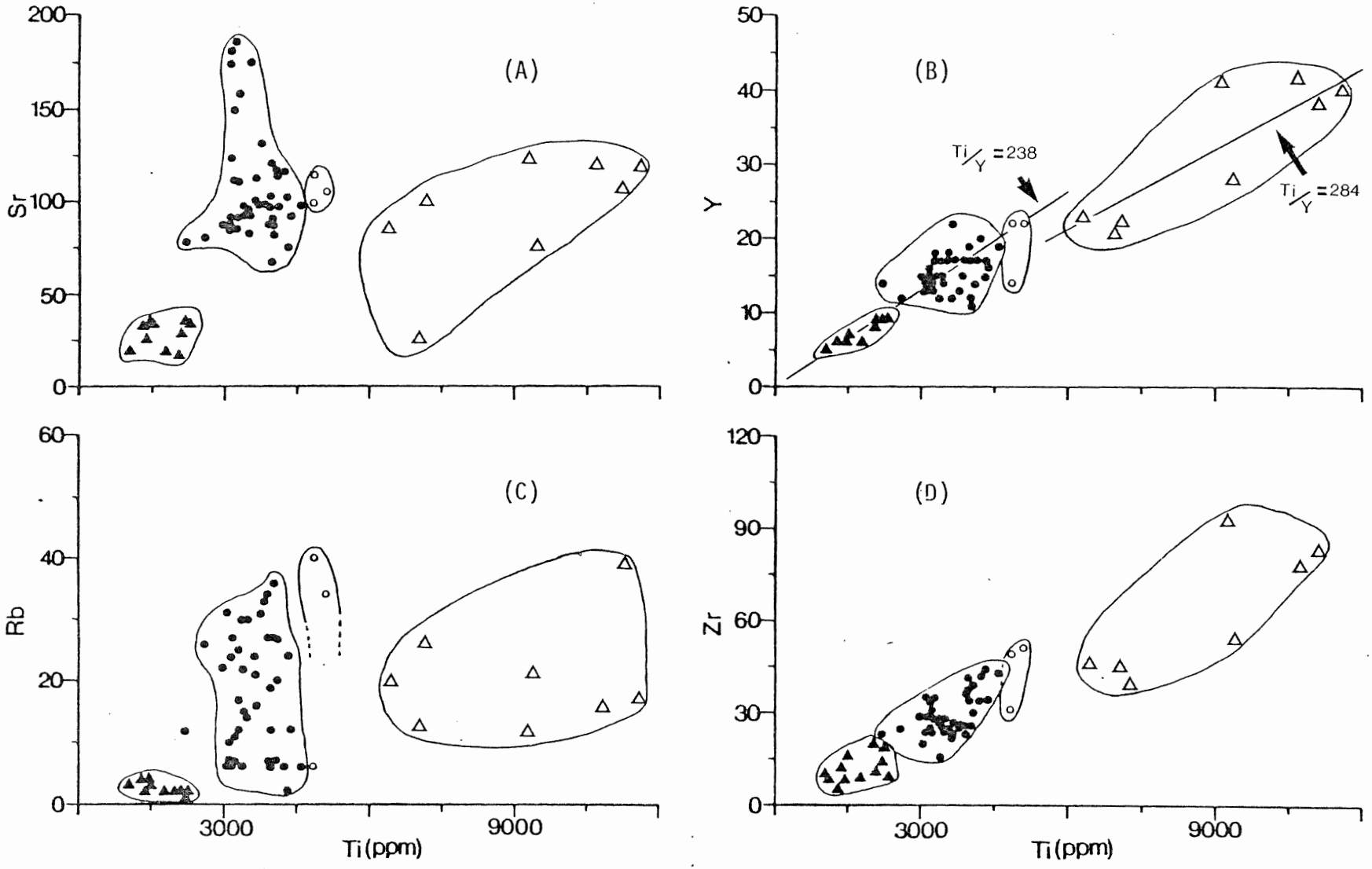

FIGURE IV-2. Variation diagrams of whole-rock trace element concentrations. (Symbols same as Figure IV-1).

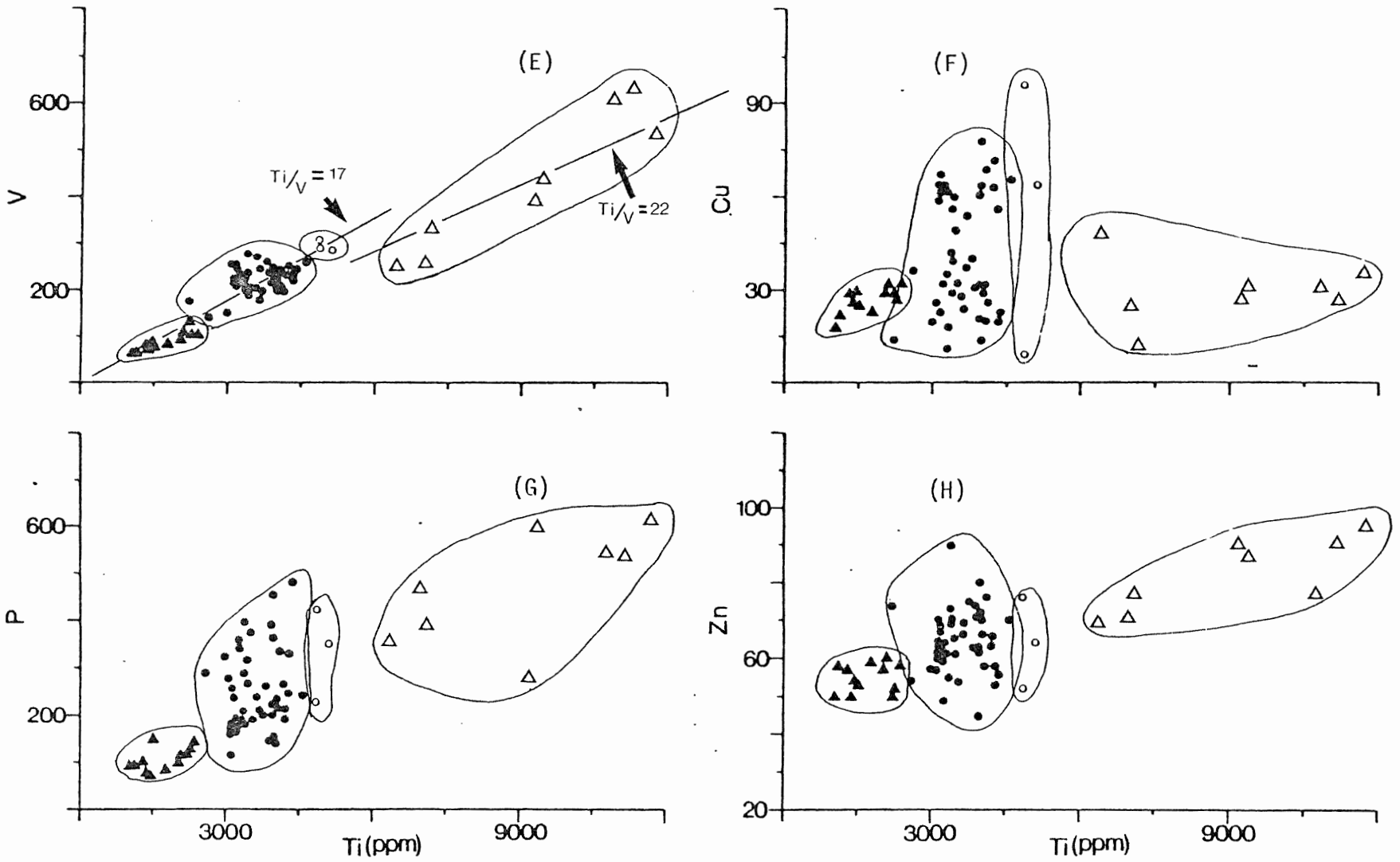

FIGURE IV-2.(cont.) Variation diagrams of whole-rock trace element concentrations. (Symbols same as Figure IV-1).

the picrites and Unit I lithologies.

Rubidium and strontium contents are highly variable within the samples analyzed, supporting the conclusion that these elements are easily mobilized during alteration.

Copper values, and to a lesser extent, zinc values, are also variable, again believed to be predominantly a result of alteration, as both are known to be easily mobilized in aqueous solutions (Rose et al., 1979). A preliminary observation is that samples which are petrographically the least altered contain the highest copper contents (around 60 ppm). In general, the evidence suggests that during low-temperature seawater alteration, zinc was relatively immobile whereas copper was readily leached from the majority of the extrusive rocks. This observation is compatible with the fact that the massive sulphide deposits found within the extrusive sequence are relatively rich in copper and poor in zinc. Between the four rock groups, however, there are no significant differences in absolute copper or zinc contents.

Chromium and nickel are extremely compatible elements, being preferentially incorporated into spinel and olivine, respectively. Figures IV-3(a and b), show the high concentrations of Ni and Cr that occur in the picritic lithologies, reflecting their abundance of these phases. Samples from Units II and III exhibit a fairly restricted range of both Ni and Cr contents, with most of the variation

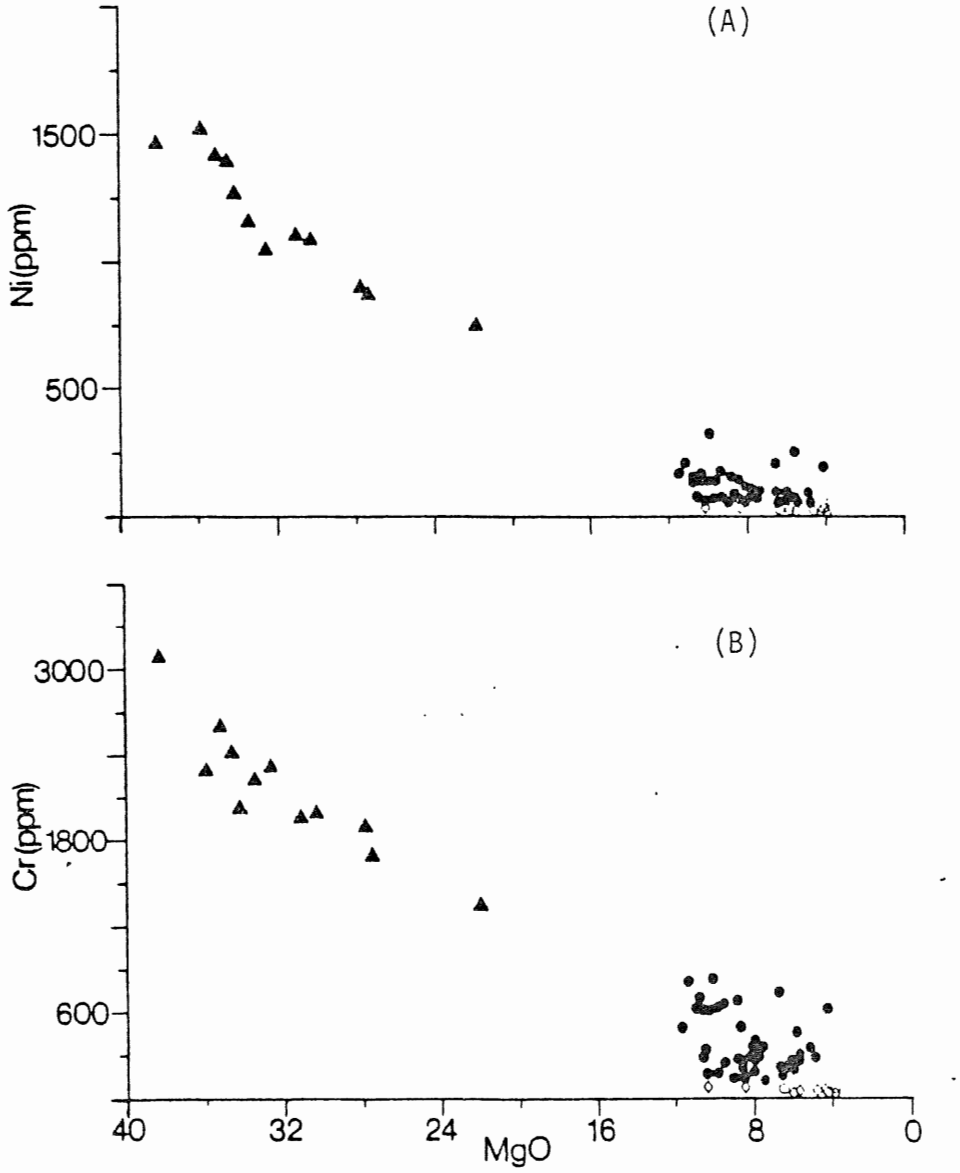

FIGURE IV-3. Variation diagrams of whole-rock Cr and Ni concentrations. (Symbols: diamond = Unit I lavas; solid circle = Unit II and III lavas; open circle = Aphyric massive flows; triangle = Picrites).

being due to differences in modal mineralogy between samples. Unit I lavas, and samples from the aphyric massive flows of Unit II, are clearly distinguished from these groups by their significantly lower amounts of both Cr and Ni.

Samples from Units II and III (including even the picritic lithologies and the aphyric flows), have slightly higher V/Ti and Y/Ti ratios than do samples from Unit I (See Figures IV-2; b + e). Such differences can not be readily explained by fractional crystallization processes and, along with the observed differences in phase relations and major element compositions between these two groups, suggest the existence of two major magma suites.

In summary, four compositional groups can be easily distinguished on nearly all the trace element variation diagrams. The HFS elements are the most useful for delineating these groups, and relations between pairs of these elements suggest the existence of two distinct magma suites.

4.5 Glass and Unaltered Pillow Geochemistry

While it is possible to distinguish four chemical groups on the basis of major and trace element compositions of whole-rock samples, it must be remembered that such an approach is limited by a number of factors. First of all, even though this study has attempted to "look past" the

effects of alteration by focussing on "immobile" elements, it is unlikely that the concentration of any element remains completely unaffected, for even if the element itself is not mobilized, the addition or removal of other elements indirectly affects the net concentration of those remaining. Secondly, the samples analyzed vary markedly in degree and style of alteration and this undoubtedly increases the "scatter" of whole-rock compositions, because the intensity, and even direction, of an element's mobility can change significantly with only slight changes in the conditions af alteration. Finally, there are chemical variations due to post-extrusion processes of differentiation (e.g. crystal settling, flowage differentiation, etc.). All three of these factors contribute to the overall variability of whole-rock compositions and, in effect, make it difficult to observe the "primary" chemical variation due solely to subsurface processes of magma generation and evolution.

In an attempt to avoid these problems, this section examines the geochemistry of glass and "unaltered", aphyric to microphyric pillow samples, both of which provide us with reliable analyses that closely approximate liquid compositions. The selection of "unaltered" pillows was based on petrographic criteria such as the presence of fresh olivine and/or groundmass glass, though the term unaltered should not be taken literally, for even the "freshest"

samples contain abundant smectites.

Figures IV-4(a-g), show the major element compositions of the glass and selected pillow samples from the Margi area, along with the two major fields of glass compositions in the massif delineated by Robinson et al., (1983). For sake of discussion, the low-Mg, high-Ti and Fe group of glass compositions will be referred to as the "arc-tholeiite" suite, and the high-Mg, low-Ti and Fe group will be referred to as the "boninite" suite. In all of the diagrams, continuous trends from the most Mg-rich pillow to the most Mg-poor glass occur, with the notable exception of the K2O-MgO plot (Figure IV-4g). The anomalously high K2O contents of the whole-rock analyses, however, are easily explained by the presence of potassium-rich smectites.

The glass analyses from Units II and III in the Margi area are clearly part of the high-Mg, "boninite" suite of glass compositions. The associated whole-rock analyses, however, indicate that the actual evolutionary path included compositions much more primitive than any preserved in the glass samples. While no glass samples were collected from Unit I, the whole-rock samples from this unit contain significantly higher amounts of both iron and titanium than do any from the overlying lavas (see Figure IV-1), and are therefore considered to be basaltic members of the "arc-tholeiite" suite.

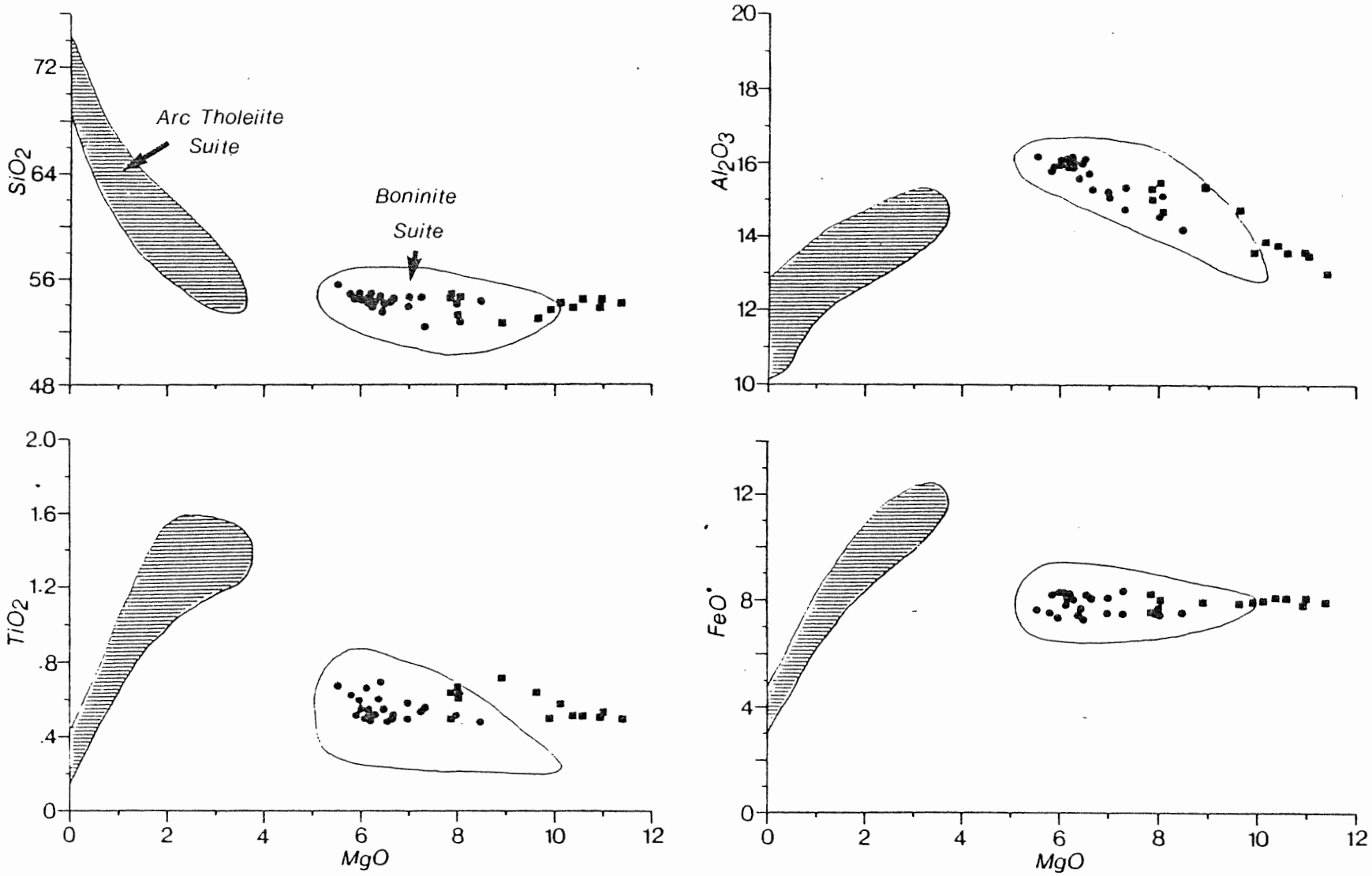

FIGURE IV-4. Variation diagrams of glass and "glassy" pillow major element oxide concentrations. (Key to symbols on following page).

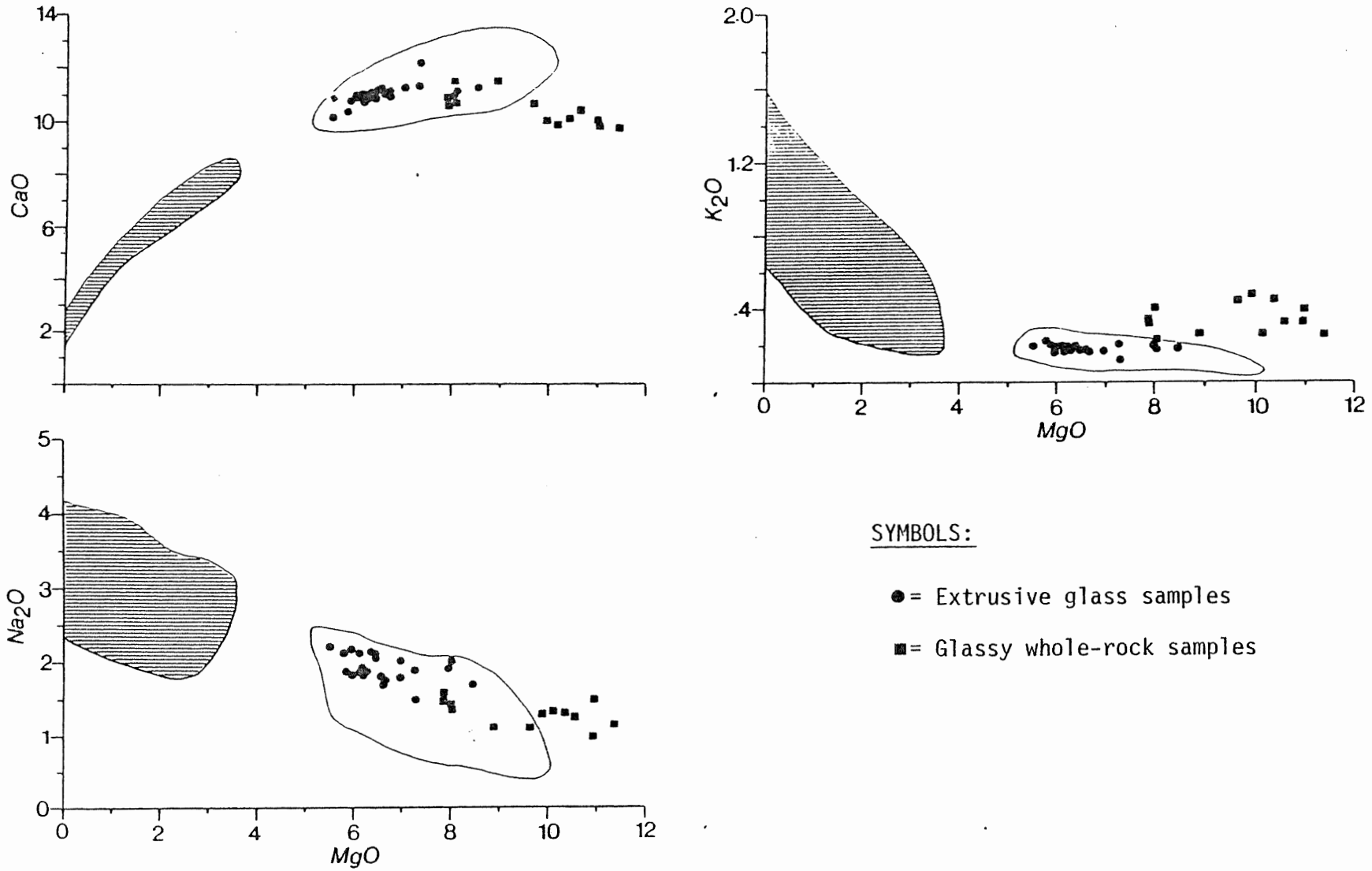

FIGURE IV-4.(cont.) Variation diagrams of glass and "glassy" pillow major element oxide concentrations.

On the basis of these diagrams, separation of the samples into smaller chemical groups does not appear to be possible. Examining just the glass analyses though, a division can be made on the basis of TiO2 and Na2O contents which corresponds to distinct stratigraphic intervals (see Figure IV-5a). The high TiO2 and Na2O analyses belong to samples from most of Unit II, while the low TiO2 and Na2O analyses belonging to samples from Unit III, and locally, the top of Unit II (lithology II-B). Whole rock samples exhibit the same pattern with respect to titanium, but not with sodium. Again, this can be easily explained as a result of alteration.

The separation of the same stratigraphic intervals also occurs on virtually any diagram which employs the HFS trace elements (See Figure IV-5b,c+d). It should be noted that the most incompatible element depleted lithologies are, in fact, from the highest stratigraphic section. Ratios between pairs of incompatible trace elements also differ between these two groups, with the most marked difference occuring in the Ti/V ratios (see Figure IV-6). Samples from Unit III (and lithology II-B) have a mean Ti/V ratio of 14.87 (+/-0.47), whereas those from Unit II have a mean Ti/V ratio of 17.30 (+/-0.52). These features suggest the presence of two slightly different parental magma compositions, however, it must be remembered that this distinction is based solely on

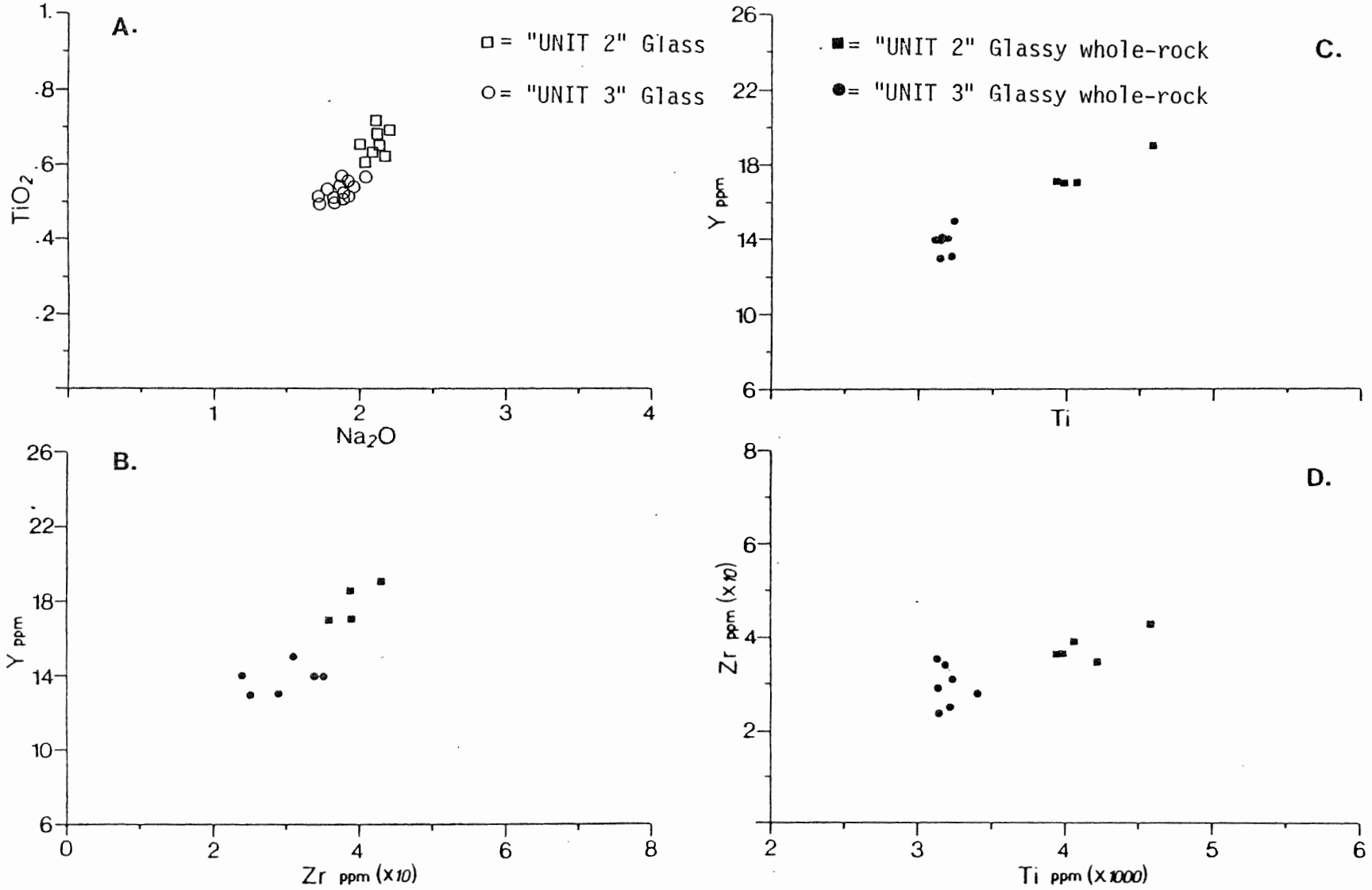

FIGURE IV-5. Variation diagrams of glass and glassy pillow minor and trace element concentrations.

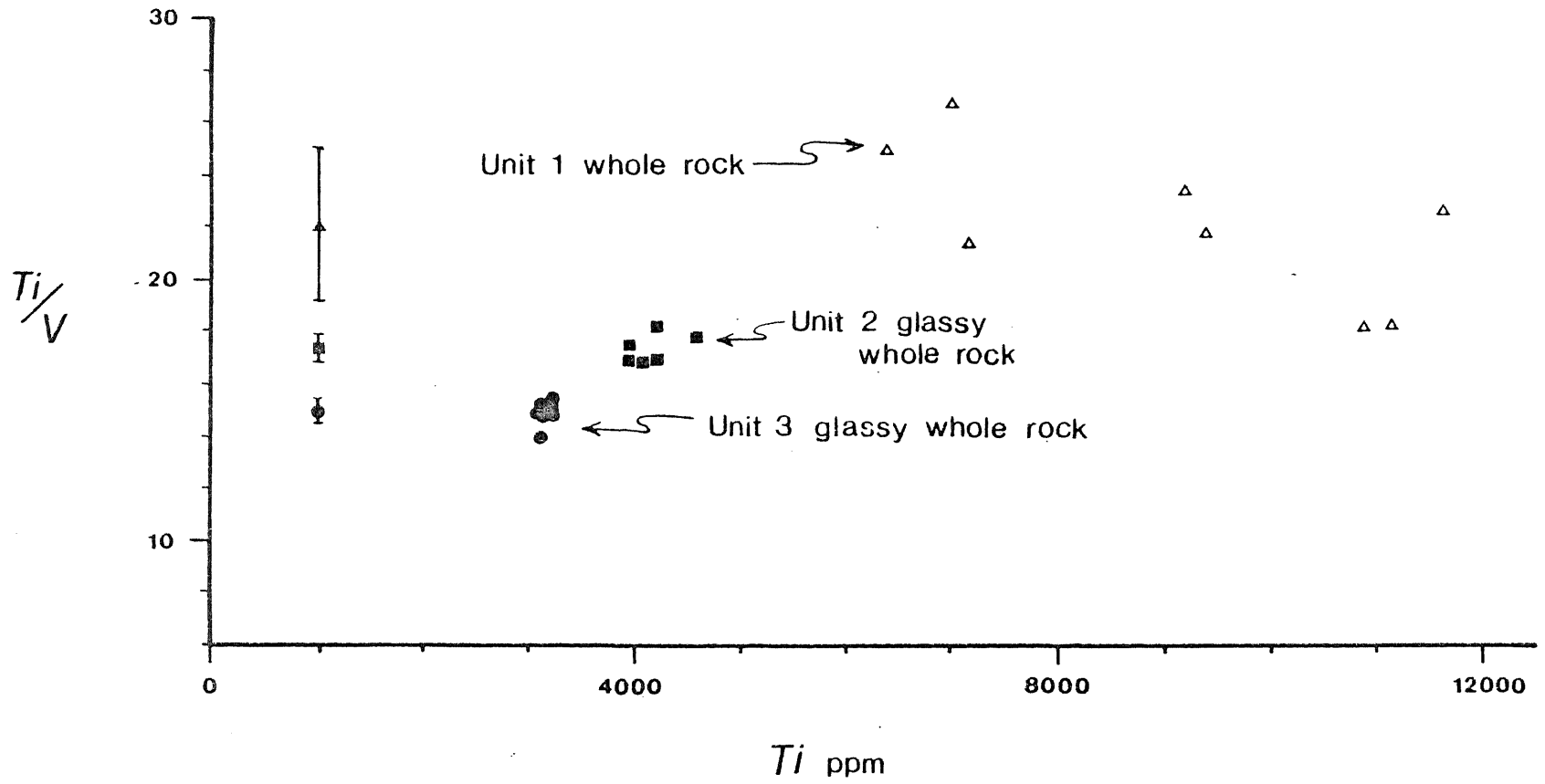

FIGURE IV-6. Ti/V ratios of selected whole-rock samples from the Margi area. (Bars at left of diagram represent mean Ti/V ratios (+/- 1 S.D.) of the three sample populations.)

slight chemical differences in a small number of samples, and that the remaining whole-rock analyses from these units can not be distinguished with any confidence. The extrusive rocks within Unit I, however, all exhibit significantly higher Ti/V ratios than do most others from the Margi area (22.09 +/-3.02), even though many are extensively altered. Clearly, these volcanics were derived from a markedly different parental magma composition.

4.6 Summary

On the basis of major and trace element chemistry, five compositional groups can be delineated in the extrusive rocks of the Margi area. Petrographic phase relations (see Chapter Three), along with major and trace element compositions indicate that these rocks belong to two major magma suites. A tentative correlation of lithologic and compositional groups with genetic suites is listed below.

Suite B_2:	3) Unit III (+ lithology IIB) 2b. (aphyric massive flows) 2a. (picritic lithologies)
Suite B_1:	2) Unit II
Suite A:	1) Unit I

Correlations of the above lithologic units and chemical suites to existing regional divisions are schematically summarized in Figure IV-7. The important points to be noted are:

1) The rocks of Unit I can be distinguished from the

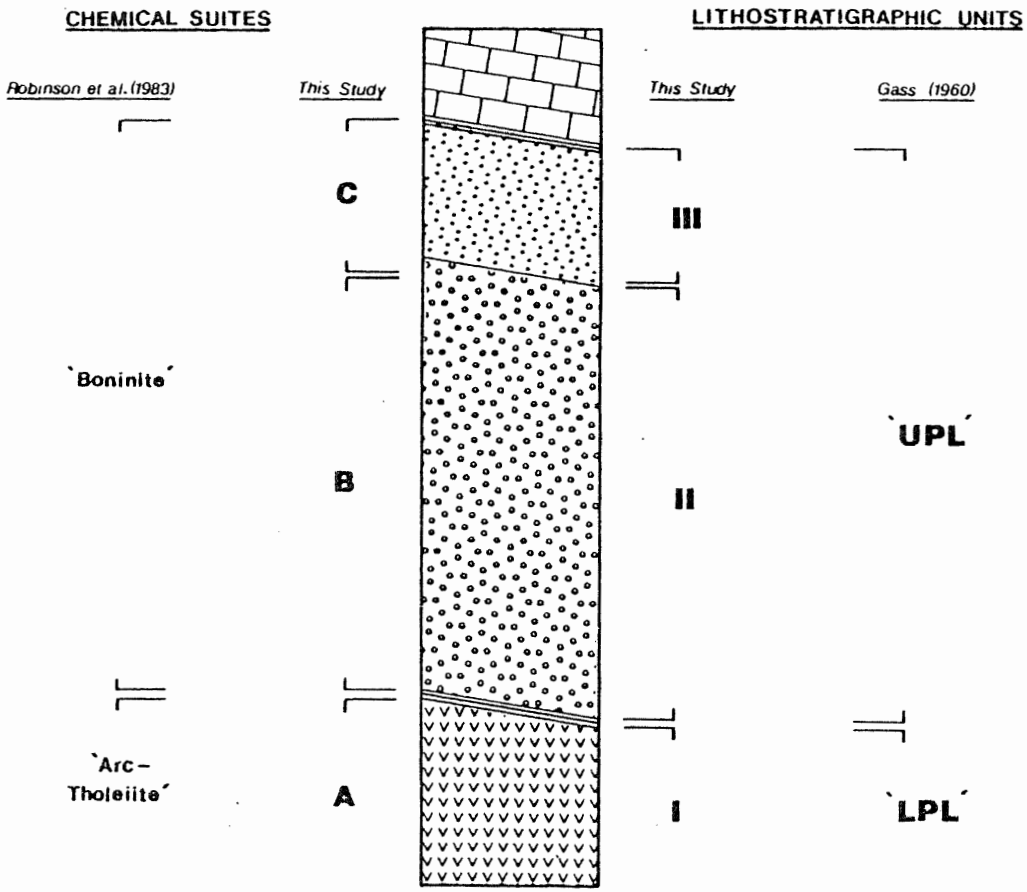

FIGURE IV-7. Correlation of lithostratigraphic units and chemical suites.

overlying volcanics by the absence of olivine and the presence of plagioclase microphenocrysts. These lavas are correlative with the classical "Lower Pillow Lava" sequence.

Chemically, the extrusive rocks in this unit are enriched in Fe, Ti, and all the incompatible trace elements relative to the overlying lavas. These features are characteristic of the "arc-tholeiite" suite of volcanics delineated in the massif by Robinson et al.,(1983).

2) Units II and III are distinguished from Unit I by the presence of olivine, and from each other by the relative abundance of olivine phenocrysts (<5% for Unit III, and >5% for Unit II). Together, these units comprise the classical olivine-phyric "Upper Pillow Lava" sequence.

Chemically, the extrusive rocks in both of these units are strongly depleted in the incompatible trace elements (relative to Unit I lavas), and contain high concentrations of MgO for the observed SiO2 content. These features are characteristic of the "boninite" suite of volcanics delineated by Robinson et al., (1983). Units II and III can also be separated by the relatively even more incompatible element depleted nature of the rocks of Unit III. This chemical division, however, is not quite coincident with the mapped lithologic boundaries of the two units, differing by the inclusion of the "glassy" olivine phyric pillows,(lithology II-B), in with chemical Suite B_2.

CHAPTER FIVE

ULTRAMAFIC LAVAS

5.1 General Statement

Considerable attention has been paid to the "ultrabasic lavas" that occur in the Margi area of Cyprus (Gass, 1958; Searle and Vokes, 1969; Malpas and Langdon, 1982; and Wang, 1983). The petrographic features of these rocks were well described by Gass (1958), who recognized two varieties of ultrabasic rocks which he respectively termed "vitrophyric" and "holocrystalline", reflecting the crystalline state of the groundmass. As illustrated in Chapter Four, all of the samples are, in some ways, compositionally similar to peridotites and peridotitic komatiites. This fact led Gass (1958), and Searle and Vokes (1969), to hypothesize that these rocks formed directly from high-magnesium, "peridotitic melts". The more recent work by Malpas and Langdon (1982), has shown that this is not the case. and that the ultrabasic nature of these rocks is due predominantly to the accumulation of olivine, which they suggest occurred within shallow level magma chambers prior to extrusion. This study supports this model to some extent, though there is strong evidence that much of the accumulation of olivine occurred within individual flow units after extrusion.

5.2 Mineralogical and Chemical Characteristics

The petrographic and chemical features of the ultrabasic lithologies (i.e. picrite-based flows and picritic pillows), were previously discussed in Chapters Two and Four. All of the samples are ultramafic as well as ultrabasic, containing between 30 and 70 modal percent olivine. A synthesis of the important features follows:

5.2.1 Picrite-based Flows (Lithology IID)

Most of the ultrabasic rocks in the Margi area occur as cumulate bases to massive flow units (see Figure III-3). The basal picritic zone is, suprisingly, relatively resistant to erosion and often forms a distinct ridge. This feature, along with the fact that the mineralogical transition from the picritic base to the aphyric flow interior is often quite sharp, has led many researchers to believe that these "ultramafic" zones are distinct flows, or intrusive units (e.g. Gass, 1958). The absence of clearly intrusive contacts, along with the absence of chilled margins between the picritic rocks and the overlying "aphyric zone", is cited as evidence for the formation of these units by the process of in-situ differentiation.

The chilled margins of these flows are poorly exposed, but when present, are typically only slightly olivine phyric. Simple volume calculations indicate that the majority of

these flows formed from lavas which contained approximately 10 to 15 % phenocrystic olivine at the time of extrusion, similar to the surrounding pillowed volcanics. Continued crystallizaton combined with redistribution processes after extrusion resulted in significant mineralogical and textural variations within these flows.

On the basis of modal mineralogy, the thickest flows can be divided into four zones: 1) A picritic base composed of approximately 50% olivine (Fo 88-93), 15% endiopside, 8% bytownitic plagioclase, along with minor chrome spinel and hypersthene. (This zone is equivalent to Gass's "holocrystalline" ultrabasic lavas. 2) A thin "olivine-pyroxené" transition zone with varying, though roughly equal, amounts of olivine, endiopside, and bytownite. 3) An aphyric, olivine-free, flow interior composed of nearly equal proportions of endiopside and bytownite (generally 30 to 40 modal % each). 4) A thin, olivine +/- clinopyroxene phyric flow top. It is important to note though, that the relative thicknesses of these "zones" are quite variable, and the picritic base can comprise anywhere from two-thirds (in the thinner flows), to less than one-fifth of the total flow thickness.

Schematic representations of the within flow mineralogic variation, along with the corresponding variations in trace and major element whole-rock chemistry, are shown for one of

the larger flows in Figures V-1 and V-2. The ultrabasic composition of the basal zone is clearly due to the presence of abundant olivine, which apparently accumulated by gravitative settling of phenocrysts shortly after extrusion. This phenomenon of "olivine settling" has been well documented in many areas: Kilauea (Murata et al., 1966); and Iceland, (Matthews et al., 1964).

The mineralogical zonation observed within these flows is, in some ways, similar to that observed in komatiitic flows (e.g. see Arndt, 1977). There are also many chemical similarities between the basal ultramafic portions of these two types of flows, and this has led some authors to refer to these rocks as "analogues of peridotitic komatiites" (Wang, 1983). Direct comparison of the ultramafic rocks of Cyprus to komatiites is misleading, however. One problem with making this analogy is that currently, there is no concensus as to the "definition" of a komatiite (Arndt et al., 1982). Chemical criteria such as MgO > 18%, and CaO/Al2O3 < 1 have been used by some authors to "recognize" komatiites (Brooks and Hart, 1974), though any olivine-rich rock, regardless of origin, will generally fit these criteria. This is an important point, for it is an implicit inference of the term komatiite that they are volcanic rocks which are "the direct crystallization products of ultramafic liquids", thereby excluding ultramafic cumulates which form by the settling of

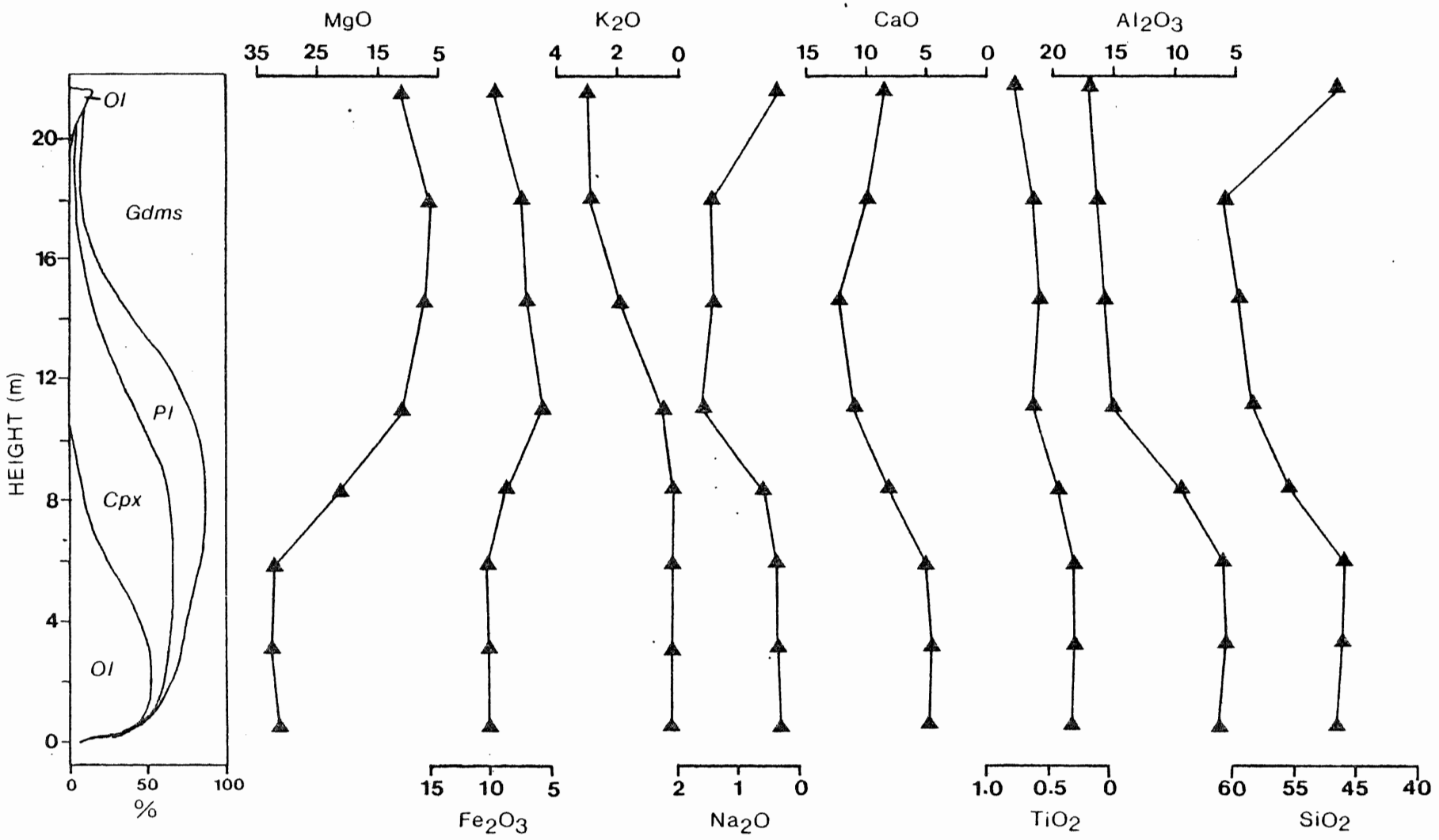

FIGURE V-1. Major element variation within a picrite-based massive flow. (See Figure II-2 for sample location)

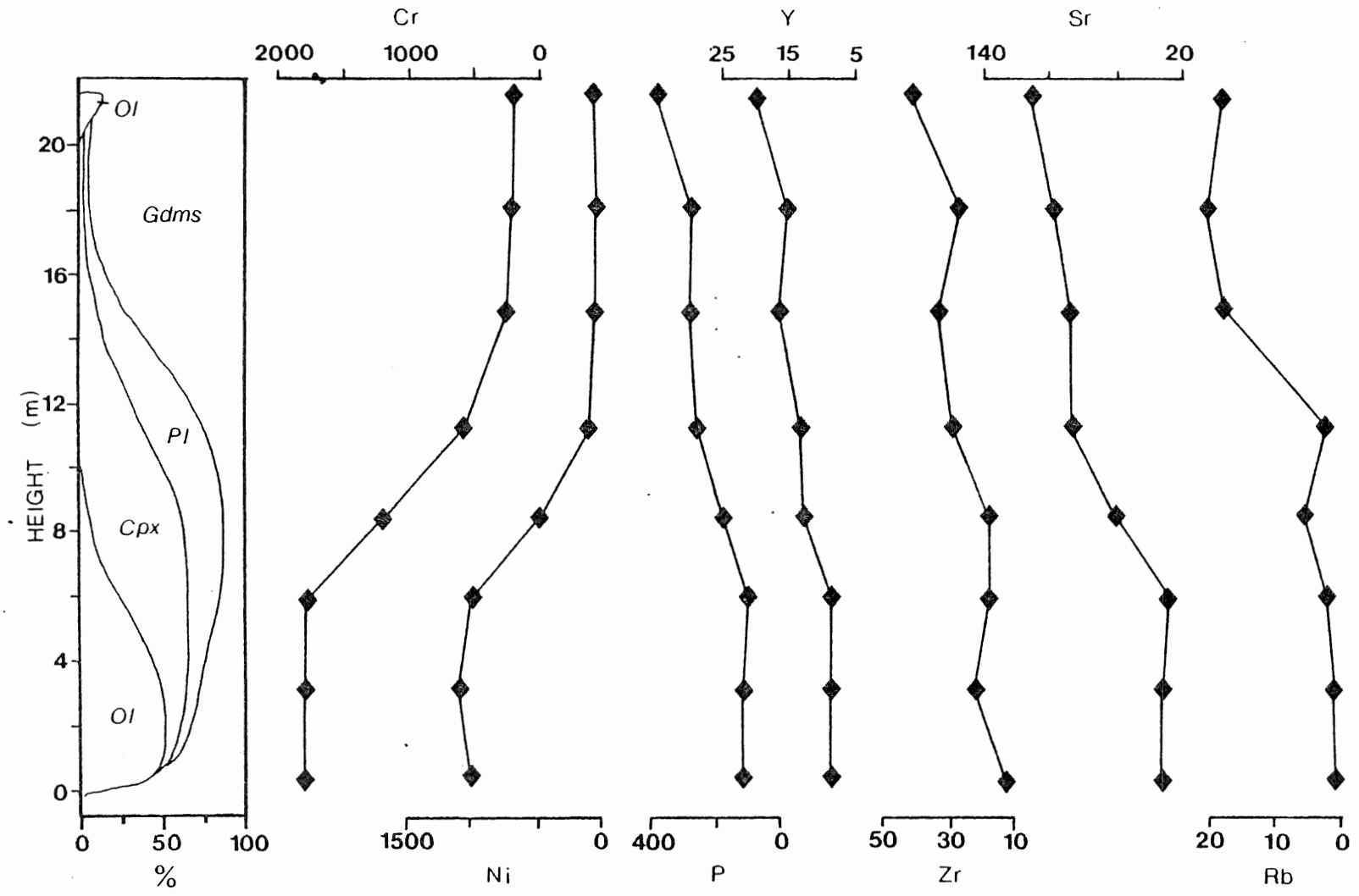

FIGURE V-2. Trace element variation within a picrite-based massive flow.

mafic minerals within basaltic flows (Cameron and Nisbet, 1982). This is perhaps the strongest argument for distinguishing the ultramafic lavas of Cyprus from komatiites, for they do occur predominantly as cumulate bases in large flows. Another point that should be emphasized is that, contrary to the observation of Searle and Vokes (1969), the olivine grains in these flow bases do show signs of disequilibrium, being rounded and corroded. This is further evidence that these ultramafic rocks did not crystallize directly from the surrounding liquid. Unfortunately, these arguments are not applicable to all the ultramafic lithologies observed in the Margi area, particularly the picritic pillows.

5.2.2 Picritic Pillows

Two small exposures of picritic pillows occur in the field area (See map 1; back pocket). Individual pillows are generally small (20 to 60 cm in diameter), spherical, and little altered (See Plate III-3). These rocks consist of 40 to 60% subhedral to euhedral olivine phenocrysts, along with minor chrome spinel, in a black glassy groundmass which contains quench clinopyroxene microlites. Olivine is homogeneously distributed within a single pillow, although there is a slight tendency for the largest grains to be concentrated in pillow cores. These rocks are equivalent to

Gass's "vitrophyric" ultrabasic lavas.

On the basis of whole-rock and mineral analyses, it is easy to show that these ultramafic pillows differ chemically from the surrounding lithologies almost entirely by the presence of olivine. The results of two least-squares mixing calculations are shown in Table V-1. These models show that by removal of approximately 60% olivine (along with minor clinopyroxene and spinel), it is possible to obtain "daughter" compositions that are indistinguishable from those of nearby "liquids".

Clearly, the abundance of olivine in these pillows can not be explained as a result of post-extrusion accumulation, and there is little petrographic evidence of disequilibrium (i.e. "rounded" grain boundaries).

5.3 Olivine-Liquid Equilibria

The distribution of ferrous iron and magnesium between olivine and liquid can be expressed as:

$$K_D = X(FeO)ol * X(MgO)liq./ X(FeO)liq * X(MgO)ol$$

where K_D is the distribution coefficient, $X(MgO)^{liq}$ is the mole fraction of MgO in the liquid phase, and X(FeO)ol is the mole fraction of ferrous iron(as an oxide) in coexisting olivine (Wood and Fraser, 1979). The value of K_D is dependent upon a large number of variables, some of which are discussed below.

TABLE V-1 Least-squares mixing calculations which relate the composition of the "ultramafic" lavas of the Margi area (sample #127), to the surrounding volcanics.

Model 1: #127 --> #38 + oliv + cpx + sp

Mineral Variables	Fractions	% of Cumulate
Olivine Fo91	0.60	0.95
Cpx En48Wo44	0.03	0.04
Chrome spinel	0.00	0.01

	SiO2	TiO2	Al2O3	FeO	MgO	Cr2O3	CaO	Na2O	K2O
#38	55.01	0.51	13.17	8.00	11.54	0.12	10.23	1.17	0.26
#127									
Obs.	45.98	0.24	5.06	8.12	35.35	0.37	4.47	0.28	0.13
Calc.	45.98	0.19	4.93	8.16	35.34	0.37	4.47	0.49	0.10

R2 = 0.05

Model 2: #127 --> #181 + oliv + cpx + sp

Mineral variables	Fractions	% of Cumulate
Olivine Fo91	0.63	0.95
Cpx En48Wo44	0.03	0.05
Chrome spinel	0.00	0.01

	SiO2	TiO2	Al2O3	FeO	MgO	Cr2O3	CaO	Na2O	K2O
#181	55.46	0.63	14.89	8.07	8.18	0.05	11.10	1.38	0.23
#127									
Obs.	45.98	0.24	5.06	8.12	35.35	0.37	4.47	0.28	0.13
Calc.	45.57	0.22	5.05	8.16	35.35	0.36	4.50	0.52	0.08

R2 = 0.07

Mineral Compositions used in models:

	SiO2	TiO2	Al2O3	FeO	MgO	Cr2O3	CaO	Na2O	K2O
Oliv	40.44	-	-	8.33	50.76	0.15	0.22	0.10	-
Cpx	52.91	0.27	2.59	5.34	16.78	0.82	21.29	-	-
Sp	-	0.20	11.64	16.63	13.75	57.72	0.06	-	-

(Olivine composition is "representative" phenocryst analyses from sample #127. Clinopyroxene and spinel compositions are "representative" phenocryst / microphenocryst analyses from an unaltered pillow (sample #154A), which is petrographicalaly and chemically similar to samples #38 and #181.)

Experimental studies and theoretical calculations (at 1 atm), have shown that the distribution coefficient (K_D) is relatively independent of temperature, at least over the temperature range of 1000 to 1400°C (Roeder and Emslie, 1970). The compositional dependence of the distribution coefficient is also known to be slight over the range of naturally occurring basaltic magma compositions, although variation does exist, depending particularly upon the degree of silica saturation of the liquid (Takahashi, 1978; Ford et al., 1983). The effect of pressure is not well-known, but for most basaltic magmas, the results of the 1 atm experiments and calculations can be applied with reasonable confidence. The effect of volatiles on the distribution coefficient is again not well known, and this may be a severe limitation to the general applicability of this equation, for the addition of volatile components drastically modifies the structure of silicate melts and, in turn, the activities of its components (Takahashi, 1978).

Nevertheless, Roeder and Emslie (1970) demonstrated that for most natural basaltic magmas, the composition of coexisting olivine depends largely on the ratio of ferrous iron to magnesium in the liquid. The relationship between total iron and ferrous iron is, in turn, dependent upon the fugacity of oxygen in the melt.

Unfortunately, very few of the samples collected for

this study were analyzed for both ferrous and ferric iron. This was primarily because most of the samples have been altered and weathered, with the result that much of the ferrous iron has been oxidized. As an attempt to ascertain the primary ferric/total iron ratio of extrusives in the Margi area, samples of glass and "fresh" pillows were powdered and analyzed for ferrous iron by wet chemistry at Dalhousie University. To avoid patches of secondary mineralization, the glass samples were crushed to approximately 0.50 mm and hand picked before powdering. These samples were also analyzed for total iron by atomic absorption. The results of these measurments are shown in Table V-2. The glass samples contain very low concentrations of ferric iron (< 0.50 wt.%), and in fact, these values may be anonamously low due to analytical errors, for in three samples total iron values were lower than those measured for just ferrous iron! On the other hand, the significantly higher values (around 2 wt. %), observed in the whole-rock samples are probably anonamously high as a result of alteration (for smectites are abundant throughout the groundmass of these samples). Thus, we appear to have a minimum ferric/total iron ratio of approximately 0.02 (mean glass), and a maximum ratio of around 0.26 (mean whole-rock). For lack of better data, the following algorithm was used to set $Fe_2O_3/FeO + Fe_2O_3$ to the "standard" (and intermediate!)

TABLE V-2 Ferrous and ferric iron concentrations in glass and "unaltered" pillow samples from the Margi area (All analyses expressed as oxide weight percents).

GLASS SAMPLES

	FeO*	FeO	Fe2O3	Fe2O3/FeO+Fe2O3
#10	7.59	7.44	0.16	0.02
#16	8.06	7.63	0.48	0.06
#32	8.10	7.82	0.31	0.04
#38	7.37	7.51	-	-
#60	8.00	7.97	0.03	0.01
#86A	7.24	7.33	-	-
#86B	7.47	7.77	-	-
				Mean 0.02

WHOLE-ROCK SAMPLES

	Fe2O3x	FeO	Fe2O3	Fe2O3/Fe2O3+FeO
#5	8.51	5.72	2.12	0.27
#10	8.25	5.60	2.04	0.27
#28	8.23	4.86	2.67	0.35
#35	8.26	4.86	2.79	0.36
#38	8.36	6.04	1.56	0.21
#86	7.91	6.00	1.20	0.17
#91	8.41	5.57	2.23	0.29
#97	8.10	5.34	2.08	0.28
#154a	7.95	5.84	1.38	0.19
#163a	8.43	5.78	1.93	0.25
#181	8.48	6.16	1.55	0.20
				Mean 0.26

FeO* = Total iron as measured by atomic absorption.
Fe2O3x = Total iron as measured by XRF and corrected for loss of volatiles.
FeO = Ferrous iron as determined by wet chemistry.
Fe2O3 = Calculated ferric iron.

value of 0.15:

$Fe_2O_3 = 0.152 * (FeOtot) + 0.0073$

$FeO = 0.863 * (FeOtot) - 0.0065$ (Zentilli, pers.comm.)

Olivine analyses were obtained with an energy dispersive microprobe system and, as a result, ferric and ferrous iron were not distinguished. This is not a significant problem though, for olivine incorporates very little ferric iron into its structure, and the ferric iron that is observed in olivine analyses (generally less than 10% of total iron), is largely due to contamination from spinel inclusions or alteration (Deer et al., 1966). Therefore, for the following calculations it is assumed that: $X(FeO)ol = X(FeOtot)ol$.

Roeder and Emslie (1970) experimentally determined K_D values for olivine/liquid pairs, and concluded that, for most natural basaltic compositions, K_D was approximately equal to 0.30. It is important to note that the K_D values they obtained ranged from 0.26 to 0.36, and that an analytical error of +/- 2% forsterite in the determination of the olivine composition can change the calculated K_D value from 0.29 to 0.34!

With these limitations and assumptions in mind, we can examine the chemical equilibrium of olivine phenocrysts in the extrusive rocks of the Margi area, and particularly, within the ultramafic lithologies. Four samples, for which coexisting glass and groundmass olivine analyses are

available, provide us with the opportunity to calculate "equilibrium" K_D values, and indirectly test the validity of assuming $K_D = 0.30$.

FeO/MgO (mole %) values for coexisting olivine and liquid in these samples are plotted in Figure V-3, along with lines for constant K_D's of 0.20, 0.30, and 0.40. Observed K_D values range from 0.30 to 0.34, which is well within the range observed by Roeder and Emslie (1970), and three of the samples have K_D values of nearly 0.30, strongly supporting the use of this value for assessing equilibrium in the remaining extrusives.

A sample from the picritic pillows (sample #127), had a fresh glassy rind, providing us with a reliable "liquid" composition. Assuming a K_D of 0.30, this glass would be in equilibrium with olivine with a forsterite content of 88%. Groundmass olivine compositions in this sample are, in fact, Fo 88, however, phenocryst compositions in this sample ranged from Fo 91 to Fo 93 (see microprobe traverse, Figure III-1). These values are substantially higher than the "equilibrium" value of Fo 88 and, conversely, if these phenocrysts were in equilibrium with the observed liquid composition, it would imply K_D values of 0.18 to 0.25, which are well below any observed by Roeder and Emslie (1970)(see Figure V-3). Clearly, the large, abundant olivine phenocrysts in the "ultramafic" pillows crystallized from a liquid much more

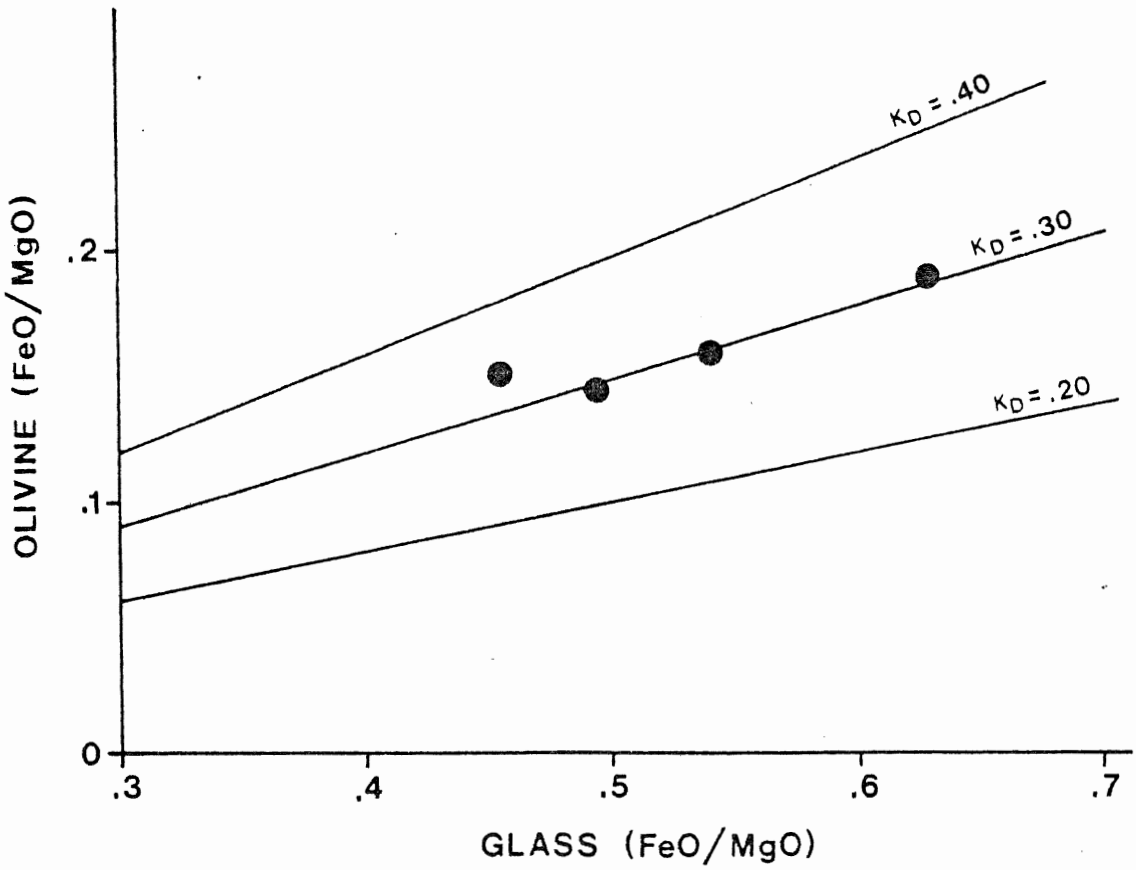

FIGURE V-3. FeO vs. MgO contents of coexisting olivine and liquid.

magnesium-rich than that with which they were extruded. In fact, to be in equilibrium with Fo92, a liquid would require a FeO/MgO ratio of approximately 0.32 which is very close to the values observed in samples from the "glassy" olivine phyric pillows (lithology IIB)(See Figure V-4).

5.4 Discussion

Searle and Vokes (1969) cited the following features to support their conclusion that the majority of the large olivine phenocrysts in the "ultrabasic" lithologies crystallized in-situ, even in the pillows, after extrusion:

1) That no picritic dikes or intrusives occur in the lower portions of the complex (i.e. that there is no evidence of highly phyric "feeders"); and 2) that there is a distinct lack of large olivine phenocrysts in the chilled rims of the ultramafic pillows and in the basal chilled margin of the larger flows.

With regard to item #1, picritic dikes <u>do</u> occur in the massif, having been observed in the Pedios canyon and south of Lythrodondas (Mehegan, pers.comm.,1984). With regard to item #2, the assumption that large olivine phenocrysts should be found in the chilled margins of the extrusives if they existed prior to eruption is, (particularly for the massive flows), poorly founded, for as shown by Bhattacharji and Smith (1964), the process of "flowage differentiation"

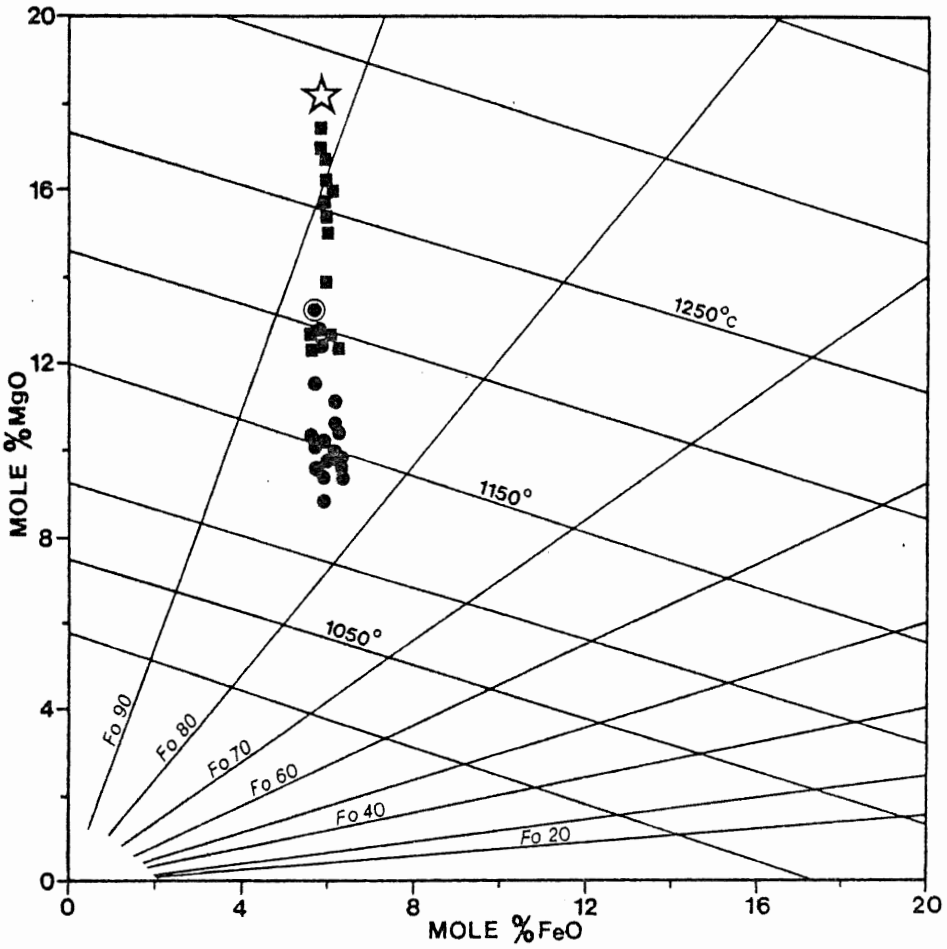

FIGURE V-4. Crystallization temperatures and compositions of olivines in equilibrium with liquids of known FeO and MgO contents. (Diagram from Roeder and Emslie, 1970). Symbols: squares = "glassy" lavas from Units II and III; circles = extrusive glass samples from Units II and III; star = theoretical parent liquid composition (see Chapter Six); outlined circle = glass sample from an "ultramafic" pillow.

effectively prevents the formation of porphyritic chilled margins. The strongest petrographic argument against the formation of the olivine in-situ is the fact that the largest grains are found within the small, glassy, picritic pillows which also contain quench morphology clinopyroxenes. In fact, there is quite a strong inverse correlation between average olivine grain size and cooling unit thickness (and obviously. cooling rate as well), which not only refutes Searle and Vokes' (1969) hypothesis, but also strengthens the conclusion reached on the basis of mineral/liquid chemistry (above), that the abundant olivine grains are not in equilibrium with the melt in which they were extruded.

5.5 Summary

The ultramafic lavas from the Margi area of Cyprus owe their ultrabasic character to the presence of 45 to 65 modal percent olivine. The majority of the ultramafic rocks were not extruded as such, having formed by post-extrusion, gravitative settling of olivine phenocrysts from moderately phyric lavas. A small proportion were extruded as picritic lavas, but the large olivine phenocrysts in these rocks are clearly of xenocrystic origin. It is postulated that these highly picritic pillows and thin flows represent samples of cumulate olivine from a shallow level magma chamber that were mixed with small amounts of liquid and extruded as a

crystal/liquid mush during periods of advanced tapping. The abundance (>50%), size (up to 20mm), and composition (>Fo90) of the olivine, as well as the presence of broad "kink bands" in some of the grains, are all features that are compatible with formation in a high-temperature environment such as a magma chamber floor.

CHAPTER SIX:

PETROGENESIS

6.1 General Statement

The composition of any igneous rock is the product of a large number of complex physio-chemical processes. Partial melting (equilibrium / disequilibrium), fractional crystallization (open / closed system), magma mixing, liquid immiscibility, assimilation, and deuteric alteration are but a few of the many possible processes. Determining which, and to what extent, individual processes have influenced the composition of a particular rock, or suite of rocks, is a problem that is not easily solved.

The role of fractional crystallization (crystal-liquid separation in particular), in modifying basaltic rock compositions has been shown to be one of the most important in many natural systems. For this reason, the emphasis of this chapter will be on ascertaining whether or not the observed chemical and petrographic variations in the extrusive rocks of the "boninite" suite in the Margi area are compatible with a simple model of fractional crystallization and, if not, examining other processes which may have been responsible for the observed discrepancies. A brief discussion of the tectonic environment in which these volcanic rocks formed is also included.

distribution of a single component is, conversely, strongly dependent upon temperature. Roeder and Emslie (1970) derived two linear expressions for the relationship between temperature and the mole proportions of FeO and MgO in the solid and liquid phases. Unfortunately, these equations were derived from a limited range of natural basaltic compositions, and do not take into account many of the possible influencing variables noted in Chapter Five (i.e. pressure, liquid composition etc). Ideally, the relations in this system should be examined thermodynamically, however, this is currently not possible, for the mixing properties and activities of species in multi-component silicate liquids are extremely complex and not fully understood (Wood and Fraser, 1978). Ford et al. (1983), took an alternative approach, and experimentally examined a wide range of natural basaltic compositions which crystallize olivine, and derived empirical expressions to represent, as closely as possible, individual component activities. The general form of their equation is:

$$\ln[X(i)ol/X(i)lq] = C_0 + C1/T + C2(P-1)/T + C_3\ln[1.5(X(mg)lq+X(fe)lq+X(ca)lq+X(mn)lq+X(cr)lq+X(ni)lq)] + C_4\ln[3X(si)^{lq}] + EC(j)\ln[1-X(j)lq]$$

where X( ) represents the cation fractions of the designated components in the superscript phases; (i) represents any one of the components Mg, Fe, Ca, and Mn; (j) represents any one of the components Al, Fe3+, Ca, Na+K, Ti and P; C_0, C_1 ...Cn

are the regression coefficients for the designated component (i) as determined by Ford et al. (1983)(See their Table 2 for values); T = temperature in degrees Kelvin; and P = pressure in bars.

Temperatures can be obtained from the above equation either by solution for the partition of a specific cation (i.e. Fe, Mg, Ca or Mn), between a particular liquid / olivine pair or from a liquid composition solely. This follows from the requirement that the divalent cations in olivine must sum to 2/3 that of the total number of cations. By choosing an arbitrary temperature, the equation can be solved respectively for X(Mg), X(Fe), X(Ca), and X(Mn) in olivine, and if the sum of these components differs from 2/3, a new temperature estimate can be made. This can be done iteratively until the calculated sum of the divalent cations in the "equilibrium" olivine is sufficiently close to 2/3. (See Ford et al. (1983) for a more comprehensive evaluation of this procedure.) The resulting temperature estimates are referred to as T(Mg), T(Fe), T(Ca), T(Mn), and T(sum), respectively. The results obtained by Ford et al. indicate that the calculated T(sum) values are the most accurate, and differ only slightly (average less than 10°C) from experimentally determined values in over 700 natural magmas.

A computer program based on the above equation was written in order to calculate values of T(Mg), T(Fe), and

T(sum) for samples of this study. It should be noted that many of the "liquid" samples used in these calculations were not analyzed for Mn, Ni, or Cr. While not major components, they do influence equilibrium conditions slightly, and thus, add another degree of uncertainty to the calculated temperatures. In all of these calculations, pressure was assumed to be 1 bar.

Results:

The calculated values of T(Mg), T(Fe), and T(sum) for approximatly 15 samples are listed in Table VI-1. The samples are of two distint types: 1) actual glass samples, and 2) "glassy" whole-rock samples, all of which are believed to represent liquids in equilibrium with olivine. "Groundmass" olivine analyses were used for calculation of T(Mg) and T(Fe) for the glass samples, whereas phenocryst analyses were used in conjunction with the whole-rock samples.

The results for the most "primitive" compositions sampled indicate that olivine (Fo90) became a liquidus phase at around 1280°C. The initial liquidus temperature of olivine in the actual parental magma, however, may have been substantially higher (around 1300°C). Along with fractionation, succeeding liquidus temperatures became lower (and olivine compositions more fayalitic), down to an observed minimum of around 1150°C.

TABLE VI-1 Liquidus temperatures for olivine as calculated with the geothermometer of Ford et al.,(1983). (P=phenocryst; G=groundmass; g=glass).

Sample ID	Olivine ID	Ol.Comp.	T(sum)	T(Mg)	T(Fe)
38	38-2 (P)	Fo 90	1281	1279	1235
10	10-3 (P)	89	1278	1271	1260
97	97-5 (P)	89	1266	1257	1261
35	35-2 (P)	88	1261	1251	1247
127g	127-2 (G)	(86)	1215	1209	1209
35g	35-5 (G)	(85)	1207	1204	1182
182g	-	-	1207	-	-
181	-	-	1199	-	-
154	154-2 (P)	87	1196	1189	1190
86	86-4 (P)	87	1198	1188	1232
38g	38-4 (G)	87	1184	1167	1220
10g	10-4 (G)	86	1160	1140	1196
86g	86-2 (G)	84	1147	1126	1176

Estimating the initial liquidus temperature of clinopyroxene is a bit more difficult. All of the samples with olivine liquidus temperatures above 1200oC lack discrete clinopyroxene grains (although quench microlites are abundant), implying that clinopyroxene was not a liquidus phase above this temperature. The first samples which contain both clinopyroxene and olivine phenocrysts have olivine liquidus temperatures ranging from 1190 to 1200oC. Unfortunately, these are whole-rock samples, and the calculated temperatures are only indicative of the initial temperature of olivine crystallization, which does not neccessarily coincide with the initial phase of clinopyroxene crystallization.

A more exact liquidus temperature for clinopyroxene can be inferred from glass samples #10 and #86. Sample #86 comes from a pillow which contains both olivine and clinopyroxene phenocrysts and groundmass grains. A liquidus temperature for the groundmass olivine in this sample of 1147oC therefore provides a lower limit for the clinopyroxene liquidus, for clearly, clinopyroxene became a liquidus phase above this temperature. Glass sample #10, on the other hand, contains only small grains of olivine and has a calculated liquidus temperature of 1160oC. Thus, it is suggested that clinopyroxene became a liquidus phase between 1147 and 1160oC; or roughly around 1155oC.

The liquidus temperature of plagioclase can not be estimated from this study, for it was not a crystallizing phase in any of the "liquids" sampled, occurring only within the crystalline groundmass of thick extrusive units. Clearly though, it became a liquidus phase at some temperature below 1145°C.

In summary, the partitioning of ferrous iron and magnesium between coexisting liquid and olivine provides a useful means of estimating liquidus temperatures of crystallizing phases in basaltic magmas when experimental methods are unavailable. The geothermometer of Ford et al. (1983), in conjunction with petrographic examinations, indicate the following phase relations for the extrusive rocks in Units II and III:

Olivine in: >1280°C
Clinopyroxene in: 1155°C
Plagioclase in: <1145°C

6.3 Closed-System Fractional Crystallization

In order to avoid as many of the effects of post-extrusion fractionation and alteration as possible, the samples examined in this section are once again limited to glass and homogeneous, glassy pillows from Units II and III. Figure VI-1 is a projection of these compositions from silica onto the plane Ol-Plag-Cpx of the normative basalt system, (analagous to the plane Fo-An-Di in the normative basalt tetrahedron of Yoder and Tilley, 1962). The trends followed

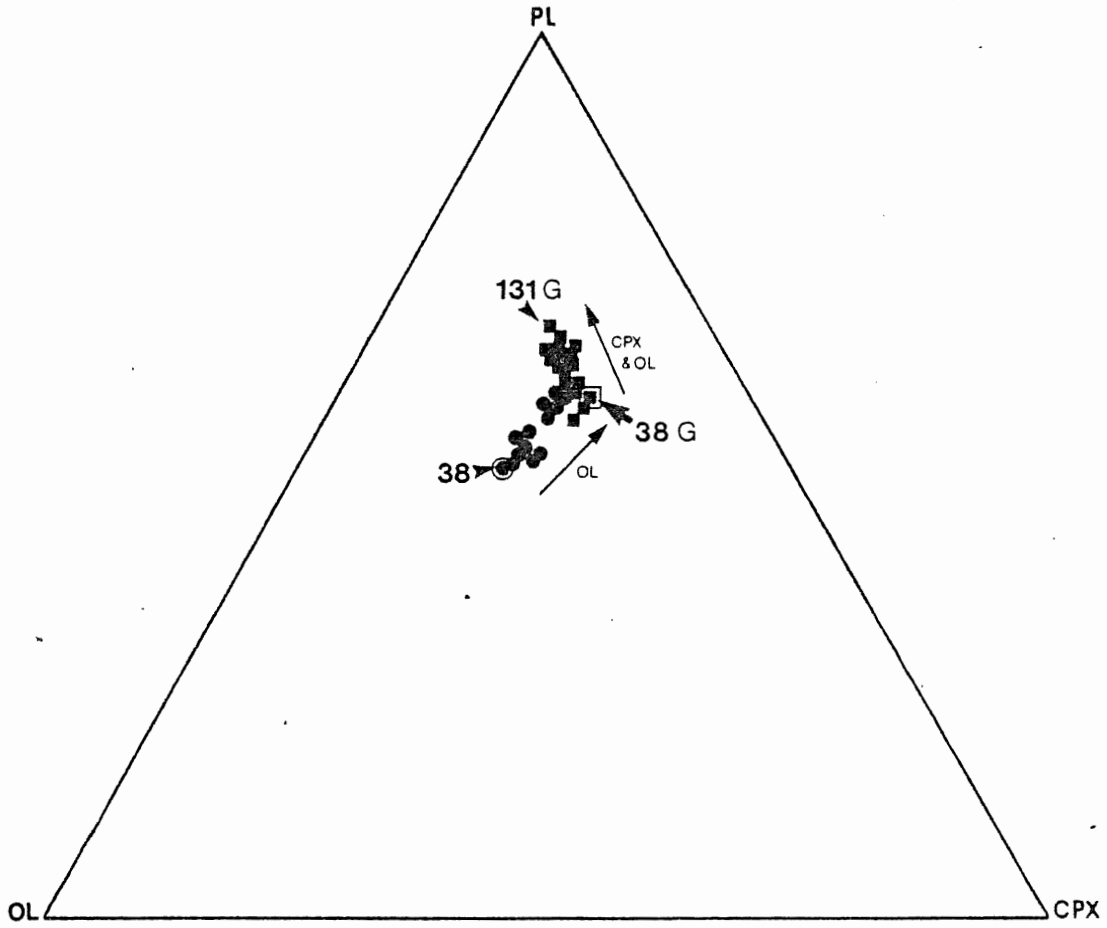

FIGURE VI-1. Whole-rock and glass compositions projected from silica onto the plane Ol-Plag-Cpx of the normative basalt system. Symbols: solid circles = "glassy" whole-rock samples from Units II and III; solid squares = extrusive glass samples from Units II and III. Numbers refer to samples used in computer modelling (see text).

by the plotted samples suggest removal of olivine followed by clinopyroxene fractionation. This supports the petrographically observed phase relations discussed above.

A much more comprehensive method of examining the process of closed-system fractional crystallization involves the use of a computer "mixing" program. Designated "parent" and "daughter" compositions are thereby related by removal and/or addition of assigned phase variables. Table VI-2 summarizes the results of three least-squares mixing calculations. The first calculation is an attempt to model the derivation of the most "evolved" glass (#131), from the most "primitive" whole-rock sample (#38) (See Figure VI-1). The "fit" of this first calculation is quite good (sum of the squares of the differences = 0.38), with most of the deviation due to relatively low Na_2O values in the whole-rock sample. This can be easily explained by depletion during alteration (See Chapter Four). The results of this calculation indicate that removal of approximately 11% olivine and 11% clinopyroxene from the parent can account for the total range of observed "liquid" compositions in Units II and III.

The two remaining calculations (Table VI-2b+c), in effect, divide the fractionation sequence into two segments. The first examines the relationship between the whole-rock and glass composition of sample #38, which is known to be

TABLE VI-2 Least squares mixing calculations for modelling crystal fractionation in the extrusives of the Margi area.

A) Model 1: #38 --> #131g + ol + cpx

Mineral Variables	Fraction	% of Cumulate
Oliv Fo88	0.11	0.49
Cpx En50Wo41	0.11	0.51

	SiO2	TiO2	Al2O3	FeO	MgO	CaO	Na2O	K2O
131g	56.63	0.68	16.45	7.77	5.64	10.37	2.24	0.24
38								
Obs.	55.01	0.51	13.17	8.00	11.54	10.23	1.17	0.26
Calc.	54.34	0.55	13.10	7.96	11.57	10.28	1.75	0.16

R2 = 0.38

B) Model 2: #38 --> #38g + ol + cpx

Mineral Variables	Fraction	% of Cumulate
Oliv Fo88	0.10	0.98
Cpx En50Wo41	0.00	0.02

	SiO2	TiO2	Al2O3	FeO	MgO	CaO	Na2O	K2O
38g	55.70	0.55	15.01	7.59	7.43	11.57	1.93	0.21
38								
Obs.	55.01	0.51	13.17	8.00	11.54	10.23	1.17	0.26
Calc.	53.65	0.49	13.34	7.96	11.59	10.33	1.71	0.19

R2 = 0.40

TABLE VI-2 (cont)

C) Model 3: #38g --> #131g + ol + cpx

Mineral Variables	Fraction	% of Cumulate
Oliv Fo88	0.01	0.04
Cpx En50Wo41	0.12	0.96

	SiO2	TiO2	Al2O3	FeO	MgO	CaO	Na2O	K2O
131g	56.63	0.68	16.45	7.77	5.64	10.37	2.24	0.20
38g								
Obs.	55.70	0.55	15.01	7.59	7.43	11.57	1.93	0.21
Calc.	56.46	0.62	14.74	7.59	7.41	11.52	1.97	0.18

R2 = 0.05

Mineral Compositions:

	SiO2	TiO2	Al2O3	FeO	MgO	CaO	Na2O	K2O
Oliv.	39.75	-	-	11.76	48.35	0.14	-	-
Cpx.	53.77	0.20	2.46	5.76	17.99	19.82	-	-

(Olivine and clinopyroxene compositions are "average" phenocryst analyses from unaltered pillows in Unit II.)

controlled by olivine fractionation, for the only phenocryst phase observed in the whole-rock sample is 9% olivine. The calculated model shows that the two compositions can be related by removal of 10% olivine from the whole-rock sample; a result which is in excellent agreement with the petrographic observations.

The final calculation derives the most evolved glass (#131), from the previous daughter (#38 glass). The results of this calculation are presented in Table VI-2c, and show that these samples are related almost entirely by fractionation of clinopyroxene (12%). It is important to point out that while there does appear to be a distinct period during which magma evolution is controlled predominantly by olivine fractionation, followed by a period dominated by clinopyroxene fractionation (see Figure VI-1), the transition is not as abrupt as the above models suggest, as is evident from numerous samples containing phenocrysts of both phases.

On the basis of the preceeding discussion, one can conclude that the observed chemical variations in the extrusive rocks of the Margi area (Units II and III), are principally the result of closed-system fractional crystallization. This is a bit too simplified however, for as noted earlier, the most "primitive" (i.e. incompatible element depleted) lithologies occur at the very top of the

stratigraphic sequence (i.e. chemical Suite B_2), and this is difficult to explain in terms of simple fractional crystallization in a single magma chamber. One could postulate a vertically "stratified" chamber which, due to vertical temperature gradients, becomes more basic with depth, and hence, upon periodic tapping an inverted evolutionary sequence is formed in the stratigraphic pile. This explanation is difficult to accept in light of the field evidence, for it is hard to imagine that much liquid remained in the magma chamber after the extrusion of the highly olivine-phyric and picritic cumulate lithologies (i.e. lithologies II-B and II-C). Perhaps the strongest argument for concluding that Suites B_1 and B_2 are not related solely by fractional crystallization, however, is based on the trace element compositions of the two groups.

Table VI-3 is another least-squares mixing calculation which attempts to derive the "evolved" lithologies of Suite B_1 from the "primitive" lithologies of Suite B_2. As with the previous models, the program determines the "best fit" mixing solution on the basis of assigned whole-rock and mineral major element compositions. Using assigned partition coefficients for the distribution of specific trace elements between the mineral phases and the melt, the program then calculates the "theoretical" trace element abundances of the daughter, which, when compared to the observed values provide

TABLE VI-3 Least squares mixing calculation which examines the chemical relationship between Suites B_1 and B2.

Model: #38 --> #86 + ol + cpx

Mineral Variables	Fraction	% of Cumulate
Oliv Fo87	0.08	0.66
Cpx En48Wo43	0.04	0.34

	SiO2	TiO2	Al2O3	FeO	MgO	CaO	Na2O	K2O
#86	54.80	0.64	15.37	8.34	7.89	11.07	1.57	0.33
38								
Obs.	55.01	0.51	13.17	8.00	11.54	10.23	1.17	0.26
Calc.	52.54	0.55	13.25	8.38	11.53	10.38	1.34	0.28

R2 = 0.45

	Parent	Predicted	Observed
Zr	25	29	39
Y	14	16	17
V	209	231	241
Ni	202	85	66
Cr	807	576	326
Ti	3117	3486	4061

Mineral Compositions:

	SiO2	TiO2	Al2O3	FeO	MgO	CaO	Na2O	K2O
Oliv.	40.08	-	-	11.91	47.84	0.17	-	-
Cpx.	53.08	0.12	2.62	5.68	16.99	20.91	-	-

(Olivine composition is "average" phenocryst composition of sample #38. Clinopyroxene composition is "average" phenocryst composition of sample #86.)

a further test of the fractionation model (see Table VI-4 for values used in the following calculations).

The attempt to model the evolution of Suite B_1 compositions (sample #86) from B_2 compositions (sample #38) results in a reasonable major element fit, except for silica (see Table VI-3). Significant discrepancies arise, however, when one compares the predicted to the observed trace element concentrations of the daughter. In all cases, the predicted values for the incompatible elements are markedly lower than those observed, most notably titanium (3486 ppm predicted : 4061 ppm observed), and zirconium (29 ppm predicted : 39 ppm observed). The predicted values of the compatible elements (Ni and Cr) are higher than those observed, but the fractionation of these elements was difficult to model because accurate partition coefficients for a chrome-spinel phase are not available. Predicted values of these elements are therefore unreliable.

Even though most of the absolute differences in incompatible element concentrations are within the range of analytical and modelling errors, the fact that <u>all</u> of the predicted concentrations are consistently lower than those observed strongly suggests that simple fractional crystallization cannot explain the entire compositional variation between Suites B_1 and B_2.

Another related matter of interest is the origin of the

TABLE VI-4 Mineral / Liquid distribution coefficients used in modelling calculations.

	Olivine	Clinopyroxene	Plagioclase
Zr	0.01*	0.50*	0.03*
Y	0.01*	0.10*	0.01*
V	0.03#	0.70#	0.00#
Ni	10.00+	2.00+	0.01+
Cr	0.10x	10.00+	0.01+
Ti	0.02*	0.50#	0.04*

(*)-from Pearce and Norry (1979)
(#)-from Shervais (1982)
(+)-from Cox et al. (1979)
(x)-from Walker (pers.comm.,1983)

aphyric massive flows, (lithology II-E). As noted in Chapter Four, samples from this lithology are the most "evolved" of any of the rocks in Units II and III, with high TiO2 values (0.80 wt. %), and low MgO values (around 4.0 wt.%). It was previously suggested that these flows were derived by differentiation from the same parent as the surrounding lithologies. To test this hypothesis, and to examine its relationship to Suite B_1 and B_2 compositions, two least-squares mixing models were calculated (see Table VI-5a+b). The first model (VI-5a), attempts to derive the composition of one of the aphyric massive flows (sample #74) from Suite B_1 compositions (sample #86), while the second model (VI-4b) attempts to derive it from Suite B_2 compositions (sample #38). For both calculations the sum of the squares of the differences is high ($>$ 2.0), primarily as a result of the high K20 content of sample #74. This is almost certainly a result of alteration, as adularia is observed in the groundmass of this sample. Disregarding K20, the calculated major element compositions are then quite reasonable for both models (sum of the squares $<$ 0.40). In agreement with our previous observations, both models indicate that the major element composition of the aphyric massive flows can be related to the surrounding lava compositions essentially by removal of clinopyroxene (around 20%). In detail, however, the calculations show that the

TABLE VI-5 Least squares mixing calculations which derive the aphyric massive flows (sample #74) from chemical Suites B_2 (sample #38) and B_1 (sample #86).

A) Model 1: #86 --> #74 + ol + cpx

Mineral Variables	Fraction	% of Cumulate
Oliv Fo87	0.03	0.11
Cpx En48Wo44	0.22	0.89

	SiO2	TiO2	Al2O3	FeO	MgO	CaO	Na2O	K2O
#74	55.52	0.80	18.46	8.00	3.91	8.58	2.24	2.48
#86								
Obs.	55.23	0.65	15.49	7.56	7.96	11.15	1.58	0.33
Calc.	54.83	0.67	14.66	7.57	7.97	11.21	1.70	1.88

R2 = 2.59 (R2 - K2O = 0.19)

	Bulk K_D	Parent	Predicted	Observed	Residual
Zr	0.090	39	50	49	-1
Y	0.446	17	20	22	2
V	0.615	241	269	288	19
Ni	2.918	66	38	46	8
Cr	7.481	326	52	46	-6
Ti	0.440	4061	4758	4859	101

Mineral Compositions:

	SiO2	TiO2	Al2O3	FeO	MgO	CaO	Na2O	K2O
Oliv.	40.12	-	-	11.99	47.73	0.16	-	-
Cpx.	52.68	0.27	2.97	5.37	16.66	21.41	-	-

(Olivine composition is "representative" phenocryst composition from sample #86. Clinopyroxene composition is "representative" phenocryst composition from sample #154A which is petrographically and chemically similar to sample #86.)

TABLE VI-5 (cont)

B) Model 2: #38 --> #74 + ol + cpx

Mineral Variables	Fraction	% of Cumulate
Oliv Fo87	0.11	0.33
Cpx En48Wo43	0.22	0.67

	SiO2	TiO2	Al2O3	FeO	MgO	CaO	Na2O	K2O
#74	55.52	0.80	18.46	8.00	3.91	8.58	2.24	2.48
#38								
Obs.	55.01	0.51	13.17	8.00	11.54	10.23	1.17	0.26
Calc.	53.23	0.56	12.92	7.91	11.62	10.37	1.50	1.66

R2 = 2.22 (R2 - K2O = 0.29)

	Bulk K_D	Parent	Predicted	Observed	Residual
Zr	0.070	255	36	49	13
Y	0.337	14	18	22	4
V	0.477	209	258	288	30
Ni	4.657	202	47	46	-1
Cr	6.712	807	81	46	-35
Ti	0.341	3117	4062	4859	797

Mineral Compositions:

	SiO2	TiO2	Al2O3	FeO	MgO	CaO	Na2O	K2O
Oliv.	40.08	-	-	11.91	47.84	0.17	-	-
Cpx.	53.08	0.12	2.62	5.68	16.99	20.91	-	-

(Olivine composition is "average" phenocryst analyses of sample #38. Clinopyroxene compositon is "average" phenocryst composition of an olivine - clinopyroxene phyric pillow from Suite B_2 (sample #14).)

observed trace element compositions are more compatible with being derived from Suite B_1 compositions than from Suite B_2 compositions. Therefore, the previous conclusion that the unusual whole-rock and mineral compositions of the aphyric massive flows were simply the end result of differentiation of "typical" Unit II compositions appears justified. It should also be noted that, compositionally, samples from these flows are, in some respects, similar to those of the "intermediate" group of extrusive glass compositions delineated by Robinson et al. (1983). This suggests that it may be possible to derive these "intermediate" liquids by differentiation from the high-Mg, "boninite" suite of glass compositions (which is correlative with Units II and III of this study). Much more field and laboratory work is needed, however, before this can be adequately demonstrated.

The results of the above modelling once again emphasize the difference in trace element compositions between Suites B_1 and B_2, and it appears unlikely that the two can be related by any simple differentiation process.

6.4 Partial Melting and Parental Magmas

While it is not within the scope of this thesis to go into the details of magma genesis, (for much more geochemical data and experimental work are necessary), a brief discussion is in order.

As outlined above, low-pressure, closed-system crystal fractionation can explain much of the observed chemical variation in the extrusive rocks of Units II and III, except for the relatively depleted nature of the lavas at the top of the stratigraphic sequence. As mentioned in the introduction to this chapter, there are countless processes that may act upon and influence the final chemical composition of an igneous rock, starting with original source composition and ending with subaerial weathering. Nevertheless, for most basaltic rocks it is, as a first approximation, justified to assume that the two most influential processes are 1) fractional crystallization, and 2) partial melting. One of the most pronounced geochemical effects of partial melting which might explain the observed discrepancy is the rapid decrease in incompatible element concentrations with slight increases in the degree of partial melting.

Features of the plutonic rocks of the massif can be used to place constraints on the processes of magma genesis. The basal 1 kilometer of the plutonic sequence consists of homogeneous, foliated harzburgite (Ol:Opx:Cpx:Sp), which contains small, lenticular bodies of dunite and localized patches of plagioclase lherzolite (Allen, 1975). In light of the experimental data of Ringwood (1969), and Green (1971), Greenbaum (1972) suggested that the tectonized harzburgite represents depleted (plagioclase lherzolite) mantle. It has

been calculated that 25 to 30% partial melting of 15 to 25 kilometers of mantle lherzolite is required to explain the estimated volume of the overlying magmatic sequence (Allen, 1975). The exteremely low concentrations of the incompatible trace elements in the extrusive rocks of this study strongly support the contention that they were derived from a "highly depleted" mantle source.

In detail, the behaviour of individual trace elements varies markedly during partial melting and fractional crystallization and thus, the concentrations of these elements can indicate the relative importance of these two processes. Figure VI-2 is a logarithmic plot of chromium versus yttrium in samples from the Margi area. Chromium, being a strongly compatible element, will decline sharply during fractional crystallization. The concentration of yttrium, however, will be strongly influenced by the degree of partial melting of the source. On the diagram, the dashed line represents the equilibrium melting trend of a plagioclase lherzolite source, with olivine, orthopyroxene, clinopyroxene, and plagioclase entering the melt in the following ratios 3:1:4:4 (from Pearce, 1980; p.268). According to Pearce (1980), Cr and Y should not participate in the processes which cause mantle heterogeneity because they are elements which are compatible with a garnet lherzolite source. Therefore, the initial source region for

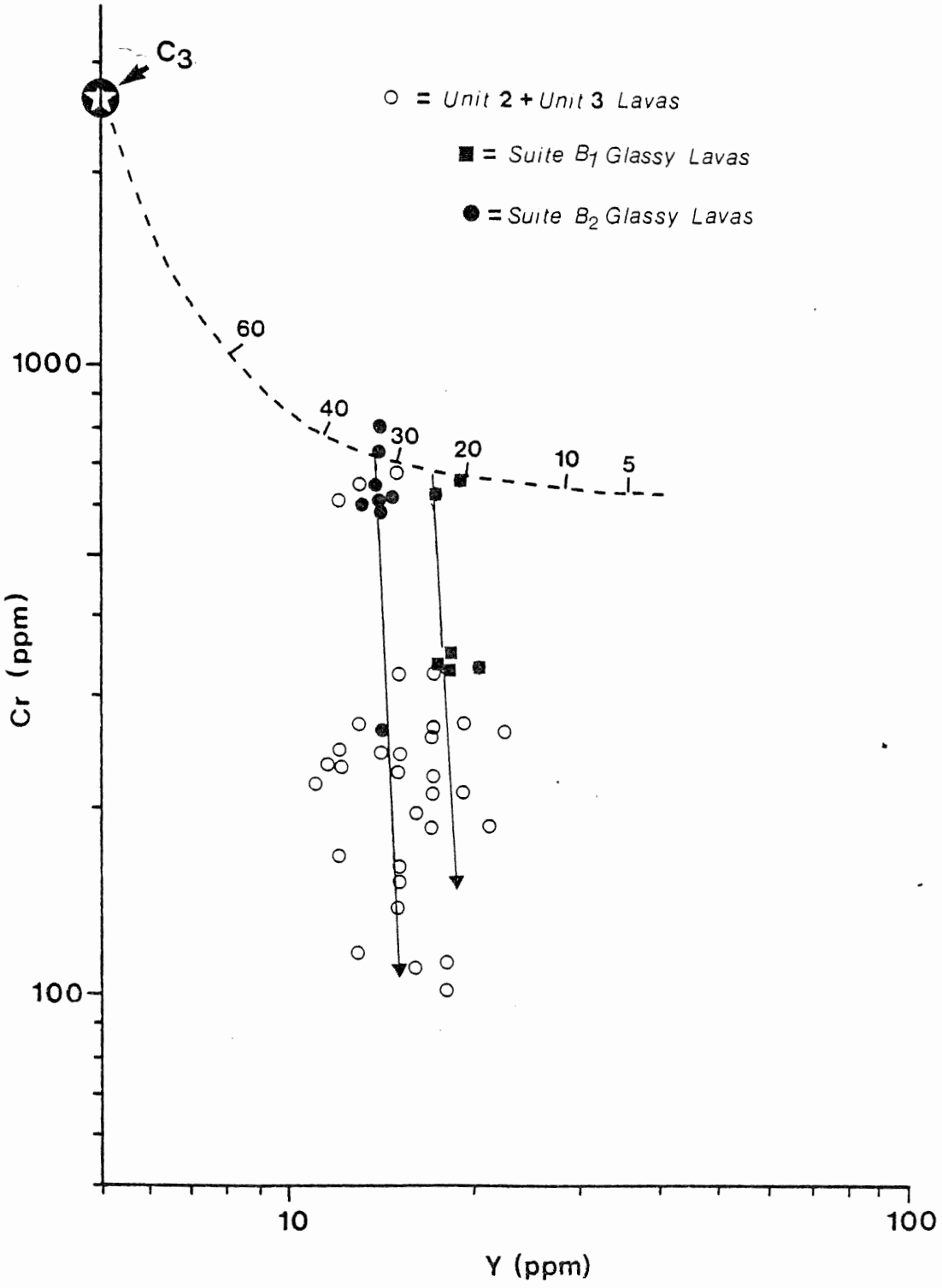

FIGURE VI-2. Modelled pathways of partial melting and fractional crystallization for Cr vs. Y.

the Troodos massif should have contained abundances of Cr and Y that were similar to those of primordial mantle (modelled here as that of C_3 chondrite). The nearly vertical lines represent closed-system fractionation of olivine, chrome-spinel, and clinopyroxene.

Although these pathways are based on a large number of assumptions (including initial source composition, mineral/liquid distribution coefficients, and style of melting and fracticnation), the diagram does illustrate a number of important features: 1) that all of the extrusive rocks in Units II and III were derived from a strongly depleted source, having undergone approximately 30% partial melting; 2) that the Cr and Y contents of the "glassy", Suite B_2 lavas are very close to those of the "theoretical" parent magma, and 3) that it is difficult to derive "unaltered" Suite B_1 type lavas from Suite B2 compositions by simple crystal fractionation, for any realistic fractionation trend will be subparallel to the chromium axis.

Figure VI-3 is a plot of titanium vs. vanadium concentrations in "unaltered" whole-rock samples from Suites B_1 and B2. Both are typically incompatible elements, however, the mineral/liquid partition coefficients for vanadium are highly dependent upon its valence state (+3, +4, or +5) which, in turn, is a function of the oxygen fugacity of the melt (Shervais, 1982). Using partition coefficients

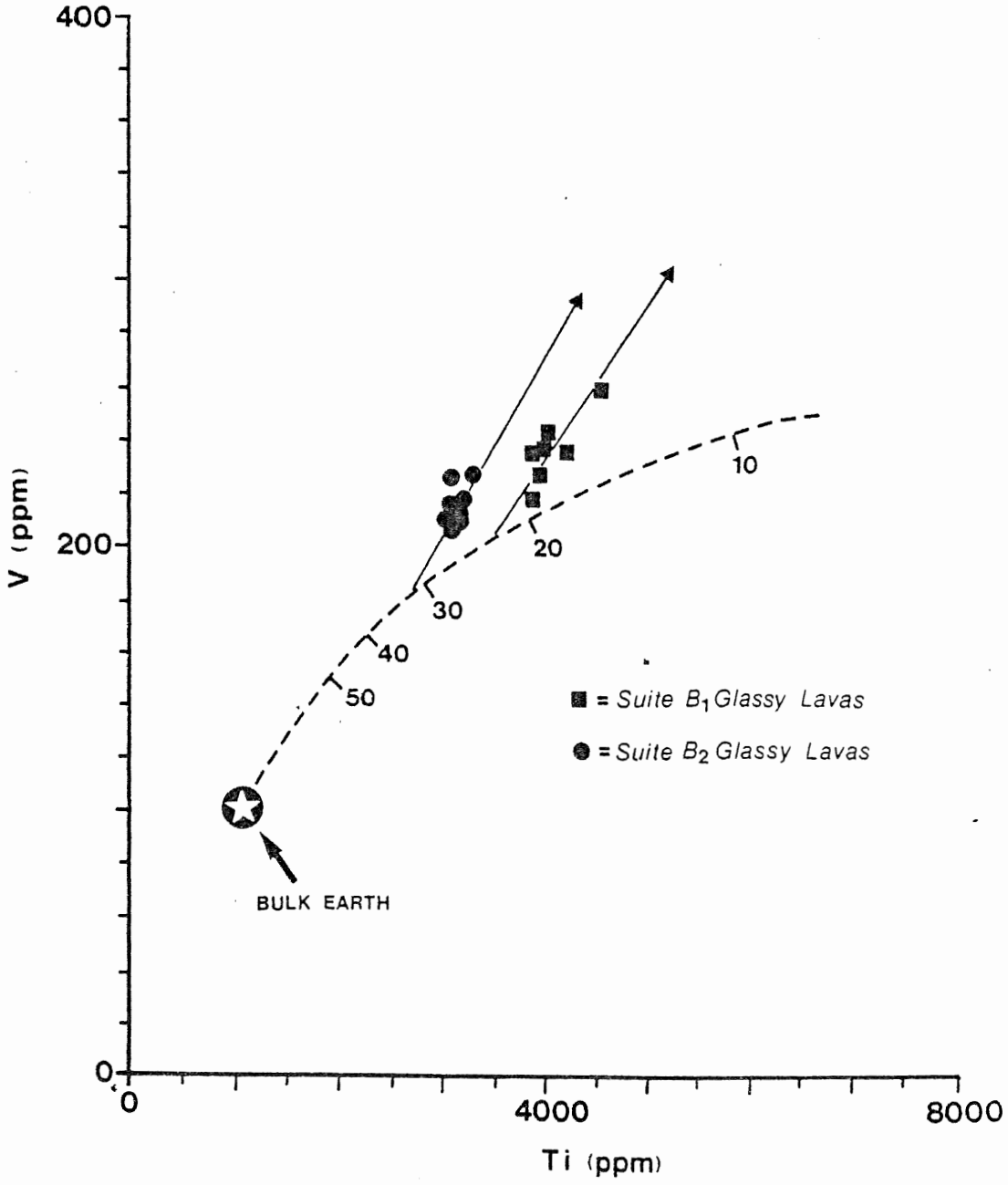

FIGURE VI-3. Modelled pathways of partial melting and fractional crystallization behavior for Ti vs. V.

determined by Shervais (1982) for vanadium (under conditions of log fO2 = -10), the genetic pathways of the extrusives of this study are modelled in terms of derivation from a bulk earth composition (after Shervais, 1982). The partial melting trend is a simple modal melting trend of a depleted spinel harzburgite source calculated from the batch melting equation of Wood and Fraser (1977). Such a model is clearly unrealistic, however, in view of the other uncertainties and assumptions, it is considered applicable for a first order approximation interpretation, particularly for high degrees of partial melting.

The diagram illustrates a number of interesting features which, in general, are consistent with the previous observations: 1) that the lavas of both Units II and III were derived from a source which has undergone 25 to 30% partial melting; and 2) that the Ti and V contents of the two suites cannot be related by simple fractional crystallization processes, for any fractionation trend will be nearly parallel to a line of constant Ti/V ratio.

It is suggested here that the differences in trace element concentrations between these suites are the result of slightly different degrees of partial melting, with Suite B_2 lavas representing the final (extruded) increment of partial melt in the Margi area. It is also suggested that the mean composition of the glassy, olivine phyric pillows (lithology

IIB), is only slightly removed from the parental magma composition of Suite B_2 and, in terms of solely major element chemistry, is also similar to that of the parental magma for Suite B_1. This is based on the following observations as well as on the modelling results discussed above: 1) chemically and petrographically the six samples from this lithology are remarkably homogeneous (see Table VI-6), 2) they are all in equilibrium with olivine (Fo 88-90), and chrome spinel, which are the predominant phases in the cumulate sequence of the massif (Laurent et al., 1980), and 3) the high olivine liquidus temperatures calculated for these samples (see Table VI-2), in combination with the relatively small size of olivine phenocrysts (generally <1.00 mm), and the remarkable quench textures preserved clearly indicate that the liquids which formed these rocks went rapidly from a very high temperature environment to being extruded. Clearly, crystal fractionation could not have played a major role in the formation of these rocks, though the possibility of slight addition or removal of olivine (and minor chrome spinel) should not be ignored. In fact, to produce olivine phenocrysts with compositions similar to those which are observed in the picritic lithologies (see Chapter Five), and the cumulate sequence (i.e. up to Fo 92), the parental magma clearly needed to be more magnesium-rich than the samples discussed. Reverse mixing calculations

TABLE VI-6 Chemical and petrographic features of samples from lithology IIB. (Oxides expressed as weight percent; trace elements expressed in parts per million).

Chemistry:

samp.#	#10	#28	#35	#38	#91	#97	Mean	(S.D.)
SiO2	54.23	53.24	53.57	54.06	54.20	53.57	53.81	(0.41)
Al2O3	13.46	13.48	13.73	12.94	13.49	13.47	13.43	(0.26)
TiO2	0.53	0.50	0.52	0.50	0.52	0.51	0.51	(0.01)
Fe2O3	8.86	8.78	8.95	8.74	8.97	8.64	8.82	(0.13)
MgO	10.94	9.83	10.33	11.34	10.53	10.88	10.64	(0.53)
CaO	10.13	10.63	10.43	10.05	10.82	10.56	10.44	(0.30)
Na2O	1.49	1.27	1.31	1.15	1.24	0.96	1.24	(0.18)
K2O	0.40	0.48	0.45	0.26	0.33	0.33	0.38	(0.08)
P2O5	0.05	-	0.02	0.04	0.02	0.06	0.03	(0.02)
TOTAL	100.09	98.22	99.31	99.07	100.12	98.97	99.30	(0.72)
(PPM)								
Ba	-	-	-	3	-	-	-	-
Rb	7	10	11	6	6	7	8	(2)
Sr	111	175	185	85	91	85	122	(46)
Y	14	14	13	14	14	15	14	(1)
Zr	34	35	25	25	24	31	29	(5)
Nb	-	-	-	-	-	-	-	-
Zn	68	63	62	62	60	59	62	(3)
Cu	62	67	64	59	64	62	63	(3)
Ni	129	131	128	202	157	144	149	(29)
Cr	614	621	601	807	601	681	654	(81)
Ti	3194	3135	3221	3117	3145	3238	3175	(50)
V	212	208	211	209	214	215	212	(3)

Petrography:

Phenocrysts:

	#10	#28	#35	#38	#91	#97	Mean
Oliv. %	6	6	8	9	8	6	7
Ave size(mm)	0.45	0.40	0.45	0.75	0.50	0.40	0.50
Max size(mm)	0.90	0.85	0.90	1.80	1.90	1.05	1.25
Compos.(Fo)	89	-	88	89	-	89	89
Groundmass:							
Quench Cpx %	55	55	40	70	55	50	55
Spinel %	2	tr	2	tr	tr	2	tr

indicate that by addition of approximately 4% olivine to the mean compositon of the glassy olivine phyric pillow samples, a theoretical parental magma can be produced which, on the basis of FeO/MgO partitioning, is in equilibrium with olivine compositions of Fo 92. Interestingly, the calculated parental magma composition need only contain 12.50 wt. percent MgO. It is therefore tempting to draw the conclusions of Chapter Five one step further and state that not only are ultramafic liquids not present in the extrusive sequence, but that they never existed during the magmatic evolution of the Troodos massif. Unfortunately, this can not be adequately substantiated at present and, aside from general petrological arguments to the contrary (e.g. Clarke and O'Hara, 1979), there is also substantial evidence for the presence of high MgO parental liquids in Cyprus in the form of fluid inclusions in olivines with MgO contents up to 16 wt.% (Malpas, pers. comm., 1984), and aphyric dikes in the plutonic sequence with MgO contents up to 17 wt. % (Dunsworth, pers. comm., 1984). Detailed experimental work on natural and synthetic materials with compositions similar to those of the lavas and "depleted mantle" of the Troodos massif, such as that currently underway at the University of Chicago, will hopefully resolve this problem.

6.5 Tectonic Environment

Much of the current interest in the Troodos Ophiolite is centered around determining the tectonic environment in which it formed, with the three most likely contenders being 1) at a major ocean ridge, 2) in a back-arc, or marginal basin, or 3) in an island-arc.

A wide range of tectonic "discrimination" diagrams for volcanic rocks have been put forth in the literature, almost all of which employ the HFS trace elements or mineral analyses as a means of "looking past" the chemical effects of alteration (Pearce and Cann, 1973; Pearce and Norry, 1979; Nisbet and Pearce, 1977; Shervais, 1982; Mullen, 1983). By using a number of these diagrams, one can, with some confidence, distinguish within-plate, ocean-ridge, and destructive plate margin (or island-arc) basalts. The extrusive rocks from Cyprus, including those of this study, often span the "ocean-ridge" and "destructive margin" fields on these diagrams, though in general, a strong "destructive margin" influence predominates (see Figure VI-4; and Pearce and Cann, 1971; 1973; Pearce, 1975; Nisbet and Pearce, 1977; and Pearce, 1980).

The paucity of pyroclastic deposits, and the presence of an extensive sheeted dike complex in the Troodos massif, along with overlying pelagic sediments, are features atypical of modern "island-arc" environments (Garcia, 1978). To

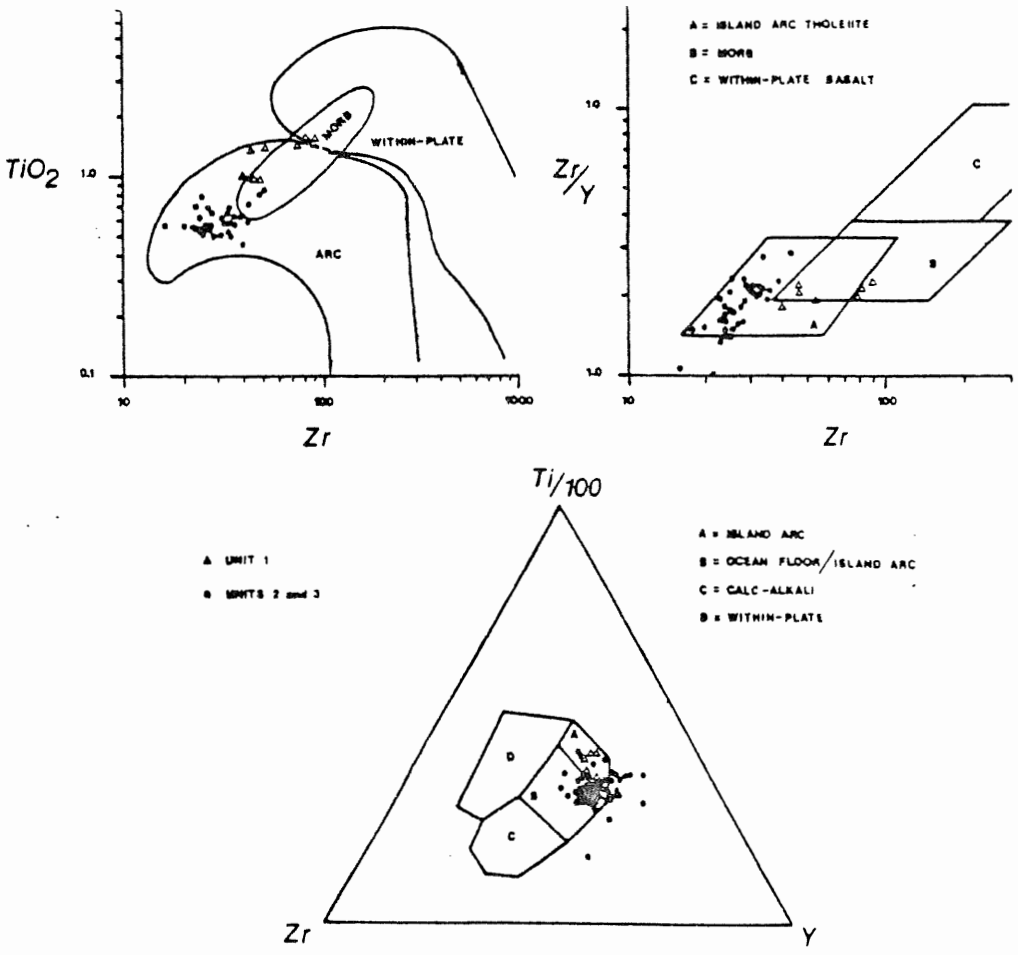

FIGURE VI-4. Trace element tectonic discriminant diagrams (from Pearce and Cann, 1971; 1973; and Pearce, 1980). All samples from the Margi area plot in the "island-arc" fields on these diagrams, although samples from Unit 1 (triangles) appear to have stronger "ocean-floor" affinities.

reconcile the apparantly contradictory field relations and chemical features, a number of researchers (e.g. Pearce, 1975), originally suggested that the massif formed in a "back-arc" or "inter-arc" basin, based primarily on the fact that existing back-arc basins are believed to be extensional in origin (Karig, 1970).

Chemically, however, most oceanic back-arc basin basalts are indistinguishable from major ocean ridge basalts, showing little evidence of subduction zone involvement (with the possible exception of high volatile contents)(Saunders et al., 1980; Dick, 1982). This observation, along with the fact that the only other in-situ occurrence of associated "arc-tholeiite" and "boninite" series volcanism is found in the Mariana and Bonin arc/fore-arc region, is evidence that the Troodos massif formed in an "island-arc", (and not a back-arc) environment.

The most recently proposed tectonic model for the formation of the Troodos Ophiolite is one which involves a complex arc and ridge/transform environment along the eastern margin of the Tethys sea (Moores et al., 1983). In this model, the Troodos massif is formed along a small spreading ridge immediately above a subduction zone. It is suggested by Moores et al.,(1983), that this unusual constructive / destructive environment was responsible, and perhaps essential, for the development and emplacement of all the

Tethyan Ophiolites.

The relationship between tectonic environment and petrogenesis is, of course, an important one. Unfortunately, a comprehensive petrogenetic / tectonic model for the formation of the Troodos Ophiolite has yet to be formulated. As previously noted, in the Bonin-Mariana region there is an association of "arc-tholeiite" and "boninite" volcanism similar to that which is observed in Cyprus, where an extrusive sequence with arc-tholeiite affinities is (generally) overlain by a high-magnesium, high-silica sequence with "boninitic" affinities. Because of these similarities, the model proposed for the formation of the Bonin-Mariana arc can also be used to partially explain the formation of the Troodos massif (Meijer, 1980; Crawford et al., 1981). Important features which the model incorporates are: 1) that boninite series lavas are clearly associated spatially and temporally with tholeiite series lavas, and generally, the boninite series lavas are younger than the tholeiites; 2) that boninite and arc-tholeiite series magmas are quartz-normative and contain high concentrations of volatiles; features which are currently accepted as being indicative of relatively shallow melting (Yoder and Tilley, 1962), and 3) that to produce high-magnesium, high-silica boninite-type lavas requires hydrous melting of depleted mantle (Kushiro, 1972; Green, 1976; Green, 1980).

For the Bonin-Mariana region it is therefore postulated that water from the subducted slab was responsible for initiating melting in the overlying mantle wedge at quite shallow depths. The melts produced were initially of arc-tholeiite composition and erupted to form a "typical" island-arc complex. Further melting of the depleted mantle, perhaps in response to mantle diapirism (Duncan et al., 1980; Crawford et al., 1981), finally produced "boninite" type melts which were extruded through the thin fore-arc crust.

Such a model explains the general chemical and stratigraphic relationships observed in both regions, however, it still does not explain the existence of an extensive sheeted dike complex in the Troodos massif. Present-day "island-arc" suites do not appear to have formed in such an extensional environment, and there are no documented "spreading ridges" that exhibit strong subduction related chemical traits. A model such as that put forth by Moores et al. (1983), where a ridge/transform system sits directly above a subduction zone. may create the neccessary environment for the formation of a suite of rocks chemically and structurally similar to the Troodos Ophiolite. Examination of similar modern-day environments (e.g. the Andaman Sea), is necessary to substantiate and expand this model.

6.6 Summary

Table VI-7 summarizes the associated magma chamber processes and extrusive activity envisoned for the Margi area. It essentially describes the geochemical evolution within a "periodically tapped, periodically replenished, continuously fractionated magma chamber" (a process which has been examined on a mathamatical basis by O'Hara, 1977; and O'Hara and Matthews, 1981). It should be noted, that although this "model" implies a small number of parental melt additions to the magma chamber, it is quite probable that many more additions of smaller amounts of magma may have occurred.

In detail, the field and geochemical features of the high-magnesium ("boninite") suite of volcanics in the Margi area are compatible with their having been derived from a continuously fractionated magma chamber which is periodically fed from a strongly depleted mantle source. Pre- and post-extrusion fractionation of olivine (up to 11%), clinopyroxene (up to 11%), and minor Cr-spinel appear to be the most important processes in controling major compositional variations within these rocks.

Incompatible trace element concentrations are consistent with derivation from a mantle source which has undergone 25 to 30% partial melting. It is suggested that the slightly lower concentrations of the incompatible elements in the

TABLE VI-7 Hypothetical magma chamber and associated extrusive activity for the Margi area, Cyprus.

	MAGMA CHAMBER ACTIVITY	EXTRUSIVE ACTIVITY
STAGE I	-Filling of chamber -Olivine fractionation	-None -(hiatus between Units I and II
STAGE II	-Tapping > Filling -Olivine and Cpx fractionation	-Formation of Unit II (Olivine + Cpx phyric lavas)
STAGE III	-Tapping >> Filling "Purging" of chamber	-Formation of Unit II (Highly Ol-phyric and picritic lavas)
STAGE IV	-Filling of chamber	-Formation of lithology IIB. (Extrusion of parental magma?)
STAGE V	-Tapping > Filling -Olivine and Cpx fractionation	-Formation of Unit III (Aphyric lithologies followed by Ol and Cpx-phyric rocks)

rocks at the top of the volcanic pile (Suite B_2), are the result of addition(s) of partial melt fractions to a shallow level magma chamber or feeder system.

CHAPTER SEVEN

SUMMARY

7.1 Data Presented

1) A detailed geologic map of the Margi area was compiled.

2) Petrographic observations were made on 110 rock samples.

3) Major element compositions of the following four mineral phases were presented: (approximate number of analyses in parantheses).

olivine (100) plagioclase (50)

pyroxene (200) spinel (40)

4) Seventy whole-rock samples were analyzed for nine major and thirteen trace elements.

5) Twenty-four extrusive glass samples were analyzed for nine major elements.

7.2 Conclusions

1) The volcanic rocks in the Margi area of Cyprus are highly variable in form (ranging from small pillows to massive flows), and lithology (ranging from aphyric to picritic). Ten distinct cooling unit lithologies were recognized and described

2) Three major lithostratigraphic units were identified:

UNIT III. Aphyric to sparsely olivine phyric pillows and thin flows

UNIT II. Olivine phyric to picritic pillows and flows

UNIT I. Aphyric and plagioclase / clinopyroxene microphyric volcanics

3) The boundary between Units I and II coincides with the previously mapped boundary between the classical Lower and Upper Pillow Lava sequences and is often marked by a thin layer of umberiferous sediment.

4) The boundary between Units I and II separates rocks which belong to two major chemical suites: Suite A (or Unit I) samples are generally basalts which contain high concentrations of FeO and TiO2 compared to the overlying lavas. These volcanics are correlative with the "arc-tholeiite" suite of extrusive compositions delineated by Robinson et al., (1983). Samples from Suites B_1 and B_2 (Units II and III) are basalt to basaltic andesite in composition, and contain relatively high concentrations of MgO, and low concentrations of TiO2 compared to samples from Unit I. These volcanics are correlative with the "boninite" suite of extrusive compositions delineated by Robinson et al., (1983).

5) The compositional variation within the rocks of the "boninite" suite in the Margi area can be largely explained by closed-system fractional crystallization of olivine (up to 11%), clinopyroxene (up to 11%), and minor chrome spinel.

6) Incompatible trace element concentrations of the "boninite" suite lavas are consistent with derivation from a strongly depleted mantle source which has undergone 25 to 30% partial melting. It is suggested that the slightly lower concentrations of the incompatible trace elements in samples from chemical Suite B_2 are the result of addition(s) of partial melt fractions to a shallow level magma chamber.

7) The "ultrabasic" lavas in the Margi area all contain 45 to 65 modal percent phenocrystic olivine. The majority of these ultramafic rocks formed by post-extrusion gravitative settling of olivine phenocrysts from moderately phyric lavas. A small portion were extruded as "picritic" lavas, but it is suggested that these represent samples of cumulate olivine from a magma chamber that were mixed with small amounts of melt and extruded as a crystal liquid mush during periods of advanced tapping.

Allen, C.R., (1975), The petrology of a portion of the Troodos complex, Cyprus., Ph.D. Thesis, University of Cambridge, Cambridge, England, 161p.

Arndt, N.T., (1977), Mineralogical and chemical variation in two thick, layered komatiitic lava flows., Carn. Inst. Wash. Year Book, p.494-502.

Arndt, N.T. and Nisbet, E.G., (1982), What is a komatiite?, In:Komatiites, Arndt. N.T., and Nisbet, E.G. (Eds.), George Allen and Unwin Pubs., London, p.19-28.

Augustithis, S.S., (1978), Atlas of textural patterns of basalts and their genetic significance., Elsvier Pub. Co., N.Y., U.S.A., 323p.

Bagnall. P.S., (1960), The geology and mineral resources of the Pano Lefkara and Larnaca area., Cyprus Geol. Surv. Dept. Mem.#5. 116p.

Baragar. W.R.A., Lambert. M.B., Baglow, N., and Gibson, I.L., (1984), Sheeted dyke complex, Troodos Ophiolite., Geol. Assoc. Canada. Program with Abstracts, v.9, p.44.

Bear, L.M., (1960), The geology and mineral resources of the Akaki - Lythrodonda area., Cyprus Geol. Surv. Dept. Mem.#5, 116p.

Bhattacharji, S. and Smith. C.H., (1964), Flowage differentiation., Science, v.145, p.150-153.

Boyle, J.F. and Robertson, A.H.F., (1983), Evolving metallogenesis at the Troodos spreading axis., (in press).

Brooks, C. and Hart, S.R., (1974), On the significance of komatiite., Geology. v.2 , p.107-110.

Cameron, W.E., and Nisbet, E.G., (1982), Phanerozoic analogues of komatiitic basalts., In: Komatiites, Arndt, N.T. and Nisbet, E.G. (Eds.), George Allen and Unwin Pubs., London, p.29-50.

Cameron, W.E., Nisbet, E.G., and Dietrich. V.J., (1980), Petrographic dissimilarities between ophiolitic and ocean - floor basalts, In:Ophiolites: Proceedings International Ophiolite Symposium. Cyprus. 1979. p.182-192.

Cann, J.R., (1970), Rb, Sr. Y, Zr. and Nb in some ocean-floor basaltic rocks., Earth Planet. Sci. Lett., v.10. p.7-11.

Cann, J.R., (1979), Metamorphism in the ocean crust., In: Deep Drilling Results in the Atlantic Ocean: Ocean Crust, Talwani, M (Ed.), p.230-238.

Carmichael, I.S.E., Turner. F.J., and Verhoogan, J., (1974), Igneous Petrology. McGraw-Hill Book Co., N.Y., 740p.

Carr, J.H. and Bear. L.M., (1960), The geology and mineral resources of the Peristerona - Lagoudhera area., Cyprus Geol. Surv. Dept. Mem. #2. p.1-79.

Clarke, D.B., and O'Hara, M.J., (1979), Nickle and the existence of high-MgO liquids in nature, Earth Planet. Sci. Lett., v.44. p.153-158.

Coish, R.A. and Taylor. L.A., (1979), The effects of cooling rate on texture and pyroxene chemistry in DSDP leg 34 basalt: A microprobe study., Earth Planet. Sci. Lett., v.42. p.389-398.

Cox, K.G., Bell. J.D., and Pankhurst, R.J., (1979), The Interpretation of Igneous Rocks, George Allen and Unwin Pubs., London, 450p.

Crawford, A.J., Beccaluva, L., and Serri. G., (1981), Tectono-magmatic evolution of the West Philippine-Mariana region and the origin of boninites, Earth Planet. Sci. Lett., v.54. p.346-356.

Deer, W.A., Howie, R.A., and Zussman, J., (1966), An Introduction to the Rock Forming Minerals, Longman Group Ltd. Pubs., London, 528p.

Desmet, A.P., (1976), Evidence of co-genesis of the Troodos Lavas, Cyprus., Geol. Magazine, v.113. p.165-168.

Dick, H.J.B., (1982), The petrology of two back-arc basins of the northern Phillipine Sea., Amer. Jour. Sci., v.282. p.644-700.

Duncan, R.A., and Green, D.H., (1980), Role of multistage melting in the formation of oceanic crust., Geology, v.8, p.22-26.

Dunsworth. S.M. and Calon, T., (1984), Relationships between deformation and magmatism in the plutonic complex, Troodos Ophiolite, Cyprus., Geol. Assoc. Canada. Program with Abstracts, v.9, p.59.

Ford, C.E., et al., (1983), Olivine - Liquid Equilibria: Temperature, pressure and composition dependence of the crystal - liquid partition coefficients for Mg, Fe2+, Ca, and Mn., Jour. Petrol., v.24. #3, p.256-265.

Garcia, M.O., (1978), Criteria for the identification of ancient volcanic arcs., Earth Science Reviews, v.14. p.147-165.

Gass, I.G., (1958), Ultrabasic pillow lavas from Cyprus., Geol. Mag., v.95. p.241-251.

Gass, I.G., (1960), The geology and mineral resources of the Dhali area., Cyprus Geol. Surv. Dept. Mem.#4. 116p.

Gass, I.G. (1968), Is the Troodos Massif of Cyprus a fragment of Mesozoic ocean floor?, Nature, v.220. p.39-42.

Gass, I.G. (1980), The Troodos massif: Its role in the unravelling of the ophiolite problem and its significance in the understanding of constructive plate margin processes., In: Ophiolites: International Ophiolite Symposium Volume, Nicosia. Cyprus., p.23-35.

Gass, I.G., and Masson-Smith. D., (1963), The geology and gravity anomalies of the Troodos massif. Cyprus., Roy. Soc. London Phil. Trans., A255. p.417-467.

Gass, I.G. and Smewing, J.D., (1973), Intrusion, extrusion, and metamorphism at constructive margins: Evidence from the Troodos massif. Cyprus., Nature, v.242. p.26-29.

Gass, I.G. et al., (1975), Comments on "The Troodos ophiolitic complex was probably formed in an island arc", By A. Miyashiro and subsequent correspondence by H. Hynes and A. Miyashiro, Earth Planet. Sci. Lett., v.25. p.236-238.

Gillis, K.M., (1984), Low temperature alteration of the extrusive sequence, Troodos ophiolite, Cyprus., (in press).

Green, D.H., (1976), Experimental testing of equilibrium partial melting of peridotite under water-saturated, high pressure conditions., Canad. Mineral., v.14, p.255-268.

Green, T.H., (1980), Island arc and continent-building magmatism - A review of petrogenic models based on experimental petrology and geochemistry., Tectonophysics, v.63, p.367-385.

Greenbaum, D., (1972), The chromitiferous rocks of the Troodos ophiolite complex, Cyprus., Econ. Geol., v.72, p.1175-1194.

Hickey. R.L., and Frey. F.A., (1982), Geochemical characteristics of boninite series volcanics: Implications for their source, Geochim. Cosmochim. Acta, v.46, p.2099-2115.

Honnorez. J., (1981), The aging of the Oceanic Crust at Low Temperature., In:The Sea, 7)The ocean lithosphere, Emiliani, C. (Ed.), John Wiley and Sons, N.Y, p.525-587.

Hynes, A., (1975), Comment on "The Troodos ophiolitic complex was probably formed in an island arc", by A. Miyashiro, Earth Planet. Sci. Lett., v.25. p.213-216.

Jorgensen, K.A. and Brooks, C.K., (1981), The Troodos Ophiolite: petrology of a fresh glassy basalt., Bull. Geol. Soc. Denmark, v.30. p.43-50.

Karig, D.E., (1970), Ridges and basins of the Tonga-Kermadec Island Arc system., Geophysical Research v.75. p.239-254.

Kidd, R.G.W., and Cann, J.R., (1974), Chilling statistics indicate an ocean-floor spreading origin for the Troodos complex, Cyprus, Earth Planet. Sci. Lett., v.24. p.151-155.

Koehlstedt, D.L., Goetze, C., and Durham. W.B., (1976), Experimental deformation of single crystal olivine with application to flow in the mantle., In:The physics and Chemistry of Minerals and Rocks, Strens, R.G.J. (Ed.), John Wiley and Sons Pubs., London, p.35-50.

Kushiro, I., (1972), Effect of water on the composition of magmas formed at high pressures., Jour. Petrol., v.13. p.311.

Laurent, R., Delaloye, M., Vaugnat, M., and Wagner, J.J., (1980), Composition of parental basaltic magma in ophiolites., In: Ophiolites: Proceedings International Ophiolite Symposium, Cyprus, 1979, Ed. A. Panayiotou, p.172-181.

Lofgren, G. et al., (1974), Experimentally reproduced textures and mineral chemistry of Apollo 15 quartz normative basalts., Proc. 5th Lunar Conf. Suppl. #5. Geochim. Cosmochim. Acta, v.1. p.549-567.

Ludden, J.N. and Thompson, G., (1979), An evaluation of the behaviour of the rare earth elements during the weathering of sea-floor basalt., Earth Planet. Sci. Lett., v.43. p.85-92.

Malpas, J. and Langdon, G.S., (1982), Ultramafic and related rocks of the Upper Pillow Lava Suite, Troodos Complex, Cyprus., Geol. Soc. Amer. Abstracts with Programs, v.14. #1-2. p.37.

Mantis, M., (1970), Upper Cretaceous - Tertiary foraminiferal zones in Cyprus., Cyprus Research Centre, v.111. p.227-324.

Mathews, W.H., Thorarinsson, S. and Church. (1964), Gravitative settling of olivine in pillows of an Icelandic basalt., Amer. Jour. Sci., v.262. p.1036-1040.

Meijer, A., (1980), Primitive arc volcanaism and a boninite series: Examples from western Pacific island arcs., In: The Tectonic and Geologic Evolution of Southeast Asian Seas and Islands., D.E. Hayes, Ed., Geophys. Monograph Series, v.23. p.269-282.

Miyashiro, A. (1973), The Troodos ophiolitic complex was probably formed in an island arc., Earth Planet. Sci. Lett., v.19. p.218-224.

Moores, E.M., (1975), Discussion of "Origin of Troodos and other ophiolites: A reply to Hynes", by Akiho Miyashiro., Earth Planet. Sci. Lett., v.25. p.223-226.

Moores, E.M., Robinson, P.T., Malpas, J., and Xenophontos, C., (1984), A model for the origin of the Troodos massif, Cyprus, and other mideast ophiolites., (in press).

Moores, E.M. and Vine, F.J., (1971), The Troodos Massif, Cyprus and other ophiolites as oceanic crust: Evaluation and implications., Phil. Trans. Roy. Soc. London, v.A-268, p.443-466.

Mottl, M.J. (1983), Metabasalts, axial hot springs, and the structure of hydrothermal systems at mid-ocean ridges., Geol. Soc. Amer. Bull., v.94. p.161-180.

Mottl, M.J. and Seyfried, W.E., (1980), Sub-seafloor hydrothermal systems: rock vs. water dominated., In: Seafloor Spreading Centers; Hydrothermal Systems, P.A. Rona and R.P. Lowell eds., p.66-82.

Mullen, E.D., (1983), MnO/TiO2/P2O5 : A minor element discriminant for basaltic rocks of oceanic environments - its implications for petrogenesis., Earth Planet. Sci. Lett., v.62. p.53-62.

Murata, K.J. and Richter, D.H., (1966), The 1959 eruption of Kilauea volcano, Hawaii; chemistry of the lavas., U.S. Geol. Surv. Prof. Pap. 537-A, p.A1-26.

Nisbet, E.G. and Pearce, J.A. (1977), Clinopyroxene compositions in mafic lavas from different tectonic settings., Cont. Mineral. Petrol., v.65. p.149-160.

O'Hara, M.J., (1977), Geochemical evolution during fractional crystallization of a periodically refilled magma chamber., Nature, v.266, p.503-507.

O'Hara, M.J., and Mathews, R.E., (1981), Geochemical evolution in an advancing, periodically replenished, periodically tapped, continuously fractionated magma chamber., Jour. Geol. Soc. Lond., v.138, p.237-277.

Onuma, K. and Tohara, T., (1983), Effect of chromium on phase relations in the join forsterite-anorthite-diopside in air at 1 atm., Cont. Mineral. Petrol., v.84. p.174-181.

Pearce, J.A., (1975), Basalt geochemistry used to investigate past tectonic environments on Cyprus., Tectonophysics, v.25. p.41-67.

Pearce, J.A., (1980), Geochemical evidence for the genesis and eruptive setting of lavas from Tethyan ophiolites., In:Ophiolites: Proceedings International Ophiolite Symposium. Cyprus, 1979, p.261-272.

Pearce, J.A. and Cann, J.R., (1971), Ophiolite origin investigated by discriminant analysis using Ti, Zr, and Y., Earth Planet. Sci. Lett., v.12. p.339-349.

Pearce, J.A. and Cann, J.R., (1973), Tectonic setting of basic volcanic rocks determined using trace element analyses., Earth Planet. Sci. Lett., v.19. p.290.

Pearce, J.A., and Norry, M.J., (1979), Petrogenetic implications of Ti, Zr, Y, and Nb variations in volcanic rocks., Contrib. Mineral. Petrol., v.69, p.33-47.

Poirier, J.P. and Nicolas, A., (1975), Deformation-induced recrystallization due to progressive misorientaton of subgrains, with special reference to mantle peridotites., Jour. Geol., v.83. #6. p.707-720.

Ringwood, A.E., (1969), Composition and evolution of the Upper Mantle., In:The Earths Crust and Upper Mantle, P.J. Hart, Ed., Geophys. Monograph #13. Amer. Geophys. Union, Washington, D.C., p.1-17.

Ringwood, A.E., (1982), Phase transformations and differentiation in subducted lithosphere: implications for mantle dynamics, basalt petrogenesis and crustal evolution., Jour. Geol., v.90. p.611.

Robertson, A.H.F., (1976), Origin of ochres and umbers: evidence from Skouriotissa. Troodos Massif. Cyprus., Trans. Inst. Min. Met., v.85. p.B245-251

Robertson, A.H.F. and Hudson, J.D., (1974), Pelagic sediments in the Cretaceous and Tertiary history of the Troodos Massif, Cyprus., Spec. Publ. Int. Assoc. Sedimentol., v.1. p.403-436.

Robertson, A.H.F. and Woodcock, N.H., (1980) Tectonic setting of the Troodos massif in the east Mediterranean., In:Ophiolites: International Ophiolite Symposium. Cyprus. 1979. A. Panayioutou, Ed., p.36-49.

Robinson, P.T., Melson, W.G., O'Hearn, T., and Schmincke, H.-U., (1983), Volcanic glass compositions of the Troodos ophiolite, Cyprus, Geology. v.11. p.400-404.

Roeder. P.L. and Emslie. R.F., (1970), Olivine-Liquid equilibrium., Contrib. Mineral. Petrol., v.29, p.275-289.

Rose. A.W., Hawkes, H.E., and Webb, J.S., (1979), Geochemistry in Mineral Exploration, Academic Press Inc., London, 657p.

Saunders, A.D., and Tarney. J., (1979), The geochemistry of basalts from a back-arc spreading centre in the East Scotia Sea. Geochim. Cosmochim. Acta. v.43. p.555-572.

Saunders, A.D., Tarney. J., Marsh. N.G., and Wood, D.A., (1980), Ophiolites as ocean crust or marginal basin crust: A geochemical approach., In:Ophiolites: Proceedings International Ophiolite Symposium. Cyprus. 1979. Ed. A. Panayiotou, p.193-204.

Schmincke, H.-U., Rautenschlein, M., Robinson, P.T., and Mehegan, J.M., (1983), Troodos extrusive series of Cyprus: A comparison with oceanic crust., Geology. v.11. p.405-409.

Schroeder. B., Thompson, G. and Ludden, J., (1980), Analysis of geologic materials using an automated X-ray fluorescence system., X-Ray Spectrometry. v.9. #4. p.198-205.

Searle, D.L. and Vokes, F.M., (1969), Layered ultrabasic lavas from Cyprus., Geol. Mag., v.106. #6. p.515-530.

Seyfried, W.E. and Mottl. M.J., (1982), Hydrothermal alteration of basalt by seawater under seawater dominated conditions., Geochim. Cosmochim. Acta. v.46, p.985-1002.

Shervais, J.W., (1982), Ti-V plots and the petrogenesis of modern ophiolitic lavas., Earth Planet. Sci. Lett., v.59, p.101-118.

Smewing. J.D., Simonian, K.O., and Gass, I.G., (1975), Metabasalts from the Troodos massif Cyprus: Genetic implications deduced from petrography and trace element geochemistry., Contrib. Mineral. Petrol., v.51. p.49-64.

Smith. R.E. and Smith. S.E., (1976), Comments on the use of Ti, Zr, Y, Sr. K, and Rb in classification of basaltic magmas., Earth Planet. Sci. Lett., v.32. p.114-120.

Spooner. E.T.C., (1977), Hydrodynamic model for the origin of the cupiferous pyrite ore deposits of Cyprus., In: Volcanic processes in ore genesis, London Inst. Min. Metall., p.58-71.

Spray. J.G. and Roddick, J.C., (1981), Evidence for Upper Cretaceous transform fault metamorphism in west Cyprus., Earth Planet. Sci. Lett., v.55. p.273-291.

Staudigal. H., Hart, S.R., and Richardson. (1981), Alteration of the oceanic crust: Processes and timing., Earth Planet. Sci. Lett., v.52. p.311-327.

Takahashi. E., (1978), Partitioning of Ni. Co, Fe, Mn, and Mg between olivine and silicate melts: compositinal dependence of partition coefficient., Geochim. Cosmochim. Acta., v.42. p.1829-1844.

Vine. F.J., and Matthews, D.H., (1963), Magnetic anomalies over oceanic ridges., Nature, v.199, p.947-949.

Wang. B-X. (1983), Analogues of komatiitic basalts: ultramafic lavas from Cyprus., Institute of Geology. Chinese Academy of Geological Sciences, (in press).

Wilson, R.A.M., (1959), The geology of the Xeros - Troodos area., Cyprus Geol. Surv. Dept. Mem.#1. 135p.

Wood. B.J., and Fraser. D.G., (1977), Elementary Thermodynamics for Geologists, Oxford University Press, London, 303p.

Yoder, H.S., and Tilley, C.E., (1962), Origin of basaltic magmas: an experimental study of natural and synthetic rock systems., Jour. Petrol., v.3. p.342-532.

APPENDIX I

TABLE OF PETROGRAPHIC DESCRIPTIONS

KEY TO ABBREVIATIONS AND SYMBOLS USED IN APPENDIX I

Sample #: Numbers used refer to individual hand specimens. Equivalent numbers are used to mark the sampled outcrop location on Map 2, back pocket.

Unit #: Roman numerals correspond to the major lithostratigraphic units defined in Chapter Two. Letters refer to individual cooling unit lithologies.

Rock Type: Major features of the sampled outcrop are abbreviated as follows: o=olivine-phyric; c=clinopyroxene phyric; x=plagioclase phyric; a=aphyric; u=picritic; p=pillow; f=flow (<5 m thick); mf=massive flow (>5 m thick); fb=flow base; ft=flow top; i=intrusive.

Phenocrysts/Vesicles/Groundmass: Minerals: ol=olivine; cpx=clinopyroxene; plag=plagioclase; sp=spinel; opx=orthopyroxene. %=Estimated modal abundance in thin section. Ave/Max size: Length of phases in thin section and expressed in mm.

Alteration and Remarks: Five levels of mineralogic alteration were distinguished. General characteristics of these are:

I.	(V. Low) -	Olivine < 30% altered +/- presence of unaltered glass in groundmass.
II.	(Low) -	Olivine > 30% altered; Clinopyroxene unaltered.
III.	(Mod.) -	Olivine > 60% altered; Clinopyroxene < 30% altered.
IV.	(High -	Clinopyroxene 30 to 60% altered.
V.	(V. High)-	Clinopyroxene > 60% altered.

Primary mineral abbreviatons same as above. Secondary mineral abbreviations as follows: cc=calcite; sm=smectite; ox=oxides; ze=zeolites; cl=celadonite; qtz=quartz.

sample #	unit #	rock type	PHENOCRYSTS mineral	%	ave.size	max.size	VESICLES %	ave.size	GROUNDMASS mineral	%	ave.size	max.size	texture	ALTERATION AND REMARKS
1	IIIB	oop	ol	2	*0.40	0.80	3	0.45	cpx	10	0.10	0.35	felty	-alt.high;groundmass opx 70% altered; sm, cc + ox common
			opx	5	0.25	0.75								
5	IIIA	op	cpx	tr	0.30	0.50	5	0.70	cpx	65	0.04	0.05	microlitic	-alt.low; 50% of groundmass altered to clays; minor cc; cpx microlites aligned.
									sp	tr	0.02	0.05		
5B	IIIB	op	ol	3	0.40	1.00	9	0.25	cpx	10	0.15	0.50	felty	-alt.v.high; sm, cc + ox common.
									plag	tr	0.04	0.15		
10	IIB	op	ol	6	0.45	0.90	2	0.45	cpx	55	0.20	0.65	quench	-alt.low;groundmass altered to smectites;quench cpx abundant
									sp	2	0.02	0.05		
11	IIA	of	ol	3	0.40	0.80	14	0.60	cpx	8	0.20	0.80	felty	-alt.high; cc, sm + ox common.
									plag	5	0.14	0.35		
13	IIIB	op	ol	2	0.30	0.75	18	0.40	cpx	30	-	0.45	felty	-alt.v.high; cpx 80% altered; sm + ox common.
									plag	3	-	-		
14	IIIB	oop	ol	tr	0.50	0.80	12	0.15	cpx	?	-	-	felty	-alt.v.high; sm + ox abundant.
			cpx	8	0.25	0.90			plag	tr	0.15	0.35		
15	IIE	amf	-	-	-	-	3	0.35	cpx	5	0.25	0.85	intersertal	-alt.mod; sm, ze + ox common; minor qtz.
									plag	65	0.35	1.00		
15A	IIE	amf	-	-	-	-	9	1.45	cpx	8	0.15	0.40	intersertal	-alt.high; cpx 50% altered; sm, ze, cc + ox abundant.
									plag	60	0.20	0.50		
20	IIIA	af	-	-	-	-	7	0.65	cpx	15	0.15	0.40	diabasic	-alt.high; cpx 50% altered; sm, ze, cc + ox abundant.
									plag	35	0.25	0.55		
22	IIA	ap	-	-	-	-	18	0.80	cpx	6	0.25	1.10	felty	-alt.mod; sm, cc + ox common;
									plag	2	0.20	0.60		
24	IIA	op	ol	10	2.00	5.00	2	0.70	cpx	3	0.12	0.40	seriate	-alt.high; cc, sm + ox abundant.
									plag	4	0.16	0.45		
									sp	tr	0.10	0.50		
25	IIA	op	ol	2	0.40	0.80	10	0.40	cpx	10	0.10	0.35	felty	-alt.high; sm, cc + ox abundant.
									plag	3	0.04	0.15		
26	IIE	amf	-	-	-	-	12	1.10	cpx	8	0.40	1.10	intersertal	-alt.high; cc, sm, ze + ox common; cpx 50% altered.
									plag	55	0.55	1.80		
27	IIA	op	ol	16	1.55	3.80	6	0.30	cpx	12	0.06	0.25	seriate	-alt.high; cc, sm + ox common
									plag	2	0.02	0.20		
28	IIB	op	ol	5	0.40	0.85	2	0.30	cpx	55	0.24	0.80	quench	-alt.v.low; ol 10% altered; glass 95% altered; cpx exhibit quench morphology.
									sp	tr	0.06	0.20		
32	IIIB	oop	ol	4	0.35	0.90	2	0.20	cpx	45	0.06	0.20	felty	-alt.high; sm + ox common.
			cpx	4	0.25	0.60								

sample #	unit #	rock type	PHENOCRYSTS mineral	%	ave.size	max.size	VESICLES %	ave.size	GROUNDMASS mineral	%	ave.size	max.size	texture	ALTERATION AND REMARKS
33	IIA	op	ol	tr	-	-	8	0.80	cpx plag	10 50	0.30 0.35	1.00 1.40	diabasic	-alt.high; cpx 20% altered; cc, ox and minor qtz.
34	IIIB	ocp	ol cpx	2 4	0.25 0.25	0.65 0.70	16	0.50	cpx plag	? 4	- 0.10	0.15 0.25	felty	-alt.high; cpx 30% altered; cc, sm + ox abundant.
35	IIB	op	ol	8	0.45	0.90	-	-	cpx sp	40 2	0.35 0.04	1.20 0.10	quench	-alt.v.low; ol 15% altered; glass 95% altered. cpx exhibit quench morphology.
37	IIIB	oci	ol cpx	tr 8	0.35 0.25	0.60 0.75	5	0.45	cpx plag	? 20	- 0.20	- 0.35	microlitic/ intersertal	-alt.high; groundmass cpx totally altered; cc, ze, sm + ox common.
38	IIB	op	ol	9	0.75	1.80	tr	0.60	cpx sp	70 tr	- 0.06	0.80 0.20	microlitic	-alt.v.low; ol 25% altered; cpx exhibit quench textures.
39	IIA	op	ol	4	0.75	2.00	6	0.65	cpx plag sp	15 4 tr	0.15 0.10 0.06	0.40 0.30 0.20	felty	-alt.v.high; groundmass cpx totally altered; cc, sm + ox abundant.
41	-	ai	-	-	-	-	12	0.45	cpx plag	15 15	0.10 0.15	0.25 0.35	intergranular	-alt.v.high; cpx 80% altered; cc, sm + ox common.
42	IID	ufb	ol	22	2.00	8.00	-	-	cpx plag sp	12 2 tr	0.10 0.06 0.10	0.30 0.20 0.25	seriate	-alt.high; cc, sm + ox common
44	IID	ufb	ol	35	3.00	6.00	-	-	cpx plag sp	12 8 2	0.60 0.60 0.08	2.20 1.60 0.30	subophitic	-alt.low; ol 60% altered; sm + ox common.
45	IIIA	af	-	-	-	-	2	0.50	cpx plag	10 8	0.20 0.25	0.40 0.60	felty	-alt.v.high; cpx 50% altered; cc, sm + ox common.
46	IIIB	op	ol	2	0.30	0.70	8	0.30	cpx plag	35 16	0.10 0.06	0.45 0.30	microlitic	-alt.mod; sm, ox + minor cc;
47	IIIB	op	ol	tr	-	-	12	0.30	cpx plag	20 8	- 0.15	0.70 0.50	felty	-alt.v.high; cpx 60% altered; cc, sm + ox abundant.
51	IID	ufb	ol	30	1.25	3.00	-	-	cpx plag	20 15	0.25 0.45	0.70 1.20	subophitic	-alt.mod; sm + ox common.
53	IID	ufb	ol	40	3.10	8.00	-	-	cpx sp	7 tr	0.40 0.10	2.00 0.35	-	-alt.v.low; ol 15% altered; sm + ox common.
54	IID	ufb	ol	35	1.45	2.70	-	-	cpx plag sp	8 6 ?	0.65 0.35 0.10	1.40 1.20 0.30	subophitic	-alt.v.low; ol 30% altered; sm, ze + ox common.
55	IIA	op	ol	18	0.95	2.60	10	0.45	cpx plag sp	8 3 tr	0.15 0.12 0.10	0.80 0.50 0.85	subophitic	-alt.v.high; cc, sm + ox abundant.

sample #	unit #	rock type	PHENOCRYSTS mineral	%	ave.size	max.size	VESICLES %	ave.size	GROUNDMASS mineral	%	ave.size	max.size	texture	ALTERATION AND REMARKS
56	IIIA	ap	-	-	-	-	12	0.50	cpx	15	0.12	0.35	microlitic	-alt.v.high; sm, cc + ox
									plag	15	0.10	0.30		abundant.
57	IIIB	ocp	ol	3	0.30	1.40	?	?	cpx	30	0.08	0.35	microlitic	-alt.high; sm + ox common;
			cpx	tr	0.25	0.70			plag	14	0.06	0.25		cpx exhibit wide size range.
61	IIIB	ocp	cpx	4	0.35	1.20	6	0.30	cpx	16	0.12	0.30	microlitic	-alt.high; cpx > 60% altered
			ol	tr	0.30	0.75			plag	8	0.10	0.20		sm + ox common.
64	IIA	op	ol	6	0.80	2.20	5	0.20	cpx	20	0.14	0.40	seriate	-alt.high; cc, sm + ox common.
									plag	4	0.04	0.10		
									sp	tr	0.10	0.25		
66	IIA	op	ol	12	4.85	10.00	6	0.40	cpx	18	0.08	0.30	intergranular	-alt.high; cpx 70% altered;
									plag	4	0.06	0.25		cc, sm, cl + ox common.
									sp	tr	0.10	0.30		
68	IIIA	af	-	-	-	-	8	0.80	cpx	10	0.12	0.30	-	-alt.high; cc, cl + ox common
									plag	3	0.06	0.25		cpx 70% altered.
72	IIIA	ap	-	-	-	-	8	0.45	cpx	10	0.14	0.45	microlitic/	-alt.high; cc + ox abundant.
									plag	12	0.06	0.30	intergranular	cpx 60% altered.
73	IIA	op	ol	16	1.20	3.60	4	0.30	cpx	15	0.20	0.50	subophitic	-alt.high; cc, sm + ox com-
									plag	2	0.04	0.20		mon; cpx 30% altered.
									sp	tr	0.12	0.30		
74	IIE	amf	-	-	-	-	6	0.60	cpx	20	0.25	0.70	diabasic	-alt.v.high; sm, ox + qtz
									plag	45	0.45	1.20		common; cpx 70% altered.
75	IID	ufb	ol	35	1.40	3.20	-	-	cpx	18	0.35	1.40	subophitic	-alt.low; ol 60% altered; sm
									plag	10	0.50	1.80		abundant; ze + ox common.
									sp	2	0.10	0.50		
77	IIA	ocp	ol	3	0.85	2.00	10	0.55	cpx	8	0.08	0.30	felty	-alt.high; cc, sm + ox abun-
			cpx	6	0.35	0.60			plag	5	0.10	0.55		dant.
81	IIC	up	ol	40	3.80	8.00	-	-	cpx	20	0.40	1.40	microlitic	-alt.low; sm, ox, ze + ox
									ol	4	0.15	0.45		common; cpx exhibit quench
									sp	2	0.15	0.40		morphology.
82	IIA	ocp	ol	3	0.40	0.85	8	0.55	plag	6	0.10	0.50	felty	-alt.mod; sm, cc + ox com-
			cpx	12	0.30	1.00								mon; cpx glomeroporphyrit-
														ic.
83	IID	ufb	ol	45	2.00	4.10	-	-	cpx	18	0.18	0.55	subophitic	-alt.v.low; ol 30% altered;
									plag	20	0.45	1.60		sm + ze common.
									sp	tr	0.10	0.30		
86	IIA	ocp	ol	6	0.60	1.50	tr	0.40	cpx	65	0.06	0.25	microlitic	-alt.low; ol 60% altered;
			cpx	8	0.30	0.85			sp	tr	0.04	0.20		minor fresh glass; sm com-
														mon.

sample #	unit #	rock type	PHENOCRYSTS mineral	%	ave.size	max.size	VESICLES %	ave.size	GROUNDMASS mineral	%	ave.size	max.size	texture	ALTERATION AND REMARKS
87	IA	ap	-	-	-	-	6	0.40	plag	tr	0.08	0.25	-	-alt.v.high; sm + ox have replaced 95% of section.
88	IID	uft	ol	4	0.60	1.00	12	0.35	plag	4	0.16	1.20	felty	-alt.high; cc, sm + ox abundant.
			cpx	14	0.30	0.70								
91	IIA	op	ol	8	0.50	1.90	-	-	cpx	55	0.25	0.90	microlitic	-alt.low; ol 40% altered; sm common; minor glass; quench cpx common.
									sp	tr	0.04	0.15		
95	IIIB	ocp	ol	tr	0.30	0.65	18	0.30	cpx	35	0.06	0.20	felty	-alt.high; groundmass cpx 40% altered; cc, sm, ox + minor ze present.
			cpx	6	0.25	0.85			plag	4	0.10	0.25		
96	IIIA	af	-	-	-	-	8	0.80	cpx	?	-	0.25	-	-alt.v.high; sm, cc, ox + ze all present.
97	IIA	op	ol	6	0.40	1.05	-	-	cpx	50	0.25	1.20	quench	-alt.v.low; ol 15% altered sm abundant; minor ox.
			sp	tr	0.30	0.35			sp	2	0.02	0.10		
98	IID	uft	ol	6	0.65	1.70	6	0.30	cpx	20	0.18	0.40	felty	-alt.high; cc + ox abundant.
									plag	4	0.08	0.45		
99	IID	ufb	ol	40	3.50	8.00	-	-	cpx	10	0.80	2.50		-alt.v.low; ol 20% altered sm, ox + cc common.
									sp	2	0.20	0.55		
100	IIA	oop	ol	3	0.65	1.60	4	0.20	plag	3	0.12	0.50	intergranular	-alt.high; cc, sm + ox.
			cpx	8	0.25	0.70			sp	tr	0.04	0.15		
									cpx	25	0.40	1.10	diabasic/	-alt.high; cc, sm + ox
101	IIA	of	ol	4	1.00	2.00	7	1.05	plag	35	0.40	1.20	intergranular	abundant.
									cpx	65	0.04	0.35	quench	-alt.low; sm, cc + ze; cpx
102	IIA	op	ol	8	1.00	2.20	3	0.35	sp	tr	0.08	0.30		exhibit quench morphology.
									cpx	8	0.35	1.00	-	-alt.mod; ol 80% altered;
103	IID	ufb	ol	45	2.40	4.10	-	-	plag	3	0.15	0.40		cc + ox common.
									sp	tr	0.06	0.30		
									cpx	18	0.25	0.80	diabasic	-alt.mod; cc, ox, sm + qtz
104	IIE	amf	-	-	-	-	-	-	plag	40	0.35	1.00		common.
									cpx	30	0.16	0.60	microlitic	-alt.v.low; ol 10% altered;
105	IIC	up	ol	40	3.50	15.00	tr	0.45	sp	2	0.12	0.50		minor fresh glass; cpx exhibit quench morphology.
									plag	tr	0.15	0.25	-	-
110	IA	ap	cpx	tr	-	0.25	8	-						
									cpx	20	0.22	1.00	diabasic/	-alt.high; cpx 40% altered;
111	IIE	amf	-	-	-	-	15	1.35	plag	30	0.16	0.70	intergranular	plag 35% altered; sm, ox + ze common.

sample #	unit #	rock type	PHENOCRYSTS mineral	%	ave.size	max.size	VESICLES %	ave.size	GROUNDMASS mineral	%	ave.size	max.size	texture	ALTERATION AND REMARKS
112	IA	op	plag	2	0.30	0.75	25	1.00	plag	25	0.15	0.35	microlitic	-alt.high; sm + ox abundant;
			opx	tr	0.35	0.80								
113	-	ai	-	-	-	-	4	0.40	cpx	18	0.10	0.35	microlitic	-alt.high; cpx 30% altered;
									plag	35	0.06	0.30		cc, ox + green sm common.
115	IIG	af	-	-	-	-	4	0.45	cpx	35	0.20	0.80	diabasic/	-alt.mod; sm + ox common.
									plag	35	0.14	1.20	intergranular	
117	II	ocf	ol	5	0.65	1.60	12	0.25	cpx	4	0.08	0.20	felty	-alt.high; cc, sm + ox com-
			opx	4	0.30	0.60			plag	3	0.06	0.25		mon.
120	IID	ufb	ol	35	1.60	4.80	2	0.70	cpx	8	0.40	1.40	subophitic	-alt.low; ol 50% altered;
									plag	15	0.35	1.80		sm + ox common.
									sp	2	0.10	0.50		
120A	IID	uft	-	-	-	-	3	0.40	cpx	40	0.40	0.85	intergranular	-alt.mod; cc, ox + sm com-
									plag	20	0.24	1.40		mon; opx strongly zoned.
121	IIA	op	ol	18	1.20	3.00	6	0.30	cpx	10	0.08	0.25	felty	-alt.high; cc, sm + ox; cpx
									plag	2	0.06	0.20		exhibit irregular morpol-
									sp	tr	0.04	0.12		ogy.
121A	IIA	op	ol	4	0.70	1.95	4	0.25	cpx	45	0.25	1.20	microlitic	-alt.low; ol 40% altered;
									sp	2	0.06	0.25		cpx exhibit quench morph-
														ology; sm + ox common.
123	IIIA	af	-	-	-	-	6	0.40	cpx	?	-	0.40	microlitic	-alt.v.high; cpx 75% altered
									plag	6	0.10	0.25		cc, sm + ox zbundznt.
124	IIA	op	ol	12	1.25	3.10	12	0.80	cpx	8	0.08	0.25	seriate	-alt.high; cpx 40% altered;
									plag	3	0.10	0.25		cc abundant; sm + ox common
125	IIA	op	ol	3	1.45	2.80	8	0.45	cpx	6	0.06	0.25	microlitic	-alt.high; groundmass cpx
			cpx	3	0.30	0.60			plag	8	0.06	0.30		75% altered; cc, sm + ox
														common.
126	IIA	op	ol	tr	0.60	0.80	10	0.70	cpx	10	0.15	0.35	microlitic	-alt.high; cpx 50% altered;
									plag	12	0.08	0.25		cc, sm + ox common.
127	IIC	up	ol	50	4.40	14.00	-	-	cpx	30	0.35	1.10	microlitic	-alt.v.low; ol 10% altered;
									sp	2	0.30	1.30		minor glass; cpx exhibit
														quench morphology; cc + sm
131	IID	ufb	ol	35	1.65	4.20	-	-	cpx	12	0.35	1.80	subophitic	-alt.low; ol 35% altered;
									plag	6	0.30	1.65		sm, ze + ox common.
									sp	2	0.10	0.35		
133	IIA	op	ol	12	0.80	3.60	?	0.35	cpx	8	0.12	0.50	-	-alt.high; cpx 55% altered;
									plag	3	0.10	0.60		cc abundant; sm + ox com-
														mon.
135	IID	ufb	ol	30	0.85	2.80	?	0.60	cpx	12	0.25	0.90	intergranular	-alt.mod; ol 70% altered;
									plag	8	0.35	1.60		mon.
									sp	2	0.10	0.30		

sample #	unit #	rock type	PHENOCRYSTS mineral	%	ave.size	max.size	VESICLES %	ave.size	GROUNDMASS mineral	%	ave.size	max.size	texture	ALTERATION AND REMARKS
136	IIA	ocp	ol	3	0.30	1.00	2	0.30	cpx	55	0.08	0.30	microlitic	-alt.v.low; ol 30% altered; sm, ox + minor cc.
			cpx	8	0.20	0.55			sp	tr	0.02	0.12		
137A	IA	(brec)	cpx	tr	0.40	0.70	-	-	plag	14	0.10	0.40	breccia	-alt.v.high; plag microlites not alligned; ox, ze + qtz.
			plag	tr	0.25	0.50								
139	IIF	of	ol	2	-	0.50	3	0.35	cpx	18	0.15	0.45	diabasic	-alt.v.high;cpx 50% altered sm. cc, qtz + ox abundant.
									plag	24	0.20	0.50		
140	IIF	of	ol				-	0.30	cpx	15	0.24	0.70	diabasic	-alt.high; ol 100% altered; cc, sm + ox.
									plag	40	0.35	1.30		
145	IA	ap	-	-	-	-	10	0.25	-	-	-	-		-alt.v.high; no primary minerls distinguishable. sm, ox + cc common.
147	-	ai	-	-	-	-	3	0.30	cpx	12	0.10	0.35	diabasic	-alt.high; cpx 30% altered; sm, cc + ox present.
									plag	20	0.15	0.40		
148	IA	af	-	-	-	-	6	0.25	cpx	?	-	0.40	microlitic	-alt.v.high; cpx 80% altered; sm + ox common; minor cc.
									plag	8	0.04	0.50		
153	IIE	amf	-	-	-	-	3	0.40	cpx	10	0.12	0.40	felty	-alt.high; cpx 40% altered; sm + ox.
									plag	4	0.10	0.60		
154A	IIA	ocp	ol	5	0.55	1.30	tr	0.45	cpx	55	0.10	0.30	microlitic	-alt.low; ol 80% altered; groundmass cpx elongate.
			cpx	8	0.20	0.50			sp	tr	0.02	0.14		
155	IID	ufb	ol	45	1.85	6.20	-	-	cpx	5	0.18	1.40	-	-alt.v.low; ol 30% altered; minor cc + ox.
									plag	2	0.12	0.80		
									sp	2	0.08	0.30		
159	IIIA	ap	-	-	-	-	8	1.20	cpx	15	0.06	0.35	diabasic/	-alt.high; cpx 80% altered; sm + ox common.
									plag	12	0.14	0.45	microlitic	
161	IIA	op	ol	3	1.80	3.60	12	0.60	cpx	-	0.04	0.25	diabasic/	-alt.high; cpx 60% altered; sm, cc + ox.
									plag	8	0.10	0.40	felty	
162	IID	ufb	ol	40	1.65	4.40	-	-	cpx	6	0.35	1.80	subophitic	-alt.low; ol 40% altered;
									plag	2	0.25	1.60		
									sp	tr	0.10	0.30		
163	IIA	op	ol	20	1.40	3.10	6	0.35	cpx	3	0.20	0.70	felty	-alt.high; cpx 40% altered;
									plag	tr	0.14	0.65		
163A	IIA	op	ol	15	1.35	2.80	2	0.40	cpx	66	0.15	0.30	quench	-alt.low; ol 40% altered; beautiful quench cpx.
									sp	2	0.08	0.20		
165	IIE	amf	-	-	-	-	6	0.65	cpx	6	0.22	0.80	felty	-alt.high; cpx 30% altered; sm + ox abundant; minor cc + ze.
									plag	12	0.20	1.20		

sample #	unit #	rock type	PHENOCRYSTS mineral	%	ave.size	max.size	VESICLES %	ave.size	GROUNDMASS mineral	%	ave.size	max.size	texture	ALTERATION AND REMARKS
172	IID	ufb	ol	30	1.25	2.85	2	0.45	cpx	15	0.20	0.55	subophitic	-alt.low; ol 40% altered;
									plag	10	0.35	3.00		sm + ox abundant.
									sp	2	0.10	0.30		
172A	IID	uft	ol	14	0.75	1.90	12	0.35	cpx	15	0.20	0.60	intergranular	-alt.high; cpx + plag part-
									plag	8	0.22	1.60		ly altered; cc, sm + ox
									sp	tr	0.10	0.35		common.
173	IIA	op	ol	6	0.45	1.70	12	0.45	cpx	12	0.14	0.40	diabasic/	-alt.high; sm, cc + ox
									plag	15	0.16	0.70	felty	abundant; minor qtz.
									sp	tr	0.10	0.50		
175	IIG	af	-	-	-	-	-	-	cpx	15	0.14	0.40	intersertal/	-alt.mod, sm + ox common.
									plag	45	0.35	1.40	diabasic	
180	IIA	op	ol	8	1.10	1.85	20	0.35	cpx	6	0.18	0.45	felty	-alt.high; cpx + plag part-
									plag	2	0.24	0.65		ly altered; sm + ox common.
181	IIA	ocp	ol	3	0.45	1.45	2	0.40	cpx	40	0.10	0.35	microlitic	-alt.low; ol 50% altered;
			cpx	8	0.25	0.50			sp	tr	0.04	0.06		sm abundant.

APPENDIX II

ANALYTICAL METHODS

ANALYTICAL METHODS

1) Whole-rock Sample Preperation

Mini-cores (1" diameter) were taken from all hand specimens. Portions of these cores were crushed in a steel jaw crusher and then powdered in an agate swing mill.

2) Major Element Analysis

For major element analysis, 1.2 grams of "dried" rock powder was mixed with 6.0 grams of lithium tetraborate and fused into a glass bead (see Schroeder et al., 1980, for details of this procedure). These beads were analyzed at the Universite de Montreal over the spring and summer of 1983 using a Phillips USA-AXS automated interactive XRF-spectrometer. Analyses were completed in three seperate runs, each calibrated against approximately 20 standards (both natural and artificial). The mean deviation of the standards along a typical calibration curve is listed below. Accuracy between runs (for relevent compositions) is shown by the standard deviation of AGV-1 and BCR-1 analyses. Precision is shown by the difference (Diff.), of the mean composition from the accepted standard value.

	Calib. Curve	AGV-1			BCR-1		
	Dev. of Stds	Mean(8)	S.D.	Diff.	Mean(4)	S.D.	Diff.
SiO2	0.345	60.50	0.26	+0.54	53.94	0.33	-0.88
TiO2	0.010	1.05	0.03	-0.02	2.22	0.02	0.00
Al2O3	0.198	17.52	0.17	+0.23	13.84	0.12	+0.17
Fe2O3	0.082	6.83	0.16	-0.03	13.31	0.32	-0.22
MgO	0.098	1.60	0.09	+0.07	3.54	0.10	+0.05
CaO	0.038	4.96	0.15	-0.01	6.95	0.10	-0.02
Na2O	0.125	4.28	0.69	-0.07	3.09	0.34	-0.20
K2O	0.034	2.95	0.07	+0.01	1.66	0.02	-0.02
P2O5	0.021	0.51	0.03	0.00	0.37	0.01	+0.04

3) FeO / CO2 / H2O Analysis

A) Ferrous Iron - (Wilson technique of visual titration)

0.2 grams of powdered sample were decomposed in a solution of hydroflouric acid and ammonium metavanadate in a polyethylene flask. The flasks were shaken for 48 hours and, after adding a mixture of H_3PO_4 and H_2SO_4, the contents were transferred to a 400 ml beaker along with 100 ml of a 5% boric acid solution. Ferrous ammonium sulfate solution and barium diphenylamine sulfonate indicator were added, and the solution was titrated with potassium dichromate to a purple end point. (See Jeffery, 1970; and Blanchard, 1982; for a more detailed description of this procedure).

B) Carbon Dioxide - (Automatic titration method)

Approximately 0.5g of rock powder and HCl were added to a pyrex flask and heated with an open flame for 5 minutes. The fumes from the boiling solution were passed through a series of chemical filters wich removed any water vapor or

sulfer dioxide. The remaining gass passed into an automatic titrating cell which titrated the carbon dioxide with sodium methylate. The weight percent of carbon dioxide was calculated by multiplying the burrette reading by a factor derived from the average of three standard sample analyses. (See Bouvier et al., 1972).

C) Water - (Penfield tube technique)

0.5 grams of rock powder was mixed with a 2:1:1 mixture of PbO_2:$PbCr_2O_4$:$NaWO_4$ and transferred into a penfield tube. The tube was heated over an acetylene flame and the escaping water was trapped in a chamber of the tube which lay in an ice bath. The differrence in the weight of the tube before and after drying was taken as the weight of total water in the sample. H_2O^- (and by subtraction, H_2O^+), was calculated by weighing 1 gram of rock powder before and after dessication at 110°C. (See Volberth, 1969).

REFERENCES

Blanchard, M-C. (1982), Geochemistry and Petrogenesis of the Fisset Brook Formation, Western Cape Breton Island, Nova Scotia, Unpub. M.Sc. Thesis, Dalhousie University, Halifax, Nova Scotia.

Bouvier, J.L., Gupta, J.G., and Abbey, S. (1972), Use of an automatic sulphur titrator in rock and mineral analysis: Determination of sulphur, total carbon, carbonate, and ferous iron, Geol. Surv. Canada Paper #72-31. 22p.

Jeffery, P.G. (1970), Chemical Methods of Rock Analysis, Pergamon Press, Oxford, N.Y., 509 p.

Schroeder, B., Thompson, G., Sulanowoka, M. and Ludden, J. (1980), Analysis of Geologic Materials using an Automated X-ray Fluorescence System, X-Ray Spectrometry, v.9, #4, p.185-205.

Volberth, A. (1969), Elemental Analysis in Geochemistry, Elsevier, Amsterdam. N.Y., 373 p.

APPENDIX III

WHOLE-ROCK AND GLASS GEOCHEMISTRY

NOTES TO APPENDIX III

Whole-Rock Chemistry

Sample #: Numbers refer to individual hand specimens. Equivalent numbers are used to mark the sampled outcrop location on Map 2, back pocket. Petrographic descriptions of samples are listed in Appendix I.

Major Elements: Analyses are expressed in oxide weight percents. All analyses were made using an XRF system at the Universite de Montreal, except for ferrous iron and the volatiles. (See Appendix II).

Trace Elements: Analyses are expressed in parts per million. All analyses were made using an XRF system at the Universite de Montreal.

Glass Chemistry

Sample #: Numbers refer to extrusive glass specimens collected from individual cooling units.

Major Elements: All analyses are expressed in oxide weight percents and were determined using a microprobe system at the Smithsonian Institute, Washington, D.C.

CIPW Norm: Norms calculated assuming Fe_2O_3/Fe_2O_3+FeO = 0.15. Abbreviations are as follows: Q=quartz; OR=orthoclase; AB=albite; AN=anorthite; DI=diopside; HY=hypersthene; MT=magnetite; IL=ilmenite; AP=apatite.

WHOLE-ROCK CHEMISTRY

SAMPLE #	5	9B	10	14	15	15A	17
SiO2	54.51	53.88	54.23	53.11	56.40	52.48	51.33
Al2O3	14.93	16.47	13.46	16.64	17.03	16.20	16.52
TiO2	0.50	0.57	0.53	0.55	0.63	0.55	0.56
Fe2O3*	9.07	9.41	8.86	10.00	7.52	8.85	10.36
MgO	7.84	9.51	10.94	5.69	6.49	8.08	10.67
CaO	11.04	4.37	10.13	10.97	9.23	10.05	3.68
Na2O	1.45	0.64	1.49	1.25	1.63	1.46	0.38
K2O	0.32	4.54	0.40	0.96	0.30	1.16	5.67
P2O5	-	0.05	0.05	0.05	0.05	0.09	0.06
TOTAL	99.66	99.45	100.09	99.22	99.28	98.92	99.22
FeO	5.72	na	5.60	na	na	na	na
CO2	0.36	0.20	0.24	0.33	0.20	0.78	0.98
H2O+	3.23	3.76	4.28	1.20	0.90	1.51	5.98
H2O-	2.91	4.59	2.30	3.17	3.94	4.17	3.37
Rb(ppm)	7	27	7	16	6	24	34
Sr	123	67	111	100	99	101	98
Y	13	12	14	17	14	12	17
Ba	-	15	-	-	-	-	7
Zr	29	34	34	27	31	23	26
Nb	3	-	-	1	-	-	-
Zn	70	72	68	69	76	66	74
Cu	67	32	62	54	96	24	32
Ni	61	61	129	47	19	66	58
Cr	269	232	614	260	44	168	268
Ti	3144	4004	3194	3684	4841	3642	3914
V	226	235	212	196	306	245	243
P	116	153	168	213	228	238	145

Fe2O3* = Total iron; (na) = not analyzed; (-) = not detected

5) Clinopyroxene phyric pillow; IIIA
9B) Aphyric pillow; IIIA
10) "Glassy" olivine phyric pillow; IIB
14) Olivine / clinopyroxene phyric pillow; IIIB
15) Aphyric massive flow (interior); IIE
15A) Aphyric massive flow (top); IIE
17) Aphyric pillow; IIIA

WHOLE-ROCK CHEMISTRY (cont.)

SAMPLE #	19	20	25	26	28	32	34
SiO2	52.48	49.89	47.74	57.49	53.24	50.98	47.27
Al2O3	16.76	15.73	14.31	15.91	13.48	16.02	15.22
TiO2	0.58	0.55	0.52	0.84	0.50	0.54	0.52
Fe2O3*	10.23	10.41	7.94	8.65	8.78	8.74	9.68
MgO	8.71	9.92	8.87	4.26	9.83	8.26	10.44
CaO	4.43	8.72	15.30	7.58	10.63	8.70	11.44
Na2O	0.40	1.16	0.48	2.47	1.27	0.67	0.43
K2O	5.62	2.40	3.97	1.71	0.48	5.28	4.31
P2O5	0.03	0.02	0.02	0.06	-	0.08	0.03
TOTAL	99.25	98.79	99.16	98.97	98.22	99.27	99.33
FeO	na	na	na	na	4.86	na	na
CO2	0.63	1.76	6.26	1.11	0.51	1.40	4.46
H2O+	5.38	3.88	4.41	2.07	4.29	1.69	5.32
H2O-	3.57	3.27	2.95	1.92	3.19	3.10	2.39
Rb(ppm)	36	17	22	34	10	21	27
Sr	82	110	88	105	175	113	150
Y	11	15	15	22	14	22	15
Ba	3	-	-	29	-	-	-
Zr	26	28	29	51	35	22	24
Nb	2	-	-	3	-	-	-
Zn	70	61	57	64	63	66	67
Cu	29	18	20	64	67	37	32
Ni	60	55	80	17	131	43	47
Cr	216	160	243	18	621	265	154
Ti	4025	3317	2985	5104	3135	3654	3190
V	197	226	148	284	208	182	247
P	141	193	324	350	170	664	238

Fe2O3* = Total iron; (na) = not analyzed; (-) = not detected

19) Aphyric pillow; IIIA
20) Aphyric thin flow; IIIA
25) Olivine phyric pillow; IIA
26) Aphyric massive flow (interior); IIE
28) "Glassy" olivine phyric pillow; IIB
32) Olivine / clinopyroxene phyric pillow; IIIB
34) Olivine / clinopyroxene phyric pillow; IIIB

WHOLE-ROCK CHEMISTRY (cont.)

SAMPLE #	35	36	38	44	45	46	47
SiO2	53.57	51.72	54.06	47.53	52.39	52.01	48.79
Al2O3	13.73	16.32	12.94	7.48	16.54	15.83	14.69
TiO2	0.52	0.55	0.50	0.35	0.57	0.53	0.68
Fe2O3*	8.95	8.94	8.74	9.70	9.50	8.85	8.30
MgO	10.33	6.08	11.34	27.45	6.60	8.03	6.73
CaO	10.43	13.16	10.05	5.29	10.15	12.26	16.86
Na2O	1.31	1.06	1.15	0.35	1.25	1.02	1.80
K2O	0.45	1.76	0.26	0.04	2.34	0.77	1.30
P2O5	0.02	0.08	0.04	0.04	0.06	0.04	0.03
TOTAL	99.31	99.67	99.07	98.24	99.41	99.34	99.19
FeO	4.86	na	6.04	na	na	na	na
CO2	0.25	3.51	0.23	0.24	0.95	1.47	2.14
H2O+	4.19	4.18	3.60	5.27	1.83	2.43	1.56
H2O-	3.97	3.03	1.47	2.43	3.65	4.95	3.38
Rb(ppm)	11	30	6	2	33	6	22
Sr	185	98	85	34	99	92	93
Y	13	17	14	9	15	12	17
Ba	-	35	3	-	-	-	-
Zr	25	27	na	19	26	28	27
Nb	-	-	na	-	-	4	-
Zn	62	55	62	52	63	73	90
Cu	64	29	59	27	31	42	39
Ni	128	46	202	875	46	86	82
Cr	601	186	807	1685	139	247	211
Ti	3221	3382	3117	2260	3841	3369	3394
V	211	276	209	104	238	226	233
P	176	291	159	128	264	209	398

Fe2O3* = Total iron; (na) = not analyzed; (-) = not detected

35) "Glassy" olivine phyric pillow; IIB
36) Olivine phyric thin flow; IIIB
38) "Glassy" olivine phyric pillow; IIB
44) Picritic flow base; IID
45) Aphyric thin flow; IIIA
46) Olivine phyric pillow; IIIB
47) Olivine phyric pillow; IIIB

WHOLE-ROCK CHEMISTRY (cont.)

SAMPLE #	48	51	53	56	57	61	68
SiO2	48.53	50.34	45.45	49.53	52.87	51.97	50.75
Al2O3	15.42	9.04	4.85	16.17	17.60	16.43	17.40
TiO2	0.50	0.33	0.19	0.56	0.58	0.54	0.59
Fe2O3*	8.19	9.62	9.01	9.38	10.41	9.16	8.30
MgO	8.62	21.94	35.13	7.48	4.94	5.70	8.49
CaO	10.32	7.49	4.00	10.53	10.84	13.25	8.53
Na2O	0.83	0.37	0.43	0.60	1.17	1.58	1.02
K2O	4.02	0.05	0.02	4.89	1.15	0.71	4.02
P2O5	0.04	0.01	0.02	0.08	0.09	-	0.05
TOTAL	96.47	99.18	99.10	99.21	99.65	99.34	99.15
FeO	na	na	na	na	na	na	na
CO2	4.82	0.38	0.28	3.60	0.48	1.80	2.93
H2O+	4.09	4.84	2.77	4.33	1.59	1.81	4.62
H2O-	3.02	3.34	1.58	2.64	3.76	2.37	3.83
Rb(ppm)	24	1	2	25	12	14	31
Sr	181	35	26	159	120	97	132
Y	16	9	6	18	19	14	13
Ba	-	-	-	56	1	-	-
Zr	24	14	12	35	37	25	25
Nb	-	-	-	-	1	-	-
Zn	64	50	50	64	80	65	75
Cu	23	29	26	35	78	49	40
Ni	55	743	1426	41	45	60	51
Cr	196	1336	2608	102	270	243	117
Ti	3144	2207	1372	3291	3980	3463	3773
V	254	130	76	213	206	203	263
P	258	118	77	342	453	267	202

Fe2O3* = Total iron; (na) = not analyzed; (-) = not detected

48) Aphyric thin flow; IIIA
51) Picritic flow base; IID
53) Picritic flow base; IID
56) Aphyric pillow; IIIA
57) Olivine / clinopyroxene phyric pillow; IIIB
61) Olivine / clinopyroxene phyric pillow; IIIB
68) Aphyric thin flow; IIIA

WHOLE-ROCK CHEMISTRY (cont.)

SAMPLE #	74	75	81	82	86	91	92
SiO2	54.68	47.69	44.41	48.96	54.56	54.20	45.27
Al2O3	18.18	7.26	5.13	14.64	15.30	13.49	6.02
TiO2	0.79	0.32	0.20	0.66	0.64	0.52	0.29
Fe2O3*	8.76	9.60	9.24	7.93	8.30	8.97	10.08
MgO	3.85	27.83	34.21	7.99	7.86	10.53	32.61
CaO	8.45	5.04	5.61	14.11	11.02	10.82	3.45
Na2O	2.21	0.29	0.19	0.55	1.56	1.24	0.23
K2O	2.44	0.05	0.12	4.31	0.33	0.33	0.03
P2O5	0.11	0.04	0.02	0.12	0.02	0.02	0.02
TOTAL	99.48	98.13	99.14	99.26	99.59	100.12	97.99
FeO	na	na	na	na	6.00	5.57	na
CO2	0.87	0.36	1.13	5.44	0.14	0.33	0.75
H2O+	1.76	6.09	3.96	3.74	3.69	4.06	6.22
H2O-	1.37	2.04	1.25	2.70	1.29	1.76	1.70
Rb(ppm)	40	2	4	27	7	6	2
Sr	114	29	33	88	117	91	17
Y	22	9	6	17	17	14	8
Ba	-	-	-	85	6	-	-
Zr	49	11	5	23	39	24	20
Nb	1	-	-	-	-	-	-
Zn	52	60	57	71	66	60	57
Cu	9	32	29	21	69	64	29
Ni	46	899	1272	98	66	157	1054
Cr	46	1894	2031	343	326	601	2322
Ti	4859	2088	1301	3930	4061	3145	2034
V	288	108	81	215	241	214	94
P	421	114	101	390	234	184	100

Fe2O3* = Total iron; (na) = not analyzed; (-) = not detected

74) Aphyric massive flow (interior); IIE
75) Picritic flow base; IID
81) Picritic pillow; IIC
82) Olivine / clinopyroxene phyric pillow; IIA
86) Olivine / clinopyroxene phyric pillow; IIA
91) "Glassy" olivine phyric pillow; IIB
92) Picritic flow base; IID

WHOLE-ROCK CHEMISTRY (cont.)

SAMPLE #	95	96	97	98	99	100	101
SiO2	51.15	51.52	53.57	53.51	42.64	49.02	53.03
Al2O3	16.15	16.47	13.47	15.71	3.89	13.76	15.29
TiO2	0.54	0.55	0.51	0.74	0.22	0.61	0.65
Fe2O3*	9.63	10.51	8.64	9.08	9.23	8.23	8.59
MgO	5.96	9.10	10.88	4.30	38.14	11.75	8.74
CaO	13.67	4.61	10.56	12.41	4.92	11.51	11.43
Na2O	1.18	1.26	0.96	1.62	0.08	0.37	0.98
K2O	0.77	5.03	0.33	1.52	0.12	3.63	0.24
P2O5	0.06	0.06	0.06	0.06	0.05	0.07	0.06
TOTAL	99.10	99.11	98.97	98.94	99.29	98.96	99.01
FeO	na	na	5.34	na	na	na	na
CO2	2.56	0.78	0.44	5.83	1.94	4.36	4.36
H2O+	1.73	4.87	3.98	3.64	5.08	4.64	1.64
H2O-	2.89	2.94	2.82	3.16	1.27	3.31	2.44
Rb(ppm)	15	60	7	26	3	20	12
Sr	97	176	85	80	20	97	92
Y	15	18	15	12	5	17	16
Ba	-	11	-	49	-	20	-
Zr	16	25	31	25	10	na	34
Nb	-	-	1	-	-	na	-
Zn	70	54	59	54	50	76	56
Cu	60	28	62	36	18	26	23
Ni	57	34	144	185	1474	160	142
Cr	228	114	681	607	3091	481	486
Ti	3425	3565	3238	2595	1032	4111	4376
V	190	271	215	139	63	199	243
P	316	190	195	290	92	334	482

Fe2O3* = Total iron; (na) = not analyzed; (-) = not detected

95) Olivine / clinopyroxene phyric pillow; IIIB
96) Aphyric thin flow; IIIA
97) "Glassy" olivine phyric pillow; IIB
98) Top of picrite-based flow; IID
99) Picritic flow base; IID
100) Olivine / clinopyroxene phyric pillow; IIA
101) Olivine phyric thin flow; IIA

WHOLE-ROCK CHEMISTRY (cont.)

SAMPLE #	102	103	110	112	115	117	120
SiO2	52.56	43.91	52.07	50.42	53.59	48.52	46.09
Al2O3	15.31	5.29	17.38	16.85	13.18	14.51	6.40
TiO2	0.72	0.29	1.53	1.57	0.60	0.59	0.35
Fe2O3*	8.74	9.69	12.44	14.28	8.38	8.75	10.12
MgO	8.87	31.09	4.12	4.56	10.54	8.84	30.31
CaO	11.77	8.22	6.27	5.88	11.16	12.34	4.62
Na2O	1.11	0.23	4.19	2.89	1.78	0.56	0.36
K2O	0.27	0.12	0.90	2.68	0.17	4.47	0.05
P2O5	0.06	0.06	0.18	0.16	0.03	0.09	0.04
TOTAL	99.40	98.90	99.09	99.31	99.42	98.68	98.35
FeO	na	na	na	na	na	na	na
CO2	0.19	3.46	0.38	0.76	0.15	5.03	0.20
H2O+	4.14	5.97	1.81	2.28	1.08	3.76	3.85
H2O-	2.68	2.00	3.27	2.82	3.17	2.74	1.67
Rb(ppm)	6	3	12	39	3	30	na
Sr	98	34	121	116	90	83	na
Y	19	7	41	40	15	17	na
Ba	13	-	13	50	17	-	-
Zr	43	16	92	na	33	24	9
Nb	-	-	-	na	-	-	-
Zn	70	53	91	95	59	61	58
Cu	66	25	27	36	61	32	32
Ni	146	1111	2	4	130	898	1090
Cr	669	1965	19	24	325	1877	1995
Ti	4583	1500	9212	11625	na	3502	2363
V	258	81	393	516	243	203	103
P	241	147	269	608	267	376	143

Fe2O3* = Total iron; (na) = not analyzed; (-) = not detected

102) Olivine phyric pillow; IIA
103) Picritic flow base; IID
110) Aphyric pillow; IA
112) Aphyric pillow; IA
115) Clinopyroxene microphyric flow (interior); IIG
117) Olivine / clinopyroxene phyric thin flow; IIA
120) Picritic flow base; IID

WHOLE-ROCK CHEMISTRY (cont.)

SAMPLE #	121	121A	123	127	136	139	141
SiO2	37.91	52.78	49.48	44.95	51.79	54.84	52.60
Al2O3	10.54	14.68	15.41	4.95	17.11	14.81	14.92
TiO2	0.50	0.64	0.54	0.23	0.58	0.61	0.63
Fe2O3*	9.29	8.72	8.97	8.82	10.37	7.91	8.33
MgO	6.74	9.60	8.23	34.55	5.17	6.18	6.17
CaO	30.96	11.01	10.77	4.37	11.77	11.61	13.55
Na2O	0.40	1.10	0.80	0.27	1.43	1.51	1.77
K2O	2.13	0.44	4.83	0.13	1.27	1.99	1.34
P2O5	0.16	0.10	0.10	0.03	0.19	0.06	0.01
TOTAL	98.61	99.08	99.14	98.28	99.66	99.53	99.31
FeO	na	na	na	na	na	na	na
CO2	15.08	0.27	3.94	0.33	0.49	2.34	3.44
H2O+	na	3.58	na	3.09	4.12	na	1.85
H2O-	na	3.18	na	0.91	2.08	na	1.92
Rb(ppm)	12	7	31	4	6	19	12
Sr	78	103	88	35	116	90	92
Y	14	17	13	6	20	19	17
Ba	-	9	68	1	2	-	-
Zr	23	36	20	8	42	41	28
Nb	-	-	1	-	-	-	-
Zn	74	63	57	54	66	45	49
Cu	14	61	26	30	72	14	11
Ni	194	171	70	1402	84	55	88
Cr	727	637	268	2430	337	211	223
Ti	2200	3946	3073	1451	4233	3971	3286
V	176	227	253	88	251	218	232
P	659	225	277	71	215	365	359

Fe2O3* = Total iron; (na) = not analyzed; (-) = not detected

121) Olivine phyric pillow (interior); IIa
121A) Olivine phyric pillow (rim); IIA
123) Aphyric flow; IIIA
127) Picritic pillow; IIC
136) Olivine / clinopyroxene phyric pillow; IIA
139) Olivine microphyric flow; IIF
141) Olivine microphyric flow; IIF

WHOLE-ROCK CHEMISTRY (cont.)

SAMPLE #	143	145	148	149	152	153	154A
SiO2	48.99	51.43	55.45	50.00	51.45	54.31	53.21
Al2O3	16.12	16.88	15.81	16.91	16.16	14.98	15.44
TiO2	1.34	1.54	0.98	0.96	0.62	0.65	0.67
Fe2O3*	12.68	13.54	11.09	10.82	8.18	8.88	8.37
MgO	6.00	5.76	4.53	8.48	8.30	7.57	7.99
CaO	9.27	6.15	8.26	5.03	9.10	7.46	11.60
Na2O	0.62	2.73	2.36	5.56	0.40	1.36	1.40
K2O	3.78	1.16	0.95	1.25	4.79	4.03	0.40
P2O5	0.18	0.15	0.13	0.14	0.06	0.10	0.02
TOTAL	98.98	99.34	99.57	99.14	99.07	99.34	99.11
FeO	na	na	na	na	na	na	5.84
CO2	4.63	0.47	0.75	0.27	3.03	0.28	0.09
H2O+	4.31	1.78	1.69	5.90	4.68	1.82	4.28
H2O-	6.85	4.49	1.66	3.63	4.36	2.13	1.57
Rb(ppm)	21	17	26	13	27	24	na
Sr	75	105	99	27	114	76	na
Y	28	38	22	21	14	17	na
Ba	66	22	4	12	134	23	7
Zr	54	81	40	46	30	na	34
Nb	-	1	-	-	-	na	-
Zn	88	91	78	72	58	53	63
Cu	31	26	12	24	20	20	63
Ni	12	3	6	29	103	83	80
Cr	18	26	30	71	266	336	382
Ti	9382	11167	7147	7008	4086	4316	4216
V	432	615	335	262	202	221	232
P	591	530	383	461	217	331	190

Fe2O3* = Total iron; (na) = not analyzed; (-) = not detected

143) Aphyric pillow; IA
145) Aphyric pillow; IA
148) Aphyric thin flow; IA
149) Aphyric pillow; IA
152) Olivine phyric pillow; IIA
153) Aphyric massive flow (top); IIE
154A) Olivine / clinopyroxene phyric pillow (rim); IIA

WHOLE-ROCK CHEMISTRY (cont.)

SAMPLE #	155	162	163A	175	177	178	181
SiO2	44.00	45.91	53.94	46.86	50.89	49.80	54.44
Al2O3	4.17	5.46	13.81	15.10	17.42	16.38	14.62
TiO2	0.17	0.30	0.58	1.34	1.49	0.90	0.62
Fe2O3*	9.00	10.36	8.84	12.15	13.62	10.73	8.80
MgO	35.86	33.47	10.08	5.76	4.80	10.41	8.03
CaO	6.01	3.44	10.25	9.22	5.60	6.47	10.90
Na2O	0.18	0.30	1.33	4.74	3.30	0.84	1.35
K2O	0.04	0.11	0.26	3.77	2.07	3.07	0.23
P2O5	-	0.05	0.08	0.15	0.15	0.11	0.05
TOTAL	99.44	99.39	99.17	99.09	99.35	98.71	99.04
FeO	na	na	5.78	na	na	na	6.16
CO2	2.88	0.33	0.28	0.78	0.28	1.33	0.14
H2O+	5.16	6.13	3.49	1.96	2.34	4.66	3.25
H2O-	1.33	2.12	1.72	3.42	3.97	3.85	1.15
Rb(ppm)	na	2	na	2	16	20	6
Sr	na	19	na	102	118	87	88
Y	na	6	na	15	41	23	17
Ba	-	-	1	-	52	31	3
Zr	8	9	28	44	78	47	36
Nb	-	-	-	-	-	-	-
Zn	58	59	69	58	78	70	62
Cu	22	23	56	56	31	48	64
Ni	1531	1164	317	243	5	35	69
Cr	2301	2229	812	450	32	56	330
Ti	1117	1771	3401	4305	10850	6397	3967
V	65	83	200	233	602	257	235
P	93	83	183	248	533	344	202

Fe2O3* = Total iron; (na) = not analyzed; (-) = not detected

155) Picritic flow base; IID
162) Picritic flow base; IID
163A) Olivine phyric pillow (rim); IIA
175) Aphyric flow (Cpx-rich base); IIG
177) Aphyric pillow; IA
178) Aphyric pillow; IA
181) Olivine / clinopyroxene phyric pillow (rim); IIA

GLASS CHEMISTRY

SAMPLE #	5	10	13	14	16	32
SiO2	53.99	54.09	54.75	54.48	54.10	54.31
Al2O3	15.03	16.10	15.90	15.90	15.90	15.70
TiO2	0.50	0.55	0.49	0.52	0.50	0.49
FeO*	8.03	7.25	8.08	8.20	8.17	8.12
MgO	6.99	6.48	6.20	5.88	6.22	6.59
CaO	11.27	11.24	10.92	10.80	10.91	11.03
Na2O	1.80	2.06	1.83	1.87	1.90	1.81
K2O	0.17	0.18	0.18	0.20	0.19	0.18
P2O5	0.07	0.07	0.07	0.06	0.07	0.08
TOTAL	97.85	98.02	98.42	97.91	97.96	98.31
CIPW NORM						
Q	8.70	8.20	10.25	10.31	9.19	9.31
OR	1.03	1.08	1.08	1.21	1.15	1.08
AB	15.54	17.76	15.71	16.14	16.39	15.56
AN	33.10	34.81	35.15	35.09	34.97	34.73
DI	19.15	17.54	15.84	15.71	16.16	16.61
HY	19.52	17.74	19.04	18.54	19.16	19.75
MT	1.82	1.64	1.82	1.85	1.85	1.83
IL	0.97	1.06	0.94	1.01	0.97	0.95
AP	0.17	0.17	0.16	0.14	0.17	0.19
TOTAL	100.00	100.00	100.00	100.00	100.00	100.00

SAMPLE #	35	38	46	47	57	60
SiO2	54.13	54.57	54.12	54.00	53.98	53.90
Al2O3	14.55	14.71	16.04	16.16	15.91	15.87
TiO2	0.52	0.54	0.51	0.52	0.54	0.53
FeO*	7.51	7.44	8.04	8.08	8.16	8.16
MgO	7.98	7.28	6.26	6.21	6.15	6.18
CaO	10.94	11.34	11.09	10.99	10.91	10.91
Na2O	1.92	1.89	1.88	1.84	1.86	1.82
K2O	0.20	0.21	0.18	0.18	0.18	0.17
P2O5	0.06	0.05	0.06	0.07	0.05	0.06
TOTAL	97.81	98.03	98.18	98.05	97.74	97.60
CIPW NORM						
Q	7.65	8.78	9.06	9.25	9.42	9.57
OR	1.21	1.27	1.08	1.08	1.09	1.03
AB	16.59	16.29	16.18	15.86	16.08	15.76
AN	31.14	31.62	35.40	35.96	35.29	35.44
DI	19.35	20.59	16.49	15.63	16.11	16.00
HY	21.21	18.60	18.84	19.22	19.00	19.19
MT	1.70	1.68	1.81	1.83	1.85	1.85
IL	1.01	1.05	0.99	1.01	1.05	1.03
AP	0.14	0.12	0.14	0.17	0.12	0.14
TOTAl	100.00	100.00	100.00	100.00	100.00	100.00

FeO* = Total Iron

SAMPLE #	61	86	93	95	127	131
SiO2	54.54	54.77	53.56	54.25	54.26	55.58
Al2O3	16.09	15.80	16.03	16.12	14.18	16.15
TiO2	0.55	0.62	0.69	0.50	0.48	0.67
FeO*	8.22	7.53	7.62	8.17	7.48	7.63
MgO	6.00	5.81	6.44	6.17	8.49	5.54
CaO	10.91	10.39	11.21	10.79	11.29	10.18
Na2O	1.84	2.13	2.11	1.85	1.70	2.20
K2O	0.18	0.22	0.18	0.18	0.19	0.20
P2O5	0.08	0.06	0.07	0.06	0.04	0.07
TOTAL	98.41	97.33	97.91	98.09	98.11	98.22
CIPW NORM						
Q	10.15	10.46	7.41	9.67	7.90	11.32
OR	1.08	1.34	1.09	1.08	1.14	1.20
AB	15.80	18.49	18.21	15.94	14.64	18.93
AN	35.63	33.77	34.42	35.79	31.05	34.17
DI	15.37	15.31	17.80	14.99	20.79	13.69
HY	18.86	17.57	17.84	19.57	21.76	17.50
MT	1.85	1.71	1.73	1.85	1.68	1.73
IL	1.06	1.21	1.34	0.97	0.93	1.29
AP	0.19	0.14	0.17	0.14	0.09	0.17
TOTAL	100.00	100.00	100.00	100.00	100.00	100.00

SAMPLE #	133	144	156	167	182	183
SiO2	54.70	54.55	54.44	54.48	52.80	54.68
Al2O3	15.94	16.06	15.30	15.31	15.11	15.58
TiO2	0.60	0.66	0.51	0.50	0.63	0.61
FeO*	7.36	7.78	8.06	8.06	7.52	7.41
MgO	5.97	6.14	6.66	6.65	8.05	6.38
CaO	10.99	10.75	11.03	11.08	11.11	10.91
Na2O	2.15	2.11	1.75	1.70	1.99	2.13
K2O	0.17	0.20	0.17	0.17	0.18	0.19
P2O5	0.06	0.08	0.05	0.06	0.07	0.06
TOTAL	97.94	98.33	97.97	98.01	97.46	97.95
CIPW NORM						
Q	9.50	9.14	9.95	10.19	5.49	9.17
OR	1.03	1.20	1.03	1.02	1.09	1.15
AB	18.55	18.13	15.09	14.66	17.26	18.38
AN	34.00	34.29	34.04	34.29	32.56	33.03
DI	17.30	15.80	17.48	17.41	18.99	17.73
HY	16.64	18.22	19.49	19.50	21.51	17.55
MT	1.67	1.75	1.82	1.82	1.71	1.67
IL	1.16	1.27	0.99	0.97	1.23	1.18
AP	0.14	0.19	0.12	0.14	0.17	0.14
TOTAL	100.00	100.00	100.00	100.00	100.00	100.00

FeO* = Total Iron

APPENDIX IV

MINERAL ANALYSES

OLIVINE ANALYSES

SAMPLE	SiO2	FeO*	MgO	CaO	MnO	NiO	Cr2O3	TOTAL
10-1)	39.75	11.70	47.98	0.13	0.10	0.15	-	99.80
10-2)	39.36	11.89	47.13	0.16	0.14	0.16	-	98.83
10-3)	39.66	10.75	48.80	0.18	0.11	0.22	0.05	99.77
10-4)	39.14	13.06	46.55	0.17	0.22	0.09	0.04	99.27
10-5)	38.92	11.15	47.72	-	-	0.12	-	97.91
35-1)	39.31	11.50	48.75	0.07	0.04	0.11	-	99.79
35-2)	39.65	11.20	48.57	0.06	0.06	0.07	-	99.62
35-3)	39.58	11.79	48.05	0.20	0.12	0.20	-	99.81
35-4)	39.86	12.74	48.25	0.22	0.15	0.22	0.07	101.52
35-5)	39.42	14.59	46.39	0.17	0.16	0.08	-	100.79
38-1)	40.24	12.17	47.58	0.20	0.19	0.21	-	100.59
38-2)	40.05	11.23	48.46	0.13	-	0.13	-	100.00
38-3)	39.95	12.00	47.77	0.16	0.16	0.21	0.09	100.33
38-4)	39.92	12.27	47.11	0.17	0.07	0.15	0.06	99.75
38-5)	40.02	12.25	48.27	0.15	0.12	0.13	-	100.94
38-6)	39.90	11.61	48.15	0.28	0.04	0.28	0.08	100.26
53-1)	40.13	7.52	51.06	0.12	-	0.29	0.09	99.20
53-2)	39.73	9.35	49.33	0.15	0.04	0.18	0.11	98.90
53-3)	39.85	8.39	50.14	-	-	0.12	-	98.50
53-4)	39.51	8.24	50.39	0.04	-	0.12	-	98.30
53-4a)	39.84	9.48	48.87	0.11	-	0.23	0.09	98.62
53-5)	39.85	8.87	49.26	0.07	-	0.07	-	98.12
54-4)	39.94	11.69	48.50	0.10	0.12	0.11	0.05	100.52
54-5)	40.07	11.70	48.69	0.18	0.16	0.21	0.13	101.26
81-1)	40.37	8.43	50.35	0.16	0.16	0.18	0.23	99.88
81-2)	39.98	8.42	50.02	0.20	0.08	0.17	0.11	98.97
81-3)	39.47	11.93	47.99	0.18	0.04	0.10	-	99.61
81-4)	39.75	8.73	49.50	0.07	-	0.12	-	98.17
81-5)	39.98	8.42	49.95	-	-	0.19	-	98.53
83-1)	39.91	11.10	48.83	0.23	0.10	0.19	-	100.38
83-2)	39.41	11.20	48.52	0.15	0.09	0.16	-	99.53
83-3)	40.02	11.76	48.76	0.20	0.14	0.20	0.09	101.16
83-4)	39.41	12.35	47.78	0.18	-	0.19	-	99.91
83-5)	38.99	12.88	47.02	0.14	-	0.08	-	99.12
86-1)	39.08	13.85	46.83	0.16	0.06	0.11	-	100.09
86-2)	39.25	15.29	45.68	0.11	0.13	0.13	-	100.59
86-3)	39.62	14.17	47.12	0.13	0.12	0.23	-	101.39
86-4)	39.72	11.75	48.32	0.14	0.10	0.15	-	100.18
86-5)	39.61	14.16	46.90	0.13	0.22	0.18	-	101.18
86-6)	38.65	15.23	45.19	0.18	0.23	0.05	-	99.54
97-1)	39.07	12.72	47.33	0.12	-	0.10	-	99.36
97-2)	39.94	10.89	49.01	0.14	0.17	0.14	0.15	100.45
97-3)	40.06	14.22	45.40	0.97	0.08	0.13	-	100.85
97-4)	40.36	11.13	49.35	0.15	0.11	0.23	0.11	101.44
97-5)	40.14	10.31	49.28	0.09	-	0.13	0.09	100.04
97-6)	39.15	10.93	48.56	0.14	0.18	0.24	0.14	99.35

OLIVINE ANALYSES (cont.)

SAMPLE	SiO2	FeO*	MgO	CaO	MnO	NiO	Cr2O3	TOTAL
99-1)	39.39	10.49	48.87	0.11	-	0.10	-	98.95
99-2)	39.88	7.08	50.96	0.12	-	0.27	0.10	98.41
99-3)	39.83	9.10	49.47	0.14	0.08	0.23	0.14	98.98
99-4)	39.95	9.19	49.57	0.19	0.14	0.20	0.18	99.44
99-5)	40.12	7.99	50.50	0.20	0.05	0.29	0.19	99.35
105-1a)	40.29	9.68	49.75	0.20	0.10	0.23	-	100.24
105-1b)	40.44	9.60	49.89	0.16	0.13	0.15	0.14	100.51
105-1c)	40.22	9.33	49.85	0.17	0.17	0.20	0.18	100.13
105-1d)	39.99	9.25	49.48	0.11	0.10	0.38	0.07	99.39
105-1e)	40.05	9.41	49.16	0.18	0.13	0.44	0.14	99.51
105-G1)	39.75	12.25	47.38	0.23	0.21	0.04	-	99.87
105-G2)	39.62	11.60	47.91	0.17	0.23	0.12	0.09	99.74
127-2a)	40.25	8.69	50.86	0.19	0.27	0.24	0.15	100.65
127-2b)	40.38	8.32	50.69	0.21	0.11	0.09	0.23	100.03
127-2c)	39.99	8.43	50.11	0.21	0.15	0.06	-	98.95
127-4a)	39.68	9.30	48.67	0.16	0.17	0.23	0.19	98.42
127-G1)	39.82	12.09	48.31	0.27	0.21	0.15	0.15	101.02
127-G2)	40.07	12.34	47.61	0.20	0.10	0.07	0.17	100.56
136-1)	39.77	12.62	47.83	0.12	0.15	0.23	0.08	100.81
136-2)	39.44	13.77	46.86	0.11	0.05	0.18	-	100.41
136-3)	38.82	15.32	45.54	0.08	0.06	0.11	-	99.92
136-4)	38.38	16.28	44.47	-	-	0.07	-	99.20
136-5)	39.33	14.38	46.05	0.15	0.16	0.11	0.05	100.25
154a-1)	40.11	14.38	46.40	0.14	0.22	0.20	0.09	101.53
154a-2)	40.14	13.09	47.59	0.19	0.13	0.30	0.05	101.50
154a-4)	39.81	13.30	47.36	0.16	0.13	0.28	-	101.04
162-1)	39.18	11.33	47.26	0.15	0.06	0.23	-	98.21
162-1a)	39.20	11.51	47.00	0.19	0.12	0.36	0.09	98.48
162-3)	39.30	11.72	46.81	0.13	0.16	0.16	-	98.29
162-4)	39.52	10.78	47.50	0.10	0.05	0.24	-	98.18
162-4a)	39.48	10.27	47.88	0.08	0.08	0.29	-	98.08
162-5)	40.13	10.44	49.25	0.20	0.17	0.34	-	100.53
163a-1)	39.67	12.42	46.41	0.17	0.21	0.09	-	98.94
163a-2)	39.26	12.27	46.44	0.18	0.15	0.23	-	98.53
163a-3)	39.41	11.93	46.70	0.18	0.14	0.23	0.07	98.66
163a-4)	39.66	12.41	46.66	0.16	0.19	0.26	-	99.33
163a-5)	39.86	10.18	47.77	0.12	0.09	0.17	-	98.19
163a-6a)	39.77	14.19	46.07	0.21	0.27	-	-	100.52
163a-6b)	40.19	10.04	49.69	0.22	0.14	0.10	0.20	100.57

OLIVINE ANALYSES (cont.)

SAMPLE	SiO2	FeO*	MgO	CaO	MnO	NiO	Cr2O3	TOTAL
#T-1	39.70	10.77	47.78	0.08	0.06	0.07	-	98.47
T-2	40.57	7.17	50.79	0.11	0.08	0.31	0.05	99.07
T-3	40.53	7.19	51.27	0.10	0.07	0.46	0.21	99.84
T-4	40.52	7.08	50.56	0.13	0.04	0.34	0.10	98.77
T-5	40.77	6.92	51.28	0.16	0.05	0.42	0.10	99.71
T-6	40.29	7.06	50.77	-	-	0.10	-	98.22
T-7	40.69	6.91	50.80	0.14	0.09	0.47	0.11	99.31
T-8	40.59	7.09	50.83	0.11	0.04	0.18	-	98.81
T-9	40.75	6.92	51.12	0.11	0.05	0.33	0.11	99.38
T-10	40.73	7.07	50.67	0.06	-	0.28	-	98.81
T-11	41.00	7.16	51.16	-	0.08	0.36	-	99.75
T-12	40.88	7.03	51.28	0.10	0.08	0.29	0.13	99.79
T-13	40.51	7.02	50.74	-	0.05	0.37	-	98.68
T-14	40.77	6.87	51.26	0.09	0.09	0.35	0.15	99.58
T-15	40.38	7.01	50.28	0.05	-	0.22	0.06	98.54
T-16	40.87	7.08	50.98	0.13	0.11	0.49	0.13	99.80
T-17	40.51	7.10	50.65	0.10	0.13	0.28	-	98.77
T-18	40.46	7.15	50.72	0.06	0.06	0.34	0.06	98.86
T-19	40.66	7.03	50.99	0.07	-	0.29	0.07	99.10
T-20	40.47	7.15	50.62	0.14	-	0.36	0.07	98.82
T-21	40.18	10.33	48.50	-	-	0.08	-	99.08
G-1	39.77	11.39	47.99	0.18	0.15	0.32	0.06	99.88

(#) Analyses T1 to T21 are consecutive points along a microprobe traverse (See Plate III-3). Grain is a large olivine phenocryst within a picritic pillow. The composition of surrounding groundmass grains is given by G-1.

(*) Total iron expressed as FeO.

(-) Not detected

PYROXENE ANALYSES

SAMPLE	SiO2	Al2O3	FeO*	MgO	CaO	TiO2	MnO	Cr2O3	TOTAL
136-1)	53.81	3.18	6.96	19.95	16.81	0.38	0.15	0.43	101.67
136-2)	53.97	2.23	4.85	18.34	20.54	0.16	-	1.22	101.32
136-3)	54.22	2.29	5.16	17.55	20.46	0.07	-	0.99	100.74
136-4)	53.04	2.53	5.24	17.23	19.59	0.14	-	0.67	98.42
136-5)	53.94	1.79	4.80	17.18	21.13	-	-	0.92	99.76
136-6)	53.32	2.55	5.15	17.53	20.08	0.28	-	1.08	99.99
136-7)	49.80	6.45	6.69	14.86	20.00	0.65	-	-	98.45
136-8)	48.97	7.64	8.34	14.62	18.23	0.71	-	-	98.52
136-9)	53.46	2.58	5.09	17.36	19.84	0.14	-	0.92	99.40
136-10)	53.21	2.33	5.90	18.16	19.16	0.28	-	0.52	99.57
136-12)	53.66	2.85	5.39	17.26	21.15	0.32	-	0.75	101.38
86-1)	52.62	2.89	6.22	18.19	18.06	0.23	-	0.81	99.02
86-2)	52.93	2.48	5.63	17.38	20.20	0.23	-	0.62	99.47
86-3c)	54.11	2.75	6.58	19.98	16.10	0.32	0.07	0.72	100.64
86-3r)	53.85	2.11	6.28	19.32	17.47	0.31	-	0.52	99.86
86-5)	53.21	2.46	4.94	17.31	20.72	0.19	-	1.17	99.99
86-6)	52.53	2.96	6.31	16.44	20.67	0.22	-	0.06	99.18
154a-1)	55.57	0.97	6.36	21.22	16.02	0.09	-	0.59	100.82
154a-2)	53.55	2.26	4.64	16.92	22.07	-	-	1.45	100.90
154a-3)	53.22	3.00	5.42	16.83	21.63	0.09	-	0.80	100.99
154a-4)	53.58	2.62	5.41	16.99	21.56	0.27	-	0.83	101.25
154a-5)	55.64	1.00	7.10	21.55	14.76	-	0.07	0.45	100.56
154a-6)	51.17	5.08	6.35	15.53	20.97	0.65	-	-	99.75
154a-7)	51.79	3.88	5.82	16.35	20.47	0.34	-	0.38	99.04
154a-8a)	53.53	2.14	5.11	17.31	20.84	0.18	-	1.21	100.32
154a-8b)	53.65	2.78	5.54	16.56	22.41	0.43	0.12	0.47	101.97
154a-8c)	54.75	1.23	6.44	19.20	18.38	0.28	0.10	0.30	100.68
154a-9c)	55.20	1.18	5.43	19.40	18.91	-	-	0.88	101.00
154a-9r)	53.87	2.11	4.55	16.84	22.89	0.13	-	1.14	101.53
154a-10)	53.12	2.75	4.90	17.17	20.92	0.26	-	1.22	100.33
14-1)	52.86	2.70	5.42	16.87	21.13	0.18	-	0.94	100.10
14-2)	52.82	2.90	6.31	16.94	20.18	0.24	0.06	0.12	99.56
14-3)	53.74	3.19	5.92	18.02	19.69	0.42	0.12	0.76	101.85
14-4)	52.64	2.66	5.49	16.37	21.43	-	-	0.53	99.13
14-5)	53.42	2.31	5.69	17.14	21.21	0.13	-	0.68	100.58
14-6)	52.65	2.89	5.60	16.47	21.67	0.20	-	0.73	100.21
14-7)	52.83	2.61	5.71	16.90	20.76	0.18	-	0.48	99.47
14-8)	53.03	2.90	5.75	16.86	21.12	-	-	0.46	100.12
14-9a)	53.50	1.67	5.64	17.41	20.44	-	-	0.48	99.14
14-9b)	53.14	2.54	5.24	16.74	21.49	-	-	0.70	99.86
14-9c)	53.12	2.50	5.75	17.20	20.90	-	-	0.67	100.14
74-1)	52.15	2.18	10.37	14.29	20.90	0.48	-	-	100.37
74-2)	52.94	2.13	8.17	16.30	20.08	0.34	0.10	-	100.06
74-4)	52.78	2.64	5.50	16.71	21.42	0.11	-	0.27	99.44
74-5)	52.80	2.62	5.35	16.45	21.84	0.20	-	0.38	99.65
74-6)	51.07	2.29	12.43	13.61	19.45	0.65	0.17	-	99.67
74-7)	52.88	2.41	7.43	16.17	20.28	0.34	0.06	-	99.56
74-8)	53.09	2.87	4.83	16.54	21.78	0.18	-	0.70	99.99
74-9)	52.87	2.39	6.79	15.44	21.41	0.34	-	-	99.25
53-1)	49.52	6.46	5.69	13.01	23.19	0.48	-	-	98.36

PYROXENE ANALYSES (cont.)

SAMPLE	SiO2	Al2O3	FeO*	MgO	CaO	TiO2	MnO	Cr2O3	TOTAL
53-2)	48.10	8.09	8.18	11.94	22.65	1.15	0.04	0.13	100.30
53-3)	48.41	7.64	7.23	12.36	22.86	0.72	-	-	99.23
53-4)	50.66	6.21	5.99	14.13	22.61	0.41	-	0.08	100.10
53-6)	47.56	8.52	9.33	11.73	21.46	1.30	-	0.05	99.95
53-7)	48.78	8.16	6.97	12.40	23.13	0.82	-	0.05	100.30
53-8)	48.64	8.10	6.85	12.34	23.30	0.79	-	-	100.02
53-10)	48.55	7.73	7.46	12.36	22.61	0.50	-	-	99.21
97-2)	49.83	10.24	8.37	13.19	17.62	0.54	0.15	0.20	100.22
97-3)	47.42	10.69	8.32	10.89	23.07	0.62	-	0.05	100.07
97-4)	50.52	8.91	6.85	12.99	20.32	0.61	0.12	-	100.32
97-5)	46.62	11.26	8.92	10.08	22.54	0.65	-	-	100.07
97-6)	47.65	9.99	9.61	11.59	20.16	0.51	-	-	99.51
97-8)	46.49	14.68	11.48	7.31	18.60	0.52	0.10	-	99.19
81-1)	49.08	10.59	6.87	10.92	20.85	0.60	-	-	98.91
81-2)	48.93	8.21	6.29	13.06	23.47	0.61	-	-	100.57
81-4)	47.79	8.74	8.64	11.79	22.46	0.71	0.05	0.06	100.25
81-5)	50.10	6.71	5.65	13.95	23.09	0.54	-	-	100.04
81-7)	48.67	8.46	7.46	12.08	23.20	0.55	-	0.07	100.49
81-8)	49.41	8.34	7.83	12.40	23.04	0.71	-	-	101.74
81-9)	49.63	7.26	5.92	13.20	23.00	0.61	-	-	99.63
81-9a)	50.43	7.27	6.44	13.58	23.21	0.44	-	0.05	101.43
81-10)	48.32	8.81	7.55	11.61	23.90	0.80	-	-	101.00
33-1)	53.42	2.71	6.54	16.39	21.83	0.18	-	-	101.07
33-2)	53.43	2.08	4.85	17.16	21.28	-	-	0.72	99.52
33-3)	54.09	1.67	5.67	17.48	21.17	-	-	0.33	100.41
33-4)	53.55	2.47	6.66	16.58	21.38	0.20	0.04	0.07	100.97
33-6)	53.65	2.28	6.52	16.25	21.46	0.29	0.04	-	100.49
33-7)	52.88	2.42	9.47	14.99	20.81	0.33	-	-	100.91
33-8)	53.15	2.33	6.81	16.06	21.23	0.07	-	0.14	99.74
33-9)	53.61	2.29	5.67	17.38	20.56	0.07	-	0.62	100.20
33-10)	53.89	2.23	5.65	16.66	21.62	0.13	-	0.45	100.50
33-11)	53.18	2.22	5.26	16.52	22.23	0.13	-	0.67	100.22
51-1)	53.70	2.04	3.85	17.01	22.84	0.16	-	1.35	100.95
51-2)	53.75	2.03	4.03	16.92	22.71	0.06	-	1.08	100.58
51-3c)	52.98	3.27	4.82	16.70	22.30	0.26	0.07	1.11	101.50
51-3r)	53.16	2.96	4.59	16.95	22.18	0.29	0.04	1.17	101.34
51-4)	53.24	2.61	4.16	16.98	22.05	0.13	-	1.53	100.69
51-5)	54.62	1.56	4.01	17.89	22.03	-	-	1.09	101.20
51-6)	53.08	2.30	4.37	17.00	21.91	0.14	-	1.52	100.31
51-7)	53.52	1.99	3.68	16.88	22.55	-	-	1.26	99.88
51-8)	54.60	1.42	4.73	18.71	20.27	-	-	0.48	100.22
51-9)	52.72	3.82	5.11	16.98	21.73	0.36	-	0.47	101.20
51-10)	53.96	2.27	4.06	17.32	22.27	-	0.06	1.57	101.51
51-11)	53.13	1.95	3.86	17.10	22.17	0.24	-	1.12	99.58
55-1)	52.62	4.23	5.33	16.15	22.35	0.53	-	0.39	101.60
55-2)	52.05	3.65	6.42	15.83	21.37	0.42	-	-	99.74
55-3)	52.59	2.82	4.64	16.62	21.58	0.27	-	0.96	99.49
55-4)	53.33	2.78	4.05	16.60	22.49	0.15	-	1.05	100.45
55-5a)	53.21	2.07	3.88	16.82	22.58	0.16	-	1.64	100.37
55-5b)	53.37	2.24	3.90	17.04	22.76	0.14	-	1.63	101.08

PYROXENE ANALYSES (cont.)

SAMPLE	SiO2	Al2O3	FeO*	MgO	CaO	TiO2	MnO	Cr2O3	TOTAL
55-6a)	51.29	4.18	5.94	15.50	22.07	0.49	-	0.10	99.58
55-6b)	52.88	2.69	4.10	16.23	22.73	0.17	-	1.31	100.12
55-6c)	54.54	1.06	4.67	18.64	20.43	0.08	0.05	0.86	100.34
83-1)	52.81	2.93	5.29	17.28	21.19	0.33	-	0.44	100.28
83-2)	52.89	2.78	5.03	16.91	21.23	0.24	-	0.74	99.82
83-3a)	52.90	2.59	4.45	16.70	21.94	0.10	-	1.00	99.68
83-3b)	52.49	3.80	4.87	16.41	22.10	0.26	-	1.14	101.08
83-3c)	53.11	3.23	4.95	16.79	21.37	0.29	-	1.22	100.97
83-4)	54.62	1.27	5.16	18.55	19.75	0.15	-	0.33	99.82
83-5)	52.88	3.70	5.57	16.84	20.87	0.44	-	0.87	101.17
35-1)	48.48	8.27	8.81	13.09	20.78	0.61	0.08	0.10	100.22
35-2)	51.21	7.76	6.68	15.02	17.34	0.30	-	-	98.32
35-3)	50.15	7.47	7.33	15.59	18.99	0.31	-	-	99.83
35-4)	45.94	11.54	10.46	9.42	22.76	0.88	-	-	100.99
35-5)	49.76	10.52	9.34	10.00	18.04	0.57	-	-	98.23
35-6)	46.06	11.05	11.16	10.55	20.20	0.89	-	-	99.90
35-7)	52.74	12.19	5.65	10.28	17.22	0.33	-	-	98.42
35-8)	49.12	9.64	7.93	11.08	19.47	0.50	-	-	97.74
35-9)	49.02	8.16	6.68	13.73	20.94	0.60	-	-	99.11
35-10)	48.90	8.25	7.28	13.89	21.10	0.56	-	-	99.98
120a-1r)	53.21	2.75	4.77	16.58	22.50	0.27	-	0.48	100.56
120a-1c)	52.81	2.51	4.22	16.52	22.63	0.06	-	1.21	99.95
120a-2r)	54.18	2.03	4.52	17.35	22.41	0.21	-	0.47	101.17
120a-2c)	52.68	3.70	5.05	16.99	20.80	0.20	-	0.67	100.10
120a-3r)	53.35	2.44	4.40	16.69	22.49	0.21	-	0.56	100.14
120a-3c)	52.51	2.94	5.34	17.42	19.58	0.28	-	0.43	98.52
120a-4)	53.23	3.38	5.11	16.63	21.86	0.45	-	0.51	101.15
120a-5)	52.71	3.55	5.00	16.25	22.55	0.38	-	-	100.45
120a-6)	52.41	2.92	5.05	16.57	21.03	0.13	-	0.33	98.44
120a-7)	52.52	3.94	5.48	16.46	22.09	0.34	0.04	0.28	101.16
120a-8c)	53.16	2.87	4.82	16.68	22.68	0.31	-	0.62	101.14
120a-8r)	53.22	2.71	5.40	16.97	21.09	0.18	-	0.25	99.82
154a-11)	49.40	8.52	7.70	14.29	20.43	0.87	0.09	-	101.30
154a-12)	54.16	1.81	5.13	17.38	21.62	0.13	-	0.46	100.70
154a-13)	47.02	10.61	10.79	12.09	20.26	0.89	-	-	101.05
162-1)	50.50	5.32	6.13	14.75	22.09	0.46	-	0.31	99.57
162-2)	51.85	3.85	5.15	15.62	22.74	0.42	-	0.11	99.74
162-4)	51.50	4.17	5.47	15.43	21.95	0.38	-	0.36	99.26
162-5)	52.65	4.18	5.26	16.24	22.68	0.20	0.09	0.27	101.57
1-1)	51.80	3.26	6.94	16.52	20.07	0.22	-	-	98.81
1-2)	53.59	2.81	5.70	17.89	19.98	0.25	0.11	0.97	101.29
1-3)	52.41	3.28	5.65	16.45	21.57	0.10	-	0.30	99.76
1-4)	53.35	2.67	5.39	16.82	21.64	0.12	-	0.29	100.29
1-5)	48.68	8.48	7.62	13.91	20.76	0.31	-	-	99.77
1-6)	53.68	2.09	5.59	17.53	20.97	0.10	-	0.51	100.48
26-1)	51.40	2.20	10.12	14.74	20.02	0.49	0.09	-	99.07
26-2)	51.76	2.14	11.10	15.33	18.99	0.39	0.33	-	100.03
26-3)	51.45	2.30	10.34	15.16	19.74	0.43	-	-	99.42
26-4)	51.69	2.41	12.28	13.84	20.19	0.56	0.12	-	101.09
25-1)	52.47	3.09	5.20	16.37	21.85	0.20	-	0.14	99.32

PYROXENE ANALYSES (cont.)

SAMPLE	SiO2	Al2O3	FeO*	MgO	CaO	TiO2	MnO	Cr2O3	TOTAL
25-2)	52.27	3.81	5.32	16.18	22.07	0.21	-	0.23	100.09
25-3)	51.53	5.33	6.95	15.56	21.34	0.63	0.07	-	101.40
25-4)	52.48	3.17	5.38	16.39	22.11	0.26	-	0.28	100.08
25-5)	54.55	1.45	6.11	19.18	18.58	0.17	0.14	0.29	100.47
121-1)	48.14	8.61	6.96	12.52	23.13	0.98	-	0.08	100.42
121-2)	47.73	9.09	6.38	11.99	22.98	0.95	-	-	99.12
121-4)	48.15	8.46	6.69	12.43	23.09	1.02	-	0.10	99.94
121-5)	48.35	7.75	6.92	12.51	23.05	0.96	-	0.14	99.67
121-6)	47.90	8.65	6.96	12.77	21.86	0.88	-	-	99.02
64-1)	52.22	4.03	6.30	16.59	20.31	0.35	-	0.29	100.09
64-2)	52.66	3.06	4.97	16.91	21.43	0.25	-	0.96	100.24
64-4)	51.64	4.13	5.57	15.83	21.29	0.37	-	0.11	98.93
64-5)	52.81	3.22	5.07	16.76	21.90	0.22	-	0.93	100.91
64-6)	52.50	2.98	5.13	16.61	21.60	0.33	-	1.16	100.32
99-1)	51.09	5.17	5.44	14.81	23.47	0.38	-	0.07	100.44
99-2)	50.09	6.11	6.16	13.85	23.48	0.52	-	-	100.21
99-3)	45.11	11.11	10.34	10.56	21.22	0.76	-	-	99.09
99-4)	50.45	5.69	6.14	14.25	22.50	0.36	-	-	99.38
99-5)	51.98	4.35	5.19	15.05	23.11	0.23	-	0.19	100.11
99-6)	52.85	3.12	4.94	16.05	23.56	0.42	0.12	0.42	101.48
99-8)	51.38	5.64	5.58	14.38	23.56	0.37	-	0.20	101.10
99-9)	50.18	6.19	6.12	13.94	23.03	0.55	-	0.17	100.17
51-P1)	55.14	1.37	14.11	24.93	4.13	0.24	0.24	-	100.95
51-P2)	54.43	1.62	14.61	25.52	2.02	0.15	0.23	-	98.58
83-P1)	54.78	1.10	13.97	23.12	6.14	0.16	0.32	-	99.60
83-P2)	54.01	1.56	18.09	23.20	2.00	0.24	0.11	-	99.22
83-P3)	50.44	2.63	20.02	21.48	1.86	0.47	0.24	-	97.13
54-1)	51.96	2.64	4.42	17.70	22.17	0.24	0.05	1.57	100.73
54-2)	53.84	1.26	4.81	19.02	20.83	0.12	-	1.04	100.92
54-3)	52.34	2.67	4.19	17.24	23.47	0.27	0.11	1.03	101.34
54-4a)	48.72	6.55	6.69	15.02	22.09	0.92	0.09	0.53	100.58
54-4b)	51.54	2.75	4.32	16.86	22.97	0.21	0.13	1.54	100.31
54-4c)	51.52	2.54	4.52	17.52	21.85	0.19	0.05	1.40	99.59
54-5a)	50.48	4.00	5.79	16.51	21.88	0.41	0.07	0.40	99.54
54-5b)	51.36	2.56	4.31	17.38	21.96	0.15	0.04	1.28	99.04
54-5c)	51.67	2.39	4.25	17.61	21.75	0.12	0.05	1.37	99.22
54-5d)	53.39	1.29	4.32	19.23	21.49	0.23	0.22	1.07	101.24
54-6)	51.67	3.64	4.91	17.16	22.36	0.28	0.08	1.54	101.65
54-7)	49.55	6.38	6.88	15.83	21.60	0.68	0.13	0.56	101.61
120-1r)	49.98	4.79	6.49	15.66	21.99	0.52	0.12	0.22	99.78
120-1c)	50.56	3.96	5.64	16.11	22.97	0.43	0.13	0.30	100.10
120-2)	49.06	2.92	19.71	15.72	11.91	1.02	0.38	-	100.72
120-3r)	50.07	4.47	6.53	16.09	21.97	0.55	0.15	0.69	100.52
120-3c)	51.03	3.91	4.97	16.73	22.50	0.48	0.12	1.14	100.88
115-2r)	52.18	1.82	5.10	17.55	21.94	0.17	0.10	0.72	99.57
115-2c)	51.83	2.61	5.92	18.08	20.25	0.23	0.13	1.26	100.31

(*) Total iron expressed as FeO
(-) Not detected

FELDSPAR ANALYSES

SAMPLE	SiO2	Al2O3	FeO*	MgO	CaO	Na2O	K2O	TOTAL
120-1a)	49.85	29.51	0.51	0.08	15.40	2.95	-	98.30
120-1b)	51.22	30.01	0.60	0.25	15.24	3.10	0.06	100.48
120-2a)	50.13	30.91	0.65	0.35	16.04	2.99	0.10	101.17
120-2b)	49.94	29.94	0.44	0.12	15.60	2.79	-	98.83
120-2c)	49.25	31.25	0.61	0.23	16.41	2.52	0.06	100.32
120-3)	49.94	30.41	0.60	0.15	15.65	2.82	-	99.57
120-4a)	49.50	30.26	0.49	-	16.11	2.43	-	98.79
120-4b)	51.12	29.68	0.54	0.16	15.04	3.15	0.04	99.73
120-4c)	51.04	29.28	0.66	0.07	14.46	3.28	-	98.80
120-5)	49.98	30.31	0.57	0.16	15.75	2.64	-	99.41
120-6)	50.71	30.45	0.60	0.27	15.70	3.09	0.08	100.91
120-7)	49.38	29.84	0.69	0.59	15.39	2.68	-	98.57
120-8)	54.29	27.16	0.69	-	11.84	4.61	-	98.59
120a-1)	50.35	29.81	0.54	-	15.23	3.05	-	98.98
120a-2)	50.42	29.91	0.71	-	15.24	3.28	0.07	99.63
120a-3)	50.45	29.96	0.38	-	15.18	2.93	-	98.90
120a-4)	51.44	29.99	0.77	0.22	14.85	3.56	0.11	99.96
120a-5)	50.94	29.54	0.42	-	14.88	3.12	-	98.89
120a-6)	49.89	29.94	0.36	-	15.52	2.77	-	98.47
120a-7)	49.99	29.96	0.54	0.07	15.53	2.91	0.04	99.04
120a-8)	50.25	29.81	0.57	0.05	15.62	2.90	0.05	99.26
120a-A1)	63.42	17.88	0.14	-	-	0.13	16.39	97.96
74-1)	54.42	28.13	0.56	-	12.17	4.74	-	100.03
74-2)	50.62	30.51	0.65	-	15.38	3.02	-	100.18
74-3a)	49.77	30.61	0.56	-	15.98	2.72	-	99.63
74-3b)	50.49	30.76	0.67	0.07	15.83	2.97	0.11	100.89
74-3c)	51.88	29.14	0.61	-	14.07	3.84	-	99.55
74-4)	54.15	28.43	0.68	-	12.62	4.89	0.12	100.89
74-5)	53.65	28.35	0.60	-	13.16	4.23	0.27	100.32
74-6)	52.20	29.53	0.86	-	14.41	3.76	0.12	100.88
74-7)	49.64	30.66	0.77	0.09	15.98	2.92	0.06	100.12
74-8)	50.67	29.52	0.83	-	14.69	3.40	0.09	99.21
74-A1)	62.36	18.11	-	-	-	-	16.12	96.51
74-A2)	61.87	17.24	0.06	-	-	-	15.91	95.09
101-1)	50.20	29.96	0.51	-	15.72	2.77	-	99.16
101-2)	51.71	29.46	0.87	-	14.68	3.61	0.04	100.39
101-3a)	50.26	30.39	0.62	0.11	15.67	3.05	0.07	100.16
101-3b)	49.32	31.20	0.39	-	16.39	2.35	-	99.65
101-3c)	55.94	26.46	0.62	-	11.01	5.31	0.10	99.45
101-4)	51.62	28.85	0.62	-	14.52	3.52	-	99.14
101-5)	50.31	29.98	0.64	-	15.36	2.89	-	99.19
101-6)	50.35	30.32	0.54	-	15.65	2.84	-	99.70

(*) Total iron expressed as FeO

(-) Not detected

OXIDE ANALYSES

	SiO2	Al2O3	FeO*	MgO	CaO	TiO2	MnO	V2O5	Cr2O3	TOTAL
154a-2)	1.19	11.66	20.75	12.08	-	0.25	0.08	0.16	53.49	99.66
154a-2a)	-	11.54	20.43	11.97	-	0.24	-	0.10	55.99	100.27
154a-3)	-	11.96	16.91	13.99	-	0.19	-	0.11	56.68	99.84
154a-4)	-	12.46	21.18	11.92	0.06	0.30	-	0.09	54.00	100.01
154a-5)	-	11.79	16.84	13.92	0.06	0.27	-	0.26	57.45	100.59
154a-7)	-	15.52	26.12	12.36	0.05	0.82	0.16	0.45	43.77	99.25
127-1)	-	13.63	19.43	13.27	0.08	0.28	0.11	0.15	52.54	99.49
127-2)	-	11.31	18.73	13.85	-	0.29	0.11	0.26	55.30	99.85
127-3a)	-	11.21	18.03	14.28	-	0.31	0.06	0.19	56.80	100.88
127-1r)	-	13.61	19.66	13.54	-	0.07	0.09	-	52.36	99.33
127-2r)	-	11.19	18.63	13.78	-	0.18	0.16	0.11	55.22	99.27
127-3b)	-	11.08	17.80	13.69	-	0.28	0.16	0.18	56.35	99.54
127-3c)	-	11.20	17.20	14.15	-	0.32	0.04	0.10	56.77	99.78
127-3d)	-	11.38	17.57	14.08	-	0.15	0.13	0.13	56.73	100.17
127-3e)	-	11.15	17.34	13.93	-	0.21	0.10	0.11	56.56	99.40
127-4b)	-	13.23	16.57	14.74	-	0.39	0.08	0.10	53.76	98.87
127-5)	-	11.70	14.32	15.45	-	0.22	0.09	0.17	56.83	98.78
127-6)	0.48	12.28	21.43	12.29	0.09	0.40	0.12	0.30	52.71	100.10
127-7)	-	11.74	13.82	15.82	-	0.11	0.13	-	56.99	98.61
127-8)	-	12.29	20.53	12.51	-	-	0.15	0.16	53.16	98.80
127-9)	-	11.99	17.77	13.82	-	0.15	0.17	0.20	55.15	99.25
127-10)	-	11.62	19.12	12.95	-	0.38	0.19	0.17	54.63	99.06
38-1a)	2.20	12.06	22.39	10.97	0.36	0.18	0.13	0.18	49.59	98.06
38-1b)	-	11.65	19.92	12.20	-	0.15	0.13	0.21	56.14	100.40
38-2)	0.18	11.35	22.62	11.55	0.14	0.29	0.12	0.19	52.99	99.43
38-3)	-	12.68	21.97	11.70	-	0.37	0.16	0.18	53.82	100.88
38-4)	-	12.12	23.09	11.98	0.13	0.53	0.12	0.12	51.69	99.78
38-5)	0.86	11.43	23.28	11.77	0.05	0.38	0.11	0.22	51.30	99.40
38-6)	-	12.30	23.41	12.04	0.07	0.48	0.13	0.27	50.99	99.69
38-7)	-	13.76	23.05	12.15	0.13	0.32	0.14	0.25	49.49	99.29
38-8)	0.52	11.94	22.38	11.69	0.10	0.36	0.11	0.14	52.38	99.62
120-1)	-	14.60	22.12	11.61	-	0.42	0.14	0.20	51.34	100.43
120-2a)	-	13.39	23.66	10.59	-	0.41	0.15	0.20	51.25	99.65
120-1r)	-	14.89	22.41	11.39	0.05	0.55	0.15	0.29	50.68	100.41
120-2b)	-	11.99	20.09	12.52	-	0.11	0.18	-	54.83	99.72
120-3)	-	14.68	17.90	14.29	-	0.31	0.11	0.13	52.18	99.60
120-4)	-	14.94	18.56	13.92	-	0.41	0.15	0.33	51.65	99.96
120-5)	-	14.28	29.29	7.53	0.05	0.39	0.14	0.19	49.39	101.27
120-6)	-	14.37	21.30	12.29	-	0.50	0.08	0.32	51.49	100.35
120-7)	-	13.72	20.77	12.78	-	0.29	0.09	0.18	51.54	99.37
120-8)	-	14.69	26.91	9.03	-	0.31	0.18	0.22	48.10	99.44

(*) Total iron expressed as FeO

(-) Not detected

MAP 1

GEOLOGIC MAP OF THE MARGI AREA, CYPRUS

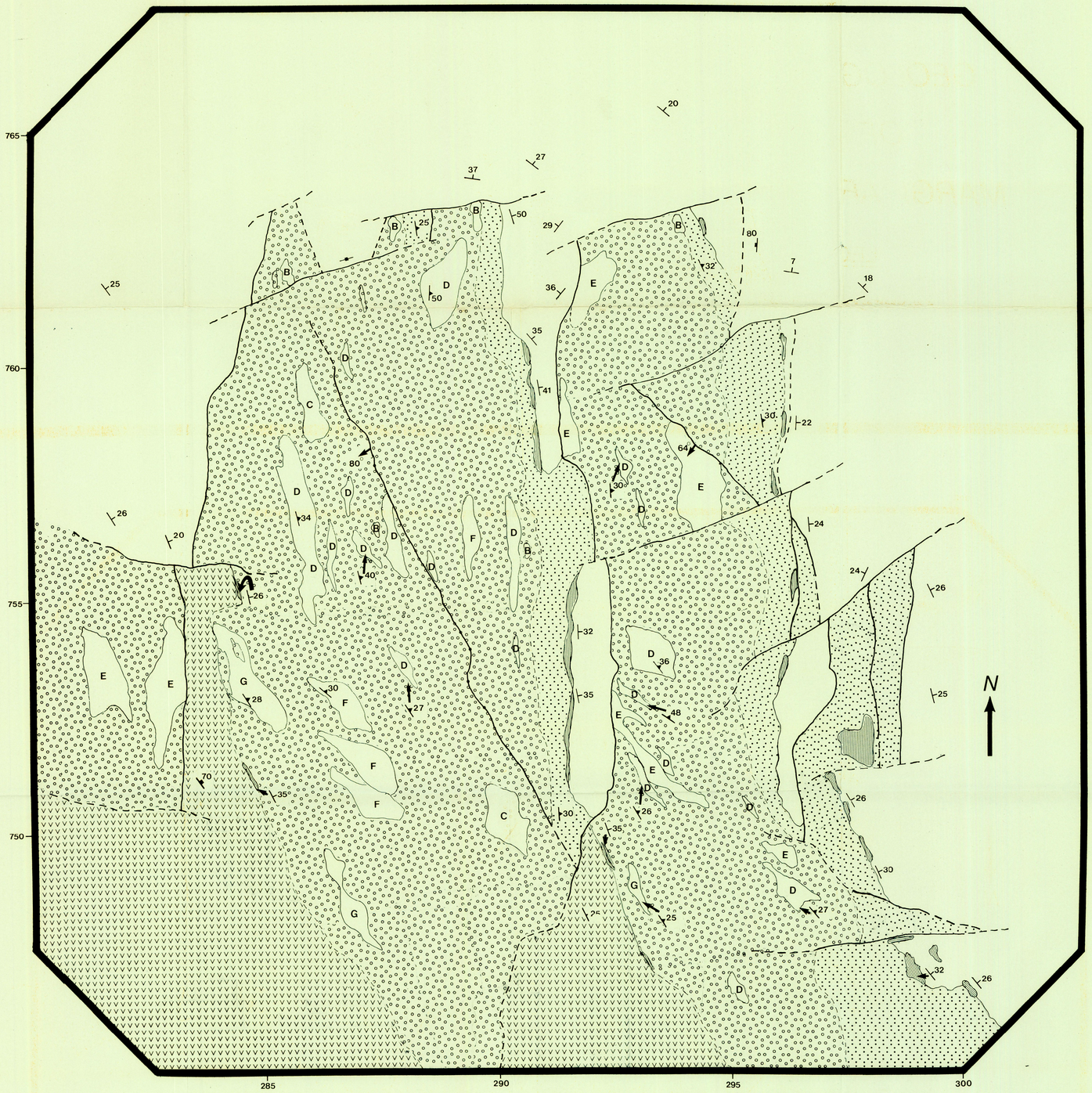

LEGEND

SEDIMENTARY ROCKS

- CHALKS
- UMBERS / CHERTS

VOLCANIC ROCKS

UNIT III
- **A.** Aphyric Pillows
- **B.** Sl. Olivine-phyric Pillows

UNIT II
- **A.** Crystalline Olivine-phyric Pillows
- **B.** Glassy Olivine-phyric Pillows
- **C.** Picritic Pillows
- **D.** Picrite-based Flows
- **E.** Aphyric Massive Flows
- **F.** Olivine-microphyric Flows
- **G.** Clinopyroxene-microphyric Flows

UNIT I
- **A.** Aphyric to Plagioclase and Clinopyroxene-phyric Volcanics

SYMBOLS

- Orientation of Bedding
- Orientation of Flow Layering
- Orientation of Jointing
- Fault Boundary and Dip (Observed / Inferred)
- Lithologic Boundary (Observed / Inferred)

SCALE

0 100 200 300 meters

1984 DAVID G. BAILEY

MAP 2

SAMPLE LOCATION MAP

LEGEND

- $\bullet^{96}$ Sample location and number
- ◉ Analyzed whole-rock
- ■ Analyzed glass
- ⊡ Analyzed whole-rock and glass

Base map from Cyprus Series D.L.S.17
1:5000 Topagraphic Sheets 39/IV;
39/V; 30/XXVIII; 30/XXIX

Contour interval = 2 meters

SCALE
0 100 200 300
meters

1984 DAVID G. BAILEY